PB83-194191

Houston Oxidant Modeling Study-1978
Volume I. Data Evaluation and Analysis

SRI International
Menlo Park, CA

Prepared for

Environmental Sciences Research Lab.
Research Triangle Park, NC

Apr 83

U.S. Department of Commerce
National Technical Information Service
NTIS

EPA-600/3-83-023a
April 1983

PB83-194191

HOUSTON OXIDANT MODELING STUDY-1978

VOLUME I. DATA EVALUATION AND ANALYSIS

by

J. R. Martinez
F. L. Ludwig
C. Maxwell
Atmospheric Science Center
SRI International
Menlo Park, California 94025

Contract 68-02-2984

Project Officers

Kenneth L. Demerjian
Basil Dimitriades
Environmental Sciences Research Laboratory
Research Triangle Park, North Carolina 27711

ENVIRONMENTAL SCIENCES RESEARCH LABORATORY
OFFICE OF RESEARCH AND DEVELOPMENT
U. S. ENVIRONMENTAL PROTECTION AGENCY
RESEARCH TRIANGLE PARK, NORTH CAROLINA 27711

REPRODUCED BY
NATIONAL TECHNICAL
INFORMATION SERVICE
U.S. DEPARTMENT OF COMMERCE
SPRINGFIELD, VA. 22161

TECHNICAL REPORT DATA
(Please read Instructions on the reverse before completing)

1. REPORT NO. EPA-600/3-83-023a	2.	3. RECIPIENT'S ACCESSION NO. PB83 194191
4. TITLE AND SUBTITLE HOUSTON OXIDANT MODELING STUDY-1978 Volume I. Data Evaluation and Analysis		5. REPORT DATE April 1983 6. PERFORMING ORGANIZATION CODE
7. AUTHOR(S) J. R. Martinez, F. L. Ludwig, C. Maxwell		8. PERFORMING ORGANIZATION REPORT NO. SRI Project 7938
9. PERFORMING ORGANIZATION NAME AND ADDRESS Atmospheric Science Center SRI International 333 Ravenswood Avenue Menlo Park, CA 94025		10. PROGRAM ELEMENT NO. CDWA1A/01-0649 (FY-83) 11. CONTRACT/GRANT NO. 68-02-2984
12. SPONSORING AGENCY NAME AND ADDRESS Environmental Sciences Research Laboratory--RTP, NC Office of Research and Development U. S. Environmental Protection Agency Research Triangle Park, NC 27711		13. TYPE OF REPORT AND PERIOD COVERED Final 14. SPONSORING AGENCY CODE EPA/600/09

15. SUPPLEMENTARY NOTES

16. ABSTRACT

During the period 15 September through 12 October 1978, the U.S. Environmental Protection Agency (EPA) conducted a special program that monitored air quality and meteorology in the Houston, Texas area. The objectives of the program were to obtain a comprehensive data base suitable for use with photochemical air-quality simulation models and to provide a detailed body of data that can be used to investigate Houston's air quality in general and photochemical oxidants (HOMS Study) and aerosols (HACS Study) in particular.

The objectives of this contract were (a) to evaluate the suitability of the 1978 Houston data base for photochemical modeling application, (b) to analyze spatial and temporal patterns of pollutant concentrations, (c) to archive data in a manner suitable for use with air quality simulation models, (d) to analyze and characterize the quality of the gaseous pollutant measurements, and (e) to use the data to evaluate the performance of the EKMA photochemical model. Results from the data evaluation and archiving work are reported in a three-volume report. (Results from the EKMA evaluation work are reported in a separate report.)

The data evaluation effort is reported in Volumes 1 and 2; the data quality characterization effort is reported in Volume 3.

17. KEY WORDS AND DOCUMENT ANALYSIS

a. DESCRIPTORS	b. IDENTIFIERS/OPEN ENDED TERMS	c. COSATI Field/Group

18. DISTRIBUTION STATEMENT RELEASE TO PUBLIC	19. SECURITY CLASS *(This Report)* UNCLASSIFIED	21. NO. OF PAGES 133
	20. SECURITY CLASS *(This page)* UNCLASSIFIED	22. PRICE

EPA Form 2220-1 (Rev. 4-77) PREVIOUS EDITION IS OBSOLETE

NOTICE

This document has been reviewed in accordance with U.S. Environmental Protection Agency policy and approved for publication. Mention of trade names or commercial products does not constitute endorsement or recommendation for use.

ABSTRACT

During the period 15 September through 12 October 1978, the U.S. Environmental Protection Agency conducted a special program that monitored air quality and meteorology in the Houston, Texas, area. The objectives of the program were to obtain a comprehensive data base suitable for use with photochemical air-quality simulation models, and to provide a detailed body of data that can be used to investigate Houston's air quality in general and photochemical oxidants and aerosols in particular.

The objectives of this study were to

- Evaluate the suitability of the 1978 Houston data base for photochemical modeling applications.
- Analyze spatial and temporal patterns of pollutant concentrations.
- Assemble a data base.

The results are reported in two volumes. Volume I describes the data evaluation and analysis, and Volume II contains a detailed guide to the data base.

This report was submitted in fulfillment of Contract No. 68-02-2984 by SRI International under the sponsorship of the U.S. Environmental Protection Agency. This report covers the period September 1978 to March 1980, and work was completed as of March 1980.

CONTENTS

Abstract iii
Figures vi
Tables ix

1. Introduction 1
    - Background 1
    - Project Objectives 1
    - Organization of the Report 2

2. Description of the Data Base from the Houston Oxidant Modeling Study 3

3. Evaluation of the Data Base from the Houston Oxidant Modeling Study 8
    - Assessment of the Usefulness of the HOMS Data Base for Modeling Purposes 8
    - Comparisons with the HAOS Data Base 13
    - Supplemental Data Needed for Modeling 21

4. Analysis of Aerometric Data 23
    - Analysis of Ozone, PAN, and NO_2 Data 23
    - Atmospheric Hydrocarbons 32
    - $NMHC/NO_x$ Ratios 53
    - Spatial Patterns in the Pollutant Data 55
    - Case Studies of Potential Modeling Days 69

5. Summary and Conclusions 94
    - General 94
    - Evaluation of HOMS Data Base 94

References 98

Appendices

A Summary of HOMS data availability for days with aircraft data 100
B Mathematical definitions for empirical orthogonal functions ... 120

FIGURES

Number		Page
1	Location of the monitoring sites during the 1978 Houston monitoring program	3
2	Summary of data availability for 1 October 1978	11
3	Locations of key monitoring sites for the 1977 Houston Area Oxidant Study	17
4	Ozone frequency distributions for the HOMS data base	25
5	Mean hourly ozone concentrations (ppb) during the HOMS monitoring period	26
6	Peak hourly ozone concentrations (ppb) during the HOMS monitoring period	27
7	Nitrogen dioxide frequency distributions for the HOMS data base	28
8	Mean hourly NO_2 concentrations (ppb) during the HOMS monitoring period	29
9	Peak hourly NO_2 concentrations (ppb) during the HOMS monitoring period	30
10	PAN frequency distributions for the HOMS data base	31
11	Average diurnal variation in NMHC concentrations at selected sites in the Houston area, May-October 1977	33
12	Time series of formaldehyde concentrations	52
13	Cumulative frequency distributions of $NMHC/NO_x$ ratios for the HOMS and HAOS	54
14	Mean ozone concentrations (ppb) and the most important empirical orthogonal functions	57
15	Average hourly values of the coefficient for the first empirical orthogonal function for ozone	58
16	Average values of the coefficient for the first empirical orthogonal function for ozone according to wind direction at Mae Drive	59
17	Mean NMHC concentrations (ppbC) and the two most important empirical orthogonal functions	60

Number Page

18 Average hourly values of the coefficients for the first two empirical orthogonal functions for NMHC...................... 62

19 Average values of the coefficients for the first two empirical orthogonal functions for NMHC according to wind direction at Mae Drive... 63

20 Mean NO_x concentrations (ppb) and the two most important empirical orthogonal functions................................ 65

21 Average values of the coefficients for the first two empirical orthogonal functions for NO_x according to wind direction at Aldine.. 67

22 Average hourly values of the coefficients for the first two empirical orthogonal functions for NO_x....................... 68

23 Weather maps for 0600 CST, 20 September 1978.................. 71

24 Ozone concentrations (ppb) at 1500 ft msl, 0600-0745 CST, 20 September 1978... 72

25 Vertical NO_x, O_3, and temperature profiles recorded east of Houston during Spirals 1, 2, and 3 on the morning flight of 20 September 1978.................. 73

26 Vertical NO_x, O_3, and temperature profiles recorded west of Houston during the morning flight of 20 September 1978.. 73

27 Ozone concentrations (ppb) at 1500 ft msl from approximately 1100-1400 CST, 20 September 1978.......... 74

28 Ozone concentrations (ppb) at ground level, 1300 CST, 20 September 1978... 75

29 Vertical cross section of ozone concentrations (ppb) downwind of Houston at approximately 1300 CST, 20 September 1978...... 75

30 Weather maps for 0600 CST, 29 September 1978.................. 77

31 Ozone concentrations (ppb) at 1500 ft msl, from approximately 0800-1115 CST, 29 September 1978.......... 78

32 Surface ozone concentrations (ppb) at ground level, 1000 CST, 29 September 1978................................. 79

33 Vertical NO_x, O_3, and temperature profiles recorded east of Houston during Spirals 1, 2, and 3 on the morning flight of 29 September 1978.................. 79

34 Ozone concentrations (ppb) at 1500 ft msl from 1320-1500 CST, 29 September 1978... 80

35 Ozone concentrations (ppb) at ground level, 1400 CST, 29 September 1978... 81

36 Vertical cross section of ozone downwind of Houston at approximately 1400 CST, 29 September 1978................. 81

Number Page

37 Weather maps for 0600 CST, 1 October 1978 82

38 Ozone concentrations (ppb) at 1500 ft msl from approximately 1150 to 1500 CST, 1 October 1978 83

39 Ozone concentrations (ppb) at ground level, 1400 CST, 1 October 1978 84

40 Vertical cross section of ozone concentrations (ppb) in the Houston area at approxmately 1400 CST, 1 October 1978 85

41 Ozone concentrations (ppb) at 1500 ft msl from approximately 1825 to 2040 CST, 1 October 1978 85

42 Ozone concentrations (ppb) at ground level, 1900 CST, 1 October 1978 86

43 Vertical cross section of ozone concentrations (ppb) in the Houston area at approximately 1900 CST, 1 October 1978 86

44 Weather maps for 0600 CST, 2 October 1978 88

45 Ozone concentrations (ppb) at 1500 ft msl from approxmately 0730-1040 CST, 2 October 1978 89

46 Ozone concentrations (ppb) at ground level, 0900 CST, 2 October 1978 90

47 Vertical NO_x, O_3, and temperature profiles recorded over central Houston during the morning flight of 2 October 1978 90

48 Ozone concentrations (ppb) at ground level, 1500 CST, 2 October 1978 91

49 Ozone concentrations (ppb) at 1500 ft msl from 1320 to 1615 CST, 2 October 1978 92

50 Vertical cross section of ozone downwind of Houston at approximately 1500 CST, 2 October 1978 93

TABLES

Number Page

1 Sites for 1978 Houston Monitoring Program...................... 4

2 Number of Hydrocarbon Samples Collected in the Houston Area, 15 September-12 October 1978................................ 6

3 Summary of Available HOMS Data for Each Aircraft Flight Date with Subjective Estimates of Their Adequacy for Modeling Purposes.. 14

4 Sites for the June Through September 1977 Houston Area Oxidant Study (HAOS)...................................... 15

5 Houston Area Oxidant Study Aircraft Data....................... 18

6 Ozone Maxima in the Houston Area............................... 24

7 Classification of Hydrocarbon Monitoring Stations in the HOMS.. 33

8 Hydrocarbon Compounds Identified by the U.S. Environmental Protection Agency... 34

9 Hydrocarbon Compounds Identified by Washington State University.. 35

10 0600-0900 (CDT) Nonmethane Hydrocarbons....................... 36

11 Principal Sources of Selected Hydrocarbons..................... 38

12 0600-0900 (CDT) Hydrocarbon Concentrations in Houston.......... 39

13 Clustering of Houston Monitoring Sites According to Hydrocarbon Concentrations.................................. 39

14 0600-0900 (CDT) Ratios of Hydrocarbon/Acetylene Concentrations (ppbC) in Houston............................ 41

15 Estimated Ambient Ratios of Hydrocarbon/Acetylene Concentrations (ppbC) in Roadway Tunnels in Los Angeles, New York, and Houston.. 42

16 0600-0900 (CDT) Concentrations of Selected Hydrocarbons Measured During the HAOS, June-October 1977................. 44

17 0600-0900 (CDT) Ratios of Hydrocarbon/Acetylene Concentrations (ppbC) Measured During the HAOS, June-October 1977... 45

Number Page

18 0600-0900 (CDT) Ratios of Benzene/Toluene Concentrations (ppbC) in the Houston Area During the HAOS, June-October 1977........................... 46

19 0600-0900 (LT) Hydrocarbon Monitoring in Denver and Southern California.. 47

20 0600-0900 (LT) Hydrocarbon Concentrations in Denver and Southern California.. 48

21 0600-0900 (CDT) Ratios of Hydrocarbon/Acetylene Concentrations (ppbC) in Denver and Southern California...... 49

22 0600-0900 (LT) Ratios of n-C_4H_{10}/C_3H_6 Concentrations (ppbC) in Houston, Denver, and Southern California.................. 50

23 Aldehydes in the Houston Area.................................. 52

24 0600-0900 (CDT) NMHC/NO_x Ratios in the Houston Area, 15 September-12 October 1978................................. 53

25 0600-0900 (CDT) NMHC/NO_x Ratios in the Houston Area, 1 May-31 October 1977... 54

SECTION 1

INTRODUCTION

BACKGROUND

During the period 15 September to 12 October 1978, the U.S. Environmental Protection Agency (EPA) conducted an intensive program that monitored air quality and meteorology in the Houston, Texas, area. The purpose of the program was twofold:

- To obtain a comprehensive, high quality data base suitable for use with photochemical air-quality simulation models.
- To provide a detailed body of aerometric data that can be used to investigate Houston's air quality in general, and photochemical oxidants and aerosols in particular.

In keeping with these objectives, the monitoring program consisted of two complementary parts known respectively as the Houston Oxidant Modeling Study (HOMS) and the Houston Aerosol Characterization Study (HACS). The data collected during the program were subsequently forwarded to SRI, where the measurements were assembled into a unified data base and subjected to various analyses, the results of which are described in this report.

Viewed from a wider perspective, the 1978 Houston program is the latest in a series of special projects, sponsored by both government and private entities, that have measured air quality in the Houston area (Lonneman and Bufalini, 1973; Decker et al., 1976; Siddiqi and Worley, 1977; Westberg, et al., 1978 and 1979; Ludwig and Martinez, 1979). The most comprehensive of these previous efforts is the Houston Area Oxidants Study (HAOS) conducted in the summer of 1977. The HAOS aerometric data have been analyzed by Ludwig and Martinez (1979), and some of their results will be compared with those obtained in the present investigation.

PROJECT OBJECTIVES

The objectives of this project are as follows:

- To evaluate the suitability of the 1978 Houston data base for use with photochemical air quality simulation models.

- To analyze pollutant concentration and meteorological data.
- To assemble a data base.

The results of this project are reported in two volumes. This volume, Volume I, describes the evaluation and analysis of the data, and Volume II contains a guide to the data base. A companion report will be published later that will examine the quality of the measurements. Also, in accordance with the project's scope of work, a paper describing preliminary results was presented at the Specialty Conference on Ozone/Oxidants sponsored by the Air Pollution Control Association (APCA) that was held in Houston in October 1979 (Martinez and Ludwig, 1979). The paper has been included in the conference proceedings published by APCA.

ORGANIZATION OF THE REPORT

Section 2 contains a brief description of the monitoring program, and Section 3 presents the evaluation of the data base. The analysis of aerometric data is described in Section 4. Section 5 contains the conclusions and recommendations of the report. The reader is referred to Volume II for a detailed description of the data archive.

SECTION 2

DESCRIPTION OF THE DATA BASE FROM THE HOUSTON OXIDANT MODELING STUDY

The geographic setting of the data base is illustrated in Figure 1. The numbers of the 25 ground-level monitoring sites in Figure 1 are keyed to Table 1, which lists station number, name, agency, parameters measured, and the Universal Transverse Mercator (UTM) coordinates of the monitoring stations. The rectangle in Figure 1 defines the boundaries of the modeling region; the UTM coordinates of its origin are 240 km E and 3270 km N. The rectangle is approximately centered on downtown Houston (Site 3).

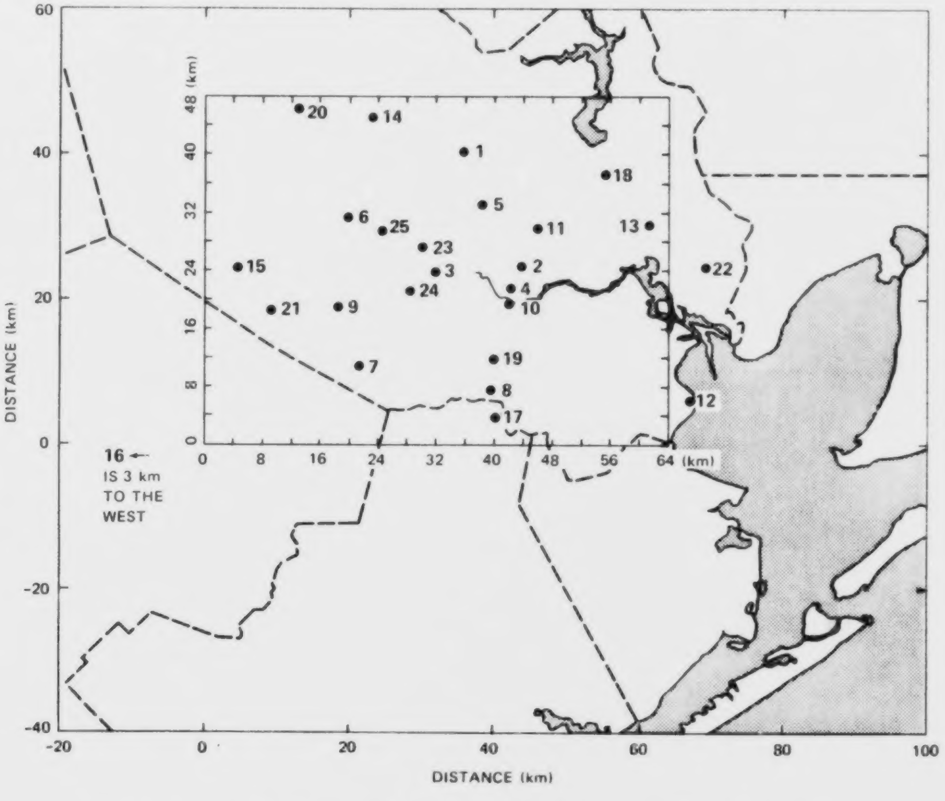

Figure 1. Location of the monitoring sites during the 1978 Houston monitoring program. Site numbers are keyed to Table 1; rectangle defines the boundaries of area modeled.

TABLE 1. SITES FOR 1978 HOUSTON MONITORING PROGRAM

Site No.	Site Name	Operating Agency	Parameters Measured	UTM Coordinates (m)
1	Aldine	Texas Air Control Board (TACB)	O_3, NO, NO_x, NO_2, SO_2, THC, CH_4, NMHC, CO, wind, temperature	275473E 3310112N
2	Mae Drive	TACB	Same as for Site 1, plus b_{scat} and detailed hydrocarbons	285303E 3295162N
3	Crawford	City of Houston	O_3, NO, NO_x, NO_2, THC, CH_4, NMHC, CO, detailed hydrocarbons, aldehydes	271648E 3293708N
4	Clinton	City of Houston	O_3, SO_2, THC, CH_4, NMHC, CO, TS, aldehydes	282382E 3291429N
5	Parkhurst	City of Houston	O_3, NO, NO_x, NO_2, THC, CH_4, NMHC, CO, detailed hydrocarbons, aldehydes	279100E 3303046N
6	Lang	City of Houston	O_3, NO, NO_x, NO_2, THC, detailed hydrocarbons	259960E 3301249N
7	Darlinghurst	City of Houston	O_3, THC	261000E 3281000N
8	Fuqua	City of Houston	O_3, NO, NO_x, NO_2, THC, CH_4, NMHC, CO, aldehydes	279296E 3278089N
9	Hornwood	EPA	O_3	258000E 3289000N
10	Pasadena	Houston Light and Power (HLP)	O_3, NO, NO_x, SO_2, wind, detailed hydrocarbons, temperature, dewpoint	282000E 3289000N
11	Channelview	HLP	Same as Site 10 without detailed hydrocarbons	286000E 3295000N
12	Seabrooke	EPA	O_3, NO, NO_x, NO_2, detailed hydrocarbons	308000E 3276000N
13	Highlands	EPA	O_3, NO, NO_x, NO_2, SO_2, wind, temperature, dewpoint, solar radiation, CO, b_{scat}, aerosols	303000E 3301000N
14	Canino	EPA	NO, NO_x, NO_2, SO_2, CO, b_{scat}	263000E 3315000N
15	Westhollow	Shell Oil Co.	O_3, NO, NO_x, NO_2, wind, CO, dewpoint, temperature, solar radiation, detailed hydrocarbons	244323E 3294203N
16	Beasley	Monsanto	O_3	216421E 3269082N

TABLE 1 (concluded)

Site No.	Site Name	Operating Agency	Parameters Measured	UTM Coordinates (m)	
17	Pearland	Washington State University (WSU)	O_3, NO, NO_x, NO_2, CH_4, NMHC, CO, dewpoint, UV, wind, temperature, detailed hydrocarbons, freon, CCl_4, methylchloroform, pressure, pibal	280000E	3274000N
18	Sheldon	WSU	O_3, NO, NO_2, acoustic sounder, detailed hydrocarbons, wind, temperature, dewpoint, PAN	295000E	3308000N
19	Hobby	EPA	Same as Site 13	279700E	3280200N
20	Jackrabbit	EPA	O_3, NO, NO_x, NO_2, PAN, SO_2, TS, THC, CH_4, NMHC, CO, b_{scat}, temperature, relative humidity, detailed hydrocarbons, freon, CCl_4, pressure, UV, VIS	252625E	3315675N
21	Alief	EPA	Same as Site 13 with UV but without CO	248600E	3289000N
22	Baytown	EPA	O_3, NO, NO_x, NO_2, SO_2, CO, b_{scat}	309000E	3295000N
23	Stude Park	EPA	Same as Site 13 with UV but without CO	269600E	3296700N
24	MacGregor	City of Houston	THC, wind, precipitation	268603E	3290782N
25	Radian Office	Radian Corp.	Pilot balloon	264780E	3298975N

A complete description of the data base, including both the HOMS and the HACS data, is presented in Volume II of this report. In this section, we will briefly discuss the important features of the data base.

Because it is intended for modeling photochemical air-quality, the data base includes the following special features:

- Detailed spatial and temporal coverage of pollutant levels in the modeling region.
- Monitoring aloft using an instrumented aircraft.
- An extensive hydrocarbon sampling program.
- Measurements of aldehydes and peroxyacetylnitrate (PAN).
- Monitoring of meteorological conditions using pilot balloons, tethersondes, and an acoustic sounder.

Figure 1 shows that the ground-level monitoring stations are well dispersed, in an attempt to describe the horizontal variations of pollutant levels. The time resolution of ground-level measurements is 1 hour for most variables but can be as long as 3 hours for some parameters, notably the hydrocarbon samples.

An instrumented aircraft operated by Washington State University (WSU) monitored pollutants aloft, making one or two daily flights. The aircraft measured O_3, NO, NO_x, b_{scat}, and condensation nuclei, and collected bag samples for detailed hydrocarbon analysis. Because the HOMS has a modeling orientation, a prime objective of the airplane flights was to obtain data that define the boundary conditions of the modeled area, since boundary conditions are required inputs of air-quality simulation models. A complete description of the aircraft data is found in Westberg et al. (1979).

The hydrocarbon sampling program collected 435 bag samples at various ground-level monitoring stations and approximately 130 samples aloft. Table 2 lists the monitoring stations, the sampling interval, and number of samples obtained. The laboratory analysis identified 64 compounds, of which there are 25 alkanes, 14 alkenes, 21 aromatics, 2 aldehydes, 1 ketone (acetone), and acetylene.

TABLE 2. NUMBER OF HYDROCARBON SAMPLES COLLECTED IN THE HOUSTON AREA, 15 SEPTEMBER—12 OCTOBER 1978

Site Name	0600-0900 (CDT)	1300-1600 (CDT)	Other Times
Mae Drive	20	17	13
Crawford	21	18	20
Parkhurst	17	17	0
Lang	16	13	0
Pasadena	19	17	0
Seabrooke	17	15	2
Westhollow	13	12	0
Pearland	28	27	0
Sheldon	25	26	0
Jackrabbit	23	18	14
Washburn Tunnel	0	0	7

Special efforts were made to monitor aldehydes and PAN. Formaldehyde and total aldehydes were monitored at Sites 3, 5, and 8, and PAN was sampled at Sites 18 and 20. The aldehydes monitoring program has been described by Joshi (1979).

Pilot-balloon (pibal) releases were made several times a day at Sites 17 and 25. Several tethersonde releases were made daily from a location near Site 12. An acoustic sounder was operated at Site 18.

The next section will evaluate the suitability of the data base for modeling purposes. Subsequent sections will analyze the data themselves.

SECTION 3

EVALUATION OF THE DATA BASE FROM THE HOUSTON OXIDANT MODELING STUDY

ASSESSMENT OF THE USEFULNESS OF THE HOMS DATA BASE FOR MODELING PURPOSES

Assessing the adequacy of a data base involves judgments that are necessarily subjective, but they can be arrived at more easily if all available pertinent information can be assembled and displayed in an easily comprehensible form. A format has been devised for displaying information for each of those days during the HOMS when aircraft data were collected. Before the formats could be developed, it was necessary to identify what kinds of information were relevant to the problem. This meant reviewing the data requirements that are common to most problems in air-quality modeling. The next section provides a brief review of the data required to operate a model and to verify results obtained.

Data Requirements for Modeling

There are two broad classes of models for simulating photochemical air-quality: grid (Eulerian) models and trajectory (Lagrangian) models. The grid models have a more general formulation from which the trajectory models can be derived by a coordinate transformation. Thus, their respective data requirements are similar in kind but may differ in degree for certain applications, since the spatial coverage of Lagrangian models can be restricted. Consequently, our discussion of data requirements for modeling will be cast in terms of Eulerian models because the data needs of Lagrangian models are a subset of those for the Eulerian.

The data needed for modeling fall into two general categories: data for input to the model and data for verifying model results. Meteorological data are necessary for operating the models and thus fall in the first category, as do measurements of the concentrations of various chemical species throughout the area. Pollutant data are also necessary for verifying modeling results, so they fall into the second category as well. The data required for operating air-quality models also include a comprehensive description of the emissions of the various chemical species treated. However, emissions information is usually compiled separately from concentration and meteorological information, and the HOMS is no exception. For this reason, our assessment of the HOMS data base with respect to its suitability for modeling applications has considered only meteorological and pollutant data.

Although there are differences from model to model in the meteorological data required, the fact that the purpose of the model is to simulate the physical phenomena that affect the formation, transport, and dilution of pollutants means that the required meteorological information will be much the same, in a general sense. Thus, if the data are suitable for the application of one model, they probably will be suitable for the application of another. The parameters listed below can be considered not only as requirements for input to air-quality models, but also as factors determining the concentrations of photochemical pollutants in the atmosphere.

The input data requirements for simulation modeling of photochemical air-quality are as follows:

Meteorological Parameters

- Wind field--horizontal (u,v) components of the wind vector must be specified in each grid cell.
- Inversion height--specified for each grid cell in the (x,y) plane.
- Temperature field--ground-level temperature in each grid cell.
- Vertical temperature gradient (lapse rate)--the vertical gradient of temperature is generally assumed to be spatially invariant in the x-y plane, so an average value is used throughout the modeling grid.
- Atmospheric stability--generally assumed to be spatially invariant.
- Solar or ultraviolet radiation--generally assumed to be spatially invariant.
- Water vapor (humidity)--generally assumed to be spatially invariant.
- Atmospheric pressure--generally assumed to be spatially invariant.

Concentrations of Chemical Constituents

- Initial conditions in each grid cell--the concentration at the start of the simulation for each of the model species.
- Boundary conditions--the concentration of each species in each grid cell on the upwind boundary and in the uppermost layer of the modeled region must be known throughout the simulation.

Other than initial conditions, which must be specified only once for each run, the meteorological variables and the boundary conditions vary with time and must be updated periodically during a simulation period. The frequency of updating required varies depending on the availability of the data and the nature of the parameters. Typically, a time resolution of one hour is used for most of the time-varying parameters except solar radiation, which is usually updated every few minutes. Thus, the data must be adequate to specify, either through direct measurement or through interpolation, values of the meteorological parameters at every grid point at intervals of an hour or less throughout the simulation. Similar requirements apply to the concentrations of chemical species within the cells around the perimeter of the modeled area and in its uppermost layer.

The requirements for model verification are somewhat less stringent than those for initialization of model runs. In general, it is sufficient to specify the concentration history of each of the most important pollutants at various points in the lowest layer of the modeling grid. The model will typically provide concentration values calculated at many more locations than it would be possible to monitor. As a general rule, the evaluation of a model will be based on comparisons of the model predictions at points that are coincident with measurements. Proper verification requires that a wide variety of conditions and geography be covered. There should be verification at sites upwind and downwind of regions of major emissions as well as at points within those regions. Sometimes the comparisons can be made with values interpolated between monitoring sites.

An Example of the Evaluation of Data for a Specific Day

In the preceding section, the factors important for the application or validation of air-quality models were outlined. An attempt has been made to display relevant information for each of the HOMS days along with the subjective evaluations derived from that information. A data summary such as that shown for 1 October 1978 in Figure 2 is available, for each day, in Appendix A. The reasons for including the different kinds of information are discussed below, along with the logic behind the evaluations of the data. The same kind of reasoning was used in arriving at the judgments shown in the data summaries given in Appendix A.

Figure 2 illustrates the approach. Because it is difficult to infer conditions aloft if no measurements have been made there, Figure 2 places considerable emphasis on the availability of such measurements, either by aircraft or balloon soundings. Furthermore, measurements aloft are made infrequently, while ground-level measurements are more abundant, so the ability to describe conditions in three dimensions depends more critically on the availability of airborne observations than on those at the surface.

The first entries on the left side of Figure 2 describe the aircraft coverage, showing that two aircraft flights were made on 1 October 1978. The first flight was made during early afternoon, from 1152 to 1500 CST. Flight levels were about 1500 ft (450 m). The next entry in Figure 2 shows that a mixed layer is estimated to have been 4000 to 5000 ft (1200 to 1500 m) deep, an estimate based on the five vertical profiles, to altitudes of about 6000 ft (1800 m), that were made during the first flight. It is important to know the flight altitude and the approximate mixing depth, to determine whether the flight took place within the mixed layer. In this case, the flights were well within the boundary layer, where constituents tend to be thoroughly and uniformly distributed in the vertical (Ludwig, 1979), so the aircraft measurements can be used to define conditions within the boundary layer. The horizontal gradients found at 1500 ft provide information that can be used to define the horizontal variability of concentration at other levels within the mixing layer. During the second flight, there was some surface destruction of ozone that made the measurements aloft unrepresentative of ground-level ozone conditions, but this was not very serious because there were 11 ground-level ozone stations in operation.

ITEM	FLIGHT 1	FLIGHT 2
AIRCRAFT COVERAGE		
START TIME	1152	1825
END TIME	1500	2040
FLIGHT LEVEL (ft)	1500 (6000)	1500 (6000)
APPROXIMATE MIXING DEPTH (ft)	4000	5000
NUMBER OF VERTICAL PROFILES	5	3
OTHER UPPER-LEVEL DATA		
TETHERSONDE		
TIMES		
LOCATION		
PILOT BALLOON (T DENOTES TEMPERATURESONDE)		
TIMES	11,13T,14,15	17T
LOCATION	25 and 17	25 and 17
SURFACE DATA — NUMBER OF SITES AVAILABLE:		
O_3	11	11
NO_x	8	8
NMHC	6	6
PAN	1	1
METEOROLOGICAL	5	5
CONDITIONS		
DAILY O_3 PEAK CONCENTRATION (ppb)	310	310
HOUR (CST)	1400	1400
SITE	Hornwood	Hornwood
GENERAL WINDS (DIRECTION/SPEED)		
850 mb	100°/5 kts	100°/5 kts
SURFACE	015°/6 kts	150°/7 kts
AIRCRAFT DATA USEFULNESS FOR		
ESTIMATION OF INITIAL CONDITIONS	Reasonably good	Poor
ESTIMATION OF BOUNDARY CONDITIONS	Reasonably good	Poor
MODEL VERIFICATION	Reasonably good	Reasonably good
ESTIMATION OF MIXING	Good	Reasonably good
DETERMINATION OF RESOLUTION REQUIREMENTS		
VERTICAL	Good	Reasonably good
HORIZONTAL	Good	Reasonably good

Maximum height of vertical profiles shown in parentheses. Location of vertical profiles is denoted by symbol ◉
Arrows denote surface and 850-mb wind direction. Dots denote location of ground monitoring sites.

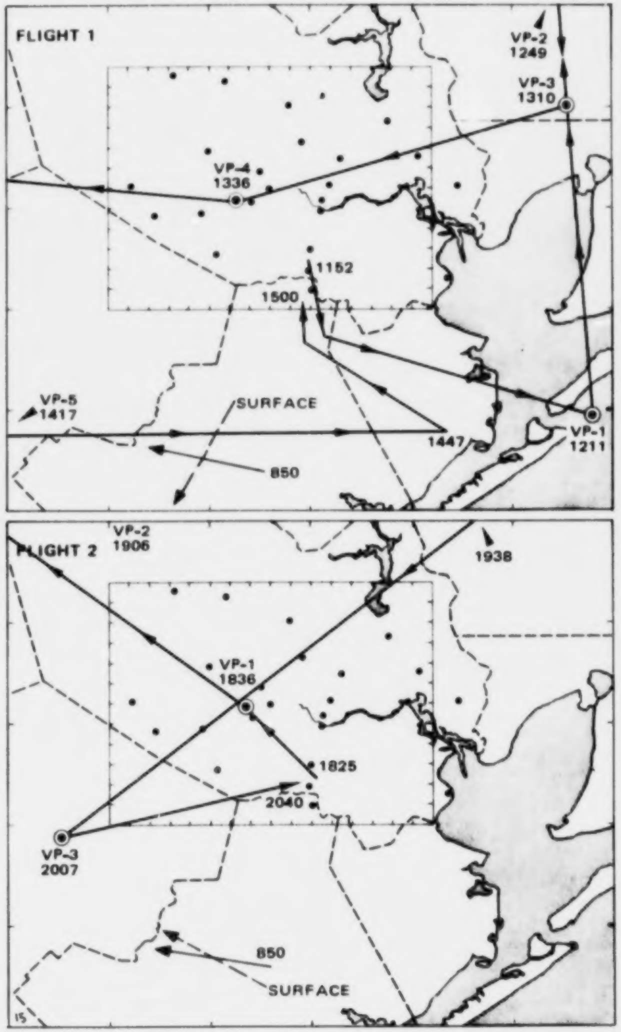

Figure 2. Summary of data availability for 1 October 1978.

Both pilot-balloon sites were in operation on 1 October, and Figure 2 shows that wind conditions aloft were well characterized during the first flight. Four observations are available from each of the two sites. Furthermore, a temperature sounding was made at each of the sites at about the middle (1300 CST) of the first flight. The available pibal, radiosonde, and aircraft data provide a good description of the mixing layer and the stability prevailing during the period. The early evening conditions of the second flight were not so well characterized. Figure 2 shows two pilot-balloon releases made during the second flight. The flight itself included only three vertical profiles.

Figure 2 shows that a large number of surface observation sites were collecting important data. The ozone concentrations were unusually high, and consequently made this day a likely candidate for modeling studies; the selection of days for analysis is discussed later. The next entry on the left side of Figure 2 shows the approximate direction and speed for the airflow in the region near the surface and at the 850-mb level, approximately 1500 m. The general airflow in the region at 850 mb was estimated from the twice-daily analyses of the National Weather Service, obtained from the National Climatic Center in Asheville, North Carolina. This information defines the upwind and downwind directions for the area. The 850-mb wind is a somewhat better indicator of regional air movement because surface winds sometimes reflect local effects or shallow circulations. Figure 2 shows that the winds aloft on 1 October 1978 were from a direction just slightly south of east. Most of the air entering the area to be modeled came from that direction, so the early afternoon flight provided a reasonably good description of the upwind boundary conditions, and initial conditions could be estimated from the available information even though the flight did not cover the northern part of the grid. Good mixing during the early afternoon should allow surface data to be extrapolated upward, with the available aircraft data used for guidance.

Figure 2 shows that the early evening data for 1 October 1978 were judged to be poor for purposes of defining boundary conditions. This is because the important upwind edge of the area was not surveyed. Similarly, there were too few aircraft measurements to provide good definitions, in three dimensions, of the distribution of ozone and other parameters. A lack of such information in the early evening is less important than for earlier hours of the day because the models are generally used to simulate conditions during the daytime hours. Therefore, initial conditions need to be specified in detail for the morning hours, but at later times only the boundary conditions (generally above or upwind of the polluted area) need to be prescribed. If boundary conditions are not accurately specified during the latter phases of a simulation with a grid model, the simulation will be most affected at the perimeter, especially the upwind perimeter. However, the most important results will frequently be in the center or downwind parts of the area, where the effects of inaccurate boundary conditions are less pronounced. If boundary conditions are badly described throughout the simulation period, the errors will propagate throughout the region, but if the situation exists only during the latter period of the run, the worst errors are likely to be confined to the least critical regions. However, verification of the results and validation of the model will depend on the availability of such data. The aircraft data should be adequate for the purpose when combined with surface measurements.

The final entries in Figure 2 provide an evaluation of the data's usefulness for estimating the spatial scale of concentration variability. Inasmuch as the available aircraft data can be used to identify features that have dimensions of a few hundred meters or less, they will generally be adequate for the purpose, provided that enough flights are taken in the area of interest. Spatial variability of concentration is of concern for modeling purposes because it defines how closely spaced the measurements must be to identify major features of concentration patterns, and how finely gridded the model calculations must be to replicate the major processes and features of the real world. Interpolation is necessary to provide initial values of all the variables for each cell of the model. The adequacy of such interpolation will depend on the scale of spatial variability and the strength of relationships among values obtained in approximate locations. It is sufficient to note here that interpolation between stations seems to provide suitable estimates of initial conditions near ground level. One would expect patterns aloft to be more regular than at the surface, so there should not be severe problems in estimating upper-level values if sufficient aircraft or sounding data are at hand.

Displays such as those shown in Figure 2 have been used to compile information for the 19 days for which aircraft data are available. The displays are relatively easy to understand and will serve to identify those cases that are interesting and have enough data to be studied and modeled in detail. These data displays are given in Appendix A. Table 3 summarizes the data available for each day and the subjective findings regarding the adequacy of the data for modeling purposes.

COMPARISONS WITH THE HAOS DATA BASE

General

During the summer of 1977, another extensive air-quality data collection program was undertaken in the Houston area. The data from that study, the Houston Area Oxidant Study (HAOS), have been summarized and analyzed elsewhere (e.g. Ludwig and Martinez, 1979; Ludwig, Martinez, and Nitz, 1979). The purpose of this section is to provide a brief review of the data available from that study. There are some differences and many similarities in the objectives of the HOMS and the HAOS; the two data sets can be considered to be complementary. The following sections discuss the HAOS data base in general terms and point out some of the strengths and weaknesses of that data base relative to the HOMS data and the objectives of HOMS.

The HAOS Monitoring Network

Table 4 lists the HAOS sites where substantial data were collected during the period June through September, 1977. Not all the sites were in operation throughout that period, but the sites shown were operational more than half the time. In addition, most of the sites were also operational during the month of October. Table 4 shows that 10 of the 22 HAOS sites were not used during HOMS. Eight of these monitored ozone, 6 monitored NO_x, and 4 measured nonmethane hydrocarbons (NMHC). Winds were measured at 7 and temperatures at 5 of the 10 HAOS sites that were not part of the HOMS network.

TABLE 3. SUMMARY OF AVAILABLE HOMS DATA FOR EACH AIRCRAFT FLIGHT DATE WITH SUBJECTIVE ESTIMATES OF THEIR ADEQUACY FOR MODELING PURPOSES

				Peak Observed Ozone Concentration (ppb)		Number of Sites Monitoring Parameters Other Than Ozone				Upper Level Observations			Subjective Evaluation of Data for Modeling*		
Date	Flight Period	In Mixing Layer?	Upwind Coverage*	Ground Station	Aloft	NO_x	NMHC	PAN	Meteorological	Pibal	Tethersonde and Temperature Sounding	Flight Profiles	Initial Condition	Boundary Condition	Model Verification
15 Sep 78	0925-1135	Yes	F	60	53	2	6	0	3	4	2	4	G	G	RG
16 Sep 78	1005-1225	Yes	F	90	55	3	7	0	3	5	2	5	RG	RG	RG
	1510-1732	Yes	P	90	126	3	7	0	3	4	0	2	P	F	F
17 Sep 78	0925-1210	Yes	G	70	81	3	6	0	4	4	2	1	F	G	G
	1950-2230	Yes	G	70	78	3	6	0	4	1	0	2	P	G	G
18 Sep 78	0930-1220	Yes	P	80	108	3	7	1	3	5	2	1	P	P	P
19 Sep 78	0742-1055	Yes	F	110	68	2	7	1	3	4	1	5	G	G	G
	1424-1707	Yes	G	110	94	2	7	1	3	5	1	2	P	G	G
20 Sep 78	0551-0748	No	P	120	53	2	7	1	3	2	2	4	F	F	P
	1055-1400	Yes	F	120	213	2	7	1	3	3	5	2	F	G	G
23 Sep 78	0545-0842	Yes	F	135	132	4	5	1	5	3	3	5	G	F	[illegible]
24 Sep 78	0625-0937	Yes	F	123	98	3	4	1	3	–	–	5	F	F	F
	1135-1520	Yes	F	123	182	3	4	1	3	–	–	2	P	F	G
25 Sep 78	0555-0900	Yes	P	164	133	6	5	1	5	3	4	5	RG	RG	RG
	1200-1500	Yes	P	164	194	6	5	1	5	3	6	1	F	F	G
26 Sep 78	0610-0905	No	P	182	108	7	6	1	5	3	2	5	G	G	F
	1030-1325	Yes	P	182	168	7	6	1	5	4	6	2	P	P	F
27 Sep 78	0745-0935	No	P	106	81	7	6	1	5	4	5	1	P	P	P
28 Sep 78	1010-1065	–	P	102	72	8	6	1	5	–	–	0	P	P	P
29 Sep 78	0820-1112	Yes	P	141	144	8	6	1	5	4	6	5	RG	RG	F
	1310-1458	Yes	P	141	175	8	6	1	5	3	7	2	F	F	G
30 Sep 78	0715-1018	No	P	105	136	8	3	1	5	5	7	5	F	F	F
	1200-1525	Yes	RG	105	174	8	3	1	5	4	9	4	F	F	G
1 Oct 78	1152-1500	Yes	RG	310	336	8	6	1	5	4	1	5	RG	RG	RG
	1825-2040	Yes	P	310	255	8	6	1	5	1	1	3	P	P	RG
2 Oct 78	0728-1038	No	G	210	122	8	6	1	5	5	5	5	RG	RG	RG
	1320-1615	Yes	RG	210	144	8	6	1	5	5	7	5	P	RG	G
4 Oct 78	0800-0915	No	F	150	106	9	5	1	5	4	3	1	P	F	P
	1655-2008	Yes	RG	150	120	9	5	1	5	2	1	2	P	G	G
5 Oct 78	0950-1302	Yes	F	190	174	8	5	1	5	5	6	5	F	G	RG
7 Oct 78	0617-0940	No	F	163	73	8	6	1	5	4	4	5	RG	RG	RG

*G = good; RG = reasonably good; F = fair; P = poor

TABLE 4. SITES FOR THE JUNE THROUGH SEPTEMBER 1977 HOUSTON AREA OXIDANT STUDY (HAOS)

Site Name	Operating Agency	Parameters Measured	Operated During HOMS
Aldine	TACB	CO, O_3, O_x, NMHC, NO_x, NO_2, NO, SO_2, THC, H_2S, meteorological	X
Crawford	City of Houston	CO, O_3, O_x, NMHC	X
Fuqua	City of Houston	O_3	X
Westhollow	Shell Oil Co.	CO, O_3, NMHC, NO_x, NO_2, NO, SO_2, THC	X
Mae Drive	TACB	CO, O_3, NMHC, NO_x, NO_2, NO, SO_2, THC, H_2S, meteorological	X
Clinton	City of Houston	CO, O_3, NMHC, SO_2	X
Parkhurst	City of Houston	O_3, NMHC, NO_x, NO_2, NO	X
MacGregor	City of Houston	O_3	X
Lang	City of Houston	O_3	X
Jackrabbit	Houston Light and Power	O_3, NO_x, NO_2, NO, SO_2, meteorological	X
Kluge	Houston Light and Power	NO_x, NO_2, NO, SO_2, meteorological	
Louetta	Houston Light and Power	NO_x, NO_2, NO, SO_2, meteorological	
Texas City	TACB	CO, O_3, NMHC, NO_x, NO_2, NO, SO_2, THC, H_2S, meteorological	
Clute	TACB	CO, O_3, NMHC, NO_x, NO_2, NO, SO_2, THC, H_2S, meteorological	
Hempstead	Rockwell	O_3, NO	
Offshore	Rockwell	O_3	
Southwest	EPA	O_3	
Bayport	Celanese	O_3, NMHC, NO_x, NO_2, NO, meteorological	
Freeport	Dow	O_3, wind	
Baytown	Gulf Chemicals	O_3	X
Beasley	Monsanto	O_3	X
Chocolate Bayou	Centenial H.C.	O_3, NMHC, NO_x, NO_2, NO, wind	

Twelve of the 24 HOMS sites were not included in the HAOS network. Those sites were

- Hornwood
- Pasadena
- Channelview
- Seabrooke
- Highlands
- Canino
- Pearland
- Sheldon
- Hobby
- Alief
- Stude Park
- Darlinghurst

All of these measured ozone, 8 measured oxides of nitrogen, 5 measured detailed hydrocarbons or NMHC, and 7 monitored wind.

It is apparent that the HAOS and the HOMS networks were comparable in scope and parameters measured, although they did not coincide site by site. Figure 3 shows the locations of the monitoring sites listed in Table 4. Comparison with Figure 1 shows that the HOMS network has greater density within the modeled area. All but three of the HOMS stations are within the rectangle bounding the model area; two of those outside the area are only a few kilometers toward the east. During HAOS, nine stations were operated in locations far outside the Houston metropolitan area and the rectangle that bounds the HOMS modeling region. The differences in network design reflect some differences in objectives between the two programs. The HOMS, with its emphasis on modeling of photochemical processes within the region bounded by the rectangle, focused its monitoring in that area to provide detailed descriptions of conditions in the area. One of the major concerns of the HAOS was to describe concentrations, especially ozone, in air entering the Gulf coast region before it passed over any of the major source areas. Thus, the HAOS network had more stations on the perimeter of the Houston-Galveston region.

The HAOS concern for the character of air entering the region extended upward, as well as horizontally, from the Houston-Galveston area. For this reason, the HAOS monitoring program also included measurements of beryllium-7 at Hartwick (see Figure 3) from mid-July through mid-September 1977 and at Kluge and Aldine from mid-September through mid-October. The motivation for the Be-7 measurements was to determine the importance of ozone originated in the stratosphere. As is discussed below, the same motivation was important in the design of the aircraft monitoring program conducted during HAOS.

Aircraft Monitoring Program for HAOS

Aircraft observations of ozone and other parameters were undertaken for the HAOS by Shauck and Alexander (1978) of Baylor University during the latter half of 1976 and the summer and early fall of 1977. These measurements focused on horizontal flights and vertical profiles at higher altitudes; data were not usually collected below a few hundred meters altitude. As noted before, one of the major purposes of the aircraft flights during HAOS was to identify and characterize possible cases where ozone had entered the area from aloft, rather than to provide three-dimensional descriptions of conditions within the boundary layer, as is required for modeling. Another consequence

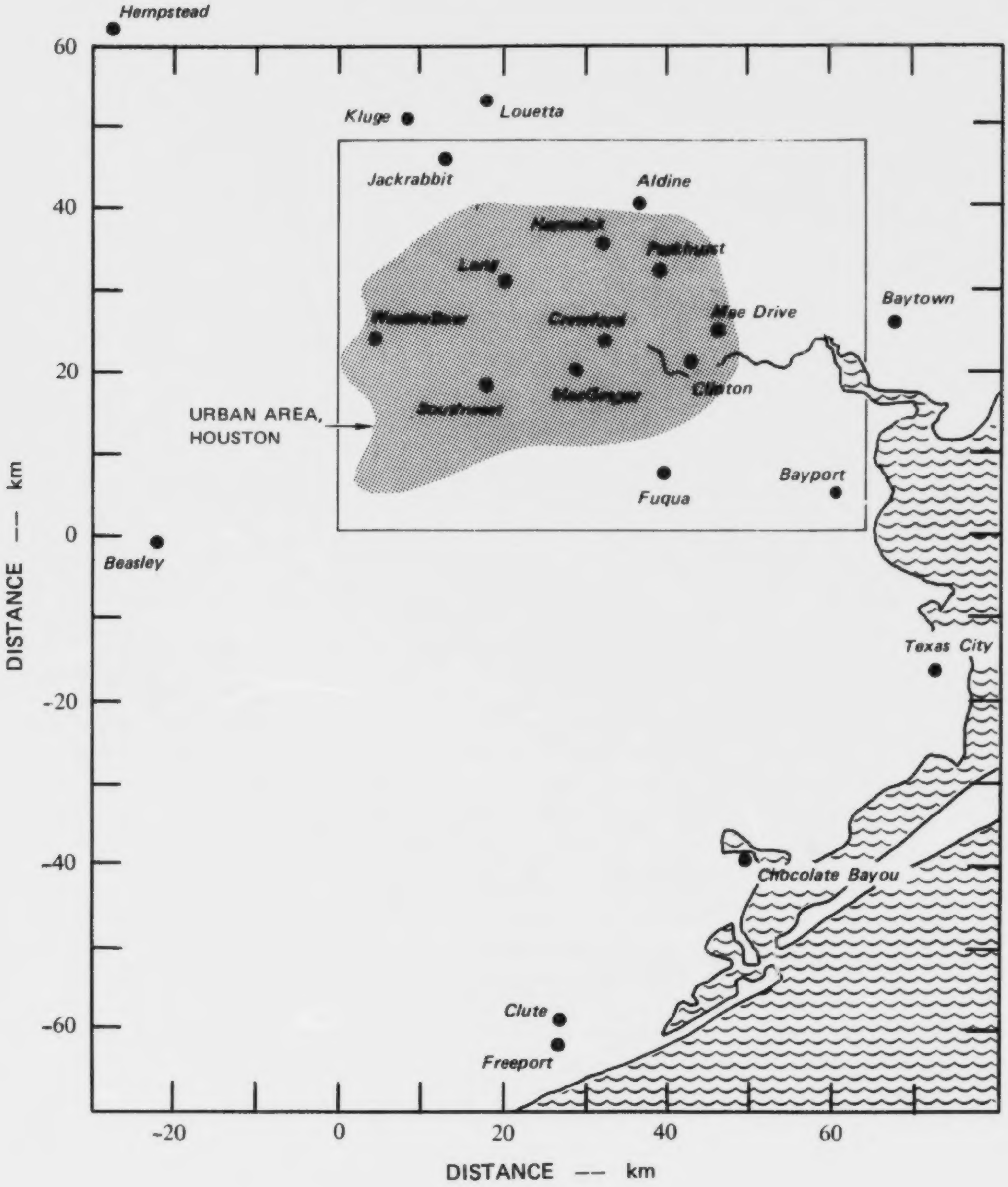

Figure 3. Locations of key monitoring sites for the 1977 Houston Area Oxidant Study.

of the HAOS objectives was that many of the flights took place almost entirely outside the modeling area. For purposes of defining the intrusion of materials from aloft, the flights did not need to be made in the immediate vicinity of Houston.

Table 5 lists the HAOS flights. The table gives beginning and end times and general itineraries for the flights. The remarks column provides

TABLE 5. HOUSTON AREA OXIDANT STUDY AIRCRAFT DATA

Date	Time (Local)	Flight Path	No. of Vertical Profiles	Profile Heights (kft msl)*	Parameters					Digitized	Remarks
					Temp.	O_3	NO	NO_x	b_{scat}		
28 Jul 76	1004-1444	Waco-Galveston-Waco	1	2.2-3.5	X	X				X	1.2 hr at Hobby Airport
29 Jul 76	0910-1611	Waco-Galveston-Waco	1	2.5-4	X	X				X	3.3 hr at Hobby Airport
13 Aug 76	1206-1656	Waco-Galveston-Waco	0		X	X				X	1.2 hr at Hobby Airport
26 Aug 76	1206-1750	Waco-Houston-College Station	0		X	X				X	2.8 hr at Hobby Airport
7 Sep 76	1210-1518	Waco-Galveston-Houston	0		X	X				X	1 hr at College Station
11 Sep 76	1114-1220	Waco (McGregor) spiral	1	0.6-1.9	X	X					
21 Sep 76	1301-1749	Waco-Galveston-Freeport-Waco	1	0.6-5	X	X					0.8 hr at Hobby Airport
22 Sep 76	1259-1831	Waco-Galveston-Freeport-Waco	0		X	X				X	1.9 hr at Hobby Airport
23 Sep 76	1520-1921	Waco-Galveston-Freeport-Waco	0		X	X				X	0.5 hr at Hobby Airport
24 Sep 76	1423-1749	Waco-Alvin-Waco	0		X	X				X	0.7 hr at Hobby Airport
25 Sep 76	1405-1810	Waco-Texas City-Waco	0		X	X				X	1.1 hr at Hobby Airport
26 Sep 76	1316-1626	Waco-Baytown-Hearne	0		X	X					0.7 hr at Hobby Airport
27 Sep 76	1448-1820	College Station-Galveston-Waco	1	0.6-7.5	X	X					0.5 hr at College Station
29 Sep 76	1227-1730	Waco-Texas City-Waco	3	3.5-4.7 3.0-4.5 2.4-4.5	X	X					1.5 hr at Hobby Airport
30 Sep 76	1337-1800	Waco-Texas City-Waco	1	4-6.5	X	X					1.2 hr at Hobby Airport
5 Nov 76	1053-1554	Waco-Galveston-Waco	2	1.7-5.5 1.5-5.5	X	X					1.3 hr at Hobby Airport
8 Nov 76	1635-1715	Spiral over Waco	1	0.6-12	X	X					
1 Dec 76	1322-1514	Waco-Navasota-Waco	0		X	X					
17 Dec 76	1035-1600	Waco-Galveston-Waco	0		X	X					1.6 hr at Lakeside
15 Feb 77	1620-2316	Waco-Houston-Waco	0		X	X					Some temperatures missing 4.1 hr at Hobby Airport
17 Jun 77	1640-	Spiral at Waco	1	0.6-10.5		X					
21 Jun 77	1442-1559	Waco-College Station-Waco	0		X	X					
22 Jun 77	1152-1528	Waco-Alvin-Conroe-Waco	2	3.0-4.0 3.5-6.5	X	X					0.5 hr at College Station
27 Jun 77	1315-1442	Waco-Houston	0		X	X					
28 Jun 77	1153-1531	Waco-Freeport	1	3.5-7.0	X	X					1.2 hr at Hobby Airport
29 Jun 77	1018-1639	Waco-Austin-Freeport-Houston-Waco	1	1-10	X	X					1.5 hr at Austin, 1 hr at Hobby Airport
1 Jul 77	1141-1711	Waco-Freeport-Houston-Waco	3	3.5-8.0 2.7-10.0 1.5-2.5	X	X					1 hr at Hobby Airport
4 Jul 77	2232-2319	Spiral at Waco	1	0.6-10.0	X	X					
5 Jul 77	1623-1708	Spiral at Waco	1	0.6-10.0	X	X					
6 Jul 77	1145-1605	Waco-Angleton-Waco	1	3.5-5.0	X	X				X	1 hr at Hobby Airport
7 Jul 77	1125-1605	Waco-Texas City-Waco	1	3.5-5.5	X	X					1 hr at Hobby Airport
11 Jul 77	1020-1503	Waco-San Antonio-Waco	0		X	X					0.5 hr at Austin, 1 hr at San Antonio, 0.6 hr at Temple

TABLE 5 (continued)

Date	Time (Local)	Flight Path	No. of Vertical Profiles	Profile Heights (kft msl)*	Parameters					Digitized	Remarks
					Temp.	O_3	NO	NO_x	b_{scat}		
13 Jul 77	1227-1737	Waco-Texas City-Waco	3	3.5-8.0 3.5-6.5 2.0-8.0	X	X				X	1.1 hr at Hobby Airport
14 Jul 77	1028-1534	Waco-Houston-Waco	1	2.5-8.0	X	X				X	0.9 hr at Hobby Airport
15 Jul 77	1034-1510	Waco-Baytown-Waco	2	2.7-6.5 4.5-6.5	X	X				X	1.3 hr at Hobby Airport
18 Jul 77	1203-1818	Waco-Galveston-Waco	2	2.5-5.5 2.5-5.0	X	X				X	1.4 hr at Hobby Airport 0.4 hr at Brenham
19 Jul 77	1203-1538	Waco-Baytown-Waco	0		X	X				X	
20 Jul 77	1649-1819	Waco-Austin-Waco	0		X	X					0.3 hr at Austin
26 Jul 77	1248-1935	Waco-Alvin-Waco	2	3.5-5.5 2.0-6.5	X	X				X	1.1 hr at Hobby Airport 1.6 hr at Hobby Airport
2 Aug 77	1319-1807	Waco-Galveston-Waco	1	2.0-6.8	X	X	X	X		X	0.6 hr at "Space Land"
4 Aug 77	1341-1607	Waco-Houston-Waco	1	3.5-9.0	X	X	X	X		X	
10 Aug 77	1335-1833	Waco-Texas City-Waco	1	3.5-5.7	X	X	X	X		X	1.1 hr at Hobby Airport
12 Aug 77	0857-1743	Waco-Houston-Waco	1	2.4-4.5	X	X	X	X		X	1.3 hr at Wieser, 4.2 hr at Hobby Airport
16 Aug 77	1108-1814	Waco-Baytown-Conroe-Columbus-Wharton-Liberty-Waco	3	3.5-6.5 3.0-6.5 1.5-7.5	X	X	X	X		X	1.3 hr at Hobby Airport 0.7 hr at Conroe
17 Aug 77	1113-1500	Waco-Temple-Waco	1	3.0-14.4	X	X	X	X			2.1 hr at Temple
19 Aug 77	1125-1547	Waco-Houston-Waco	1	2.5-5.0	X	X	X	X			1 hr at College Station
22 Aug 77	0954-1555	Waco-Baytown-Waco	1	2.8-4.5	X	X	X	X			2.8 hr at Hobby Airport
24 Aug 77	1104-1648	Waco-LaPorte-Waco	1	3.0-5.0	X	X	X	X			1.2 hr at LaPorte, 0.3 hr at Hearne
26 Aug 77	1225-1842	Waco-Baytown-Waco	0		X	X	X	X			1 hr at Sugarland, 1.1 hr at Conroe
30 Aug 77	1116-1310	Waco-Temple-Waco	2	0.6-7.0 1.0-10.0	X	X	X	X			Many missing NO/NO_x data 0.8 hr at Temple
20 Sep 77	1229-1857	Waco-Austin-Columbus-Waco	0		X	X					2.4 hr at Temple, 1 hr at Austin, 0.8 hr at College Station
21 Sep 77	1142-1714	Waco-Texas City-Waco	3	2.0-6.5 3.0-6.5 3.0-6.5	X	X				X	1.4 hr at Hooks
22 Sep 77	1041-1646	Waco-Galveston-Waco	1	2.5-5.0	X	X				X	1.3 hr at Galveston
3 Oct 77	0954-1514	Waco-Austin-Waco	0		X	X			X		4.2 hr at Austin
4 Oct 77	0832-1729	Waco-Texas City-Waco	6	1.0-4.8 2.5-4.5 2.5-4.5 3.0-4.5 0.6-3.5 2.5-4.5	X	X			X	X	2.2 hr at Austin, 1.4 hr at LaPorte
5 Oct 77	0918-1757	Waco-Baytown-Waco	2	2.0-5.0 2.5-5.0	X	X	X	X	X	X	1.5 hr at Temple, 1.6 hr at LaPorte, 1 hr at LaPorte
6 Oct 77	1135-1751	Waco-Freeport-Waco	0		X	X	X	X	X	X	1.7 hr at Hooks, 0.6 hr at Sugarland
7 Oct 77	1336-1555	Waco-Conroe-Waco	1	2.0-3.5	X	X	X	X	X		

TABLE 5 (concluded)

					Parameters						
Date	Time (Local)	Flight Path	No. of Vertical Profiles	Profile Heights (kft msl)*	Temp.	O_3	NO	NO_x	b_{scat}	Digitized	Remarks
9 Oct 77	1142-1752	Waco-Galveston-Waco	3	2.0-2.5 2.0-2.5 2.0-2.5	X	X	X	X	X		0.8 hr at Hobby Airport, 0.7 hr at LaPorte
11 Oct 77	1405-1532	Temple-Prairie View-Temple	0		X	X	X	X	X		
12 Oct 77	1159-1608	Waco-Alvin-Waco	0		X	X	X	X	X		0.9 hr at Hobby Airport
19 Oct 77	1017-1554	Waco-Alvin-Waco	1	2.0-6.5	X	X	X	X	X	X	1.1 hr at Hobby Airport
20 Oct 77	1056-1811	Waco-Galveston-Freeport-Waco	2	2.5-5.0 2.0-6.0	X	X	X	X	X	X	1.3 hr at Hobby Airport
21 Oct 77	1218-1736	Waco-Alvin-Waco	0		X	X	X	X	X		0.8 hr at Humphrey
26 Oct 77	1058-1642	Waco-Galveston-Waco	0		X	X	X	X	X	X	1 hr at Hobby Airport
27 Oct 77	1146-2007	Waco-Galveston-Waco	3	2.5-5.0 2.5-5.5 2.0-5.0	X	X	X	X	X		2.2 hr at LaPorte, 0.9 hr at Hobby Airport
28 Oct 77	1249-2153	Waco-Houston-Beaumont-Offshore-Baytown-Hooks-Houston-Waco	3	2.0-5.5 2.0-5.5 2.5-5.5	X	X	X	X	X	X	1.3 hr at Hobby Airport, 1.6 hr at Hooks
29 Oct 77	1209-2313	Waco-Offshore-Waco	11	3.0-7.7 2.5-5.5 3.5-6.0 3.5-7.0 3.5-6.5 2.0-7.0 2.0-7.0 2.5-7.0 3.5-7.0 2.5-7.0 2.5-7.0	X	X			X	X	0.8 hr at Lakeside
30 Oct 77	1211-1529	Waco-Baytown-Waco	2	2.0-7.0 2.5-3.5	X	X			X		
2 Nov 77	0836-1438	Waco-Alvin-Waco	1	2.5-10.0	X	X			X		1.4 hr at Hobby Airport
4 Nov 77	0949-1821	Waco-Galveston-Waco	2	2.0-5.5 2.0-5.5	X	X			X		1.1 hr at Hobby Airport 1.0 hr at Lakeside
22 Nov 77	1156-1419	Waco-Austin-Waco	0		X	X			X		1.2 hr at Austin

*Altitudes are given in thousands of feet (kft) above mean sea level (msl).

information about which airports were visited and times spent on the ground. The flight path description in the table is very general; the flights frequently included points not on a direct route between the points listed. The number of vertical profiles flown is shown, along with the upper and lower bounds on those profiles.

Vertical profiles are defined as those cases where the aircraft spiraled while changing altitude (rather than the gradual altitude changes that sometimes occurred over long horizontal distances during takeoff, landing, or other parts of the flight). The data have been digitized from some of the flights where ozone concentrations in excess of 150 ppb were observed (Ludwig, Martinez, and Nitz, 1979) and that fact is also indicated in Table 5. Table 5 shows that only temperature and ozone concentrations were measured during the early flights. Later, beginning August 1977, NO and NO_x were also measured; nephelometer measurements of total backscatter (b_{scat}) began in October, 1977.

Relative Strengths and Weaknesses of the Two Data Bases

In the context of this report, strengths and weaknesses of the two data bases are defined in terms of their usefulness for model applications and testing. Inasmuch as this was one of the objectives of the data collection program undertaken for HOMS, it is not surprising that that data base is more suitable in many respects for modeling purposes than are the data from HAOS. Nevertheless, there are two very important areas in which the HAOS data are superior. Of greatest importance is the time span over which the HAOS was conducted; most of the stations were operated for four or five months during the summer and early fall, as opposed to approximately one month for HOMS. Thus, HAOS provides a potentially wider variety of conditions.

The second area in which the HAOS data have advantages over the HOMS data is the spatial coverage. However, there are offsetting weaknesses associated with this. The HAOS data were collected over a much larger geographical region, as can be seen by comparing Figures 1 and 3; the HAOS studies provided more measurements to the south and southeast of Houston. Although this is not essential to the modeling of conditions within the smaller rectangular area, it is quite useful for providing a measure of "background" conditions, uninfluenced by emissions in Galveston or other coastal regions when the winds are from the south or southeast. Inasmuch as the total numbers of stations operated during the two programs were approximately equal, the greater geographical spead of the HAOS stations requires a corresponding decrease in station density within the modeled area. Thus, the HAOS data could not be used to describe the distribution of materials within the modeled area with as much detail as could the HOMS.

It is not surprising that the HOMS aircraft data are superior to those from HAOS for modeling uses. The HOMS aircraft data were collected for modeling purposes, while the HAOS data were to be used to examine influxes of ozone from aloft. The aircraft data from HOMS can be used to derive three-dimensional distributions of materials within the mixed layer over the modeled area. As a general rule, the HAOS aircraft data were collected above the mixed layer and frequently beyond the region of greatest interest for modeling the effects of Houston area emissions.

There were also some differences in the character, quality, and usefulness of air-quality data, especially the detailed hydrocarbon analysis between the HAOS and HOMS. The significance of these differences is addressed in a later section.

SUPPLEMENTAL DATA NEEDED FOR MODELING

Because the HOMS was undertaken specifically to provide information useful to modelers, there are not many instances where one can suggest that more data should have been collected or that the operation should have been conducted differently. Nevertheless, there are a few, and it is instructive to examine these so that when similar studies are undertaken in the future, such considerations can be incorporated into their design.

The station locations shown in Figure 1 can be seen to be distributed reasonably well through the modeling area. However, it is apparent that the corners of the rectangle are not as well covered as the interior regions. The southwest and northwest corners are without monitors and the region between Site 12 (just outside the eastern boundary of the rectangle) and the north-south line of monitors (from Site 17 to Site 11) has no monitoring sites.

With the exception of the corners, the modeling region is well covered with regard to ozone, but the situation is not as good for other major constituents. If we imagine the modeling region to be divided by a diagonal from northwest to southeast, we discover that there are only two stations monitoring NMHC in the southwestern part of the region. Those two sites (8 and 17) are very close together, so that most of the southwest half of the region cannot be characterized with regard to this important constituent. This same part of the modeling region is better characterized for NO_x than for NMHC, but there still are important gaps. Although there are five stations monitoring NO_x in the southwest half of the rectangle, they are not spread uniformly through the area. Three sites are clustered (8, 17, and 19) and the other two NO_x sites in the southwest half of the rectangle (15 and 21) are also very close together. Only one site (17) in the southwest half of the rectangle made detailed hydrocarbon analyses.

Obviously, a more uniform distribution of sites, monitoring all the important constituents, would be desirable. To a limited extent, aircraft measurements could be used to supplement the ground-monitoring network and provide measurements for areas where ozone, NO_x, or HC were not measured at the surface network, but this is effective only during periods of good mixing. Good mixing ensures sufficient uniformity in the vertical distribution of concentrations that the measurements made aloft will be characteristic of conditions at lower altitudes. When mixing is good, fewer vertical profiles are required, because measurements made at almost any level within the mixing layer will do a reasonably good job of characterizing conditions throughout the depth of that layer. It is obvious from Table 2 that this fact was recognized in the design of the HOMS aircraft monitoring program. In almost all instances, more vertical profiles were taken with the aircraft in the morning, when mixing was restricted, than in the afternoon, when it was less likely to be so. However, it is also evident from Table 2 that conditions at the boundaries of the modeled area were not always well described by the flight paths that were taken.

Future programs of this type could be improved by using flight paths that provide data describing the boundary conditions for the area of interest. If attention were focused on the smaller modeling area, then it might be possible to circumnavigate the perimeter of the area at more than one altitude and perhaps traverse the area once or twice. Flight paths such as those just described, plus a limited number of vertical profiles, especially upwind and downwind, would be very useful for providing the necesssary three-dimensional descriptions of conditions throughout the modeling volume and time span.

SECTION 4

ANALYSIS OF AEROMETRIC DATA

The sections that follow describe various analyses of air quality and meteorological data collected during the HOMS. In particular, the following topics are considered:

- Patterns of O_3, PAN, and NO_2 concentrations
- Atmospheric hydrocarbons
- 0600-0900 (CDT) NMHC and NO_x
- Spatial patterns of NMHC, NO_x, and O_3
- Case studies of potential modeling days.

ANALYSIS OF OZONE, PAN, AND NO_2 DATA

To set the stage for the discussions that follow, we will examine from a historical perspective the ozone conditions that prevailed during the HOMS. In particular, the HOMS conditions will be compared with those existing in 1977, which was a meteorologically typical year (Ludwig and Martinez, 1979). Ozone concentrations during 15 September to 12 October 1978 were generally higher than in the comparable period in 1977. Table 6 compares the number of sites in 1977 and 1978 when hourly O_3 exceeded 120 ppb, which is the ambient air-quality standard. The table also lists the daily maximum ozone and the monitoring station where it was recorded. The ozone standard was exceeded on 7 days in 1977 and on 13 days in 1978. Moreover, only three days in 1978 had ozone maxima below 80 ppb, whereas this was the case on 16 days in 1977. The highest concentration recorded during this period in 1978 was 310 ppb, which occurred at the Hornwood site on 1 October. For comparison, the highest ozone level reported in the Houston area during all of 1977 was 309 ppb, which occurred at the Crawford site on 8 June. The highest ozone ever measured in the region was 321 ppb, recorded at Aldine on 13 June 1975. Thus, the interval 15 September to 12 October 1978 clearly encompasses a period of intense photochemical activity and contains one of the highest ozone concentrations ever recorded in the area. This is especially fortunate for modeling applications that focus on worst-case conditions.

Table 6 shows that an ozone episode occurred during 1 to 6 October 1978. The episode covered a large area on 1, 2, 4, and 5 October, with between five and nine stations recording O_3 levels over 120 ppb. This episode is of particular interest for modeling applications, and will be the subject of a case study presented in a subsequent section.

TABLE 6. OZONE MAXIMA IN THE HOUSTON AREA

Date	Number of Sites with $O_3 > 120$ ppb		Daily Maximum O_3 (ppb)		Location of Maximum O_3	
	1977	1978	1977	1978	1977	1978
15 Sep	1	0	175	60	Jackrabbit	Aldine
16 Sep	0	0	114	90	Jackrabbit	Aldine
17 Sep	0	0	57	70	Jackrabbit	Aldine
18 Sep	0	0	40	80	Aldine	Aldine
19 Sep	0	0	37	110	Parkhurst, Jackrabbit, Beasley	Aldine
20 Sep	0	0	111	120	Southwest	Aldine
21 Sep	6	0	255	117	Parkhurst	Jackrabbit
22 Sep	5	0	224	119	Jackrabbit	Pearland
23 Sep	0	1	66	135	Southwest	Beasley
24 Sep	0	1	44	123	Parkhurst	Pearland
25 Sep	0	3	36	164	Parkhurst, Aldine	Pearland
26 Sep	0	4	37	182	Parkhurst, Aldine	Pearland
27 Sep	0	0	54	106	Parkhurst	Pearland
28 Sep	0	0	64	88	Parkhurst	Beasley
29 Sep	0	1	60	141	Parkhurst	Pearland
30 Sep	0	0	42	105	Jackrabbit	Darlinghurst
1 Oct	0	9	33	310	Crawford	Hornwood
2 Oct	0	5	34	210	Clinton	Aldine
3 Oct	0	1	51	128	Jackrabbit	Jackrabbit
4 Oct	4	6	137	150	Westhollow	Hornwood, Aldine
5 Oct	4	6	223	190	Jackrabbit	Crawford
6 Oct	2	0	173	101	Beasley	Jackrabbit
7 Oct	0	1	66	163	Parkhurst	Darlinghurst
8 Oct	1	0	169	94	Clinton	Sheldon
9 Oct	0	0	111	120	Beasley	Aldine
10 Oct	0	2	86	150	Clinton	Aldine
11 Oct	0	1	116	133	Parkhurst	Sheldon
12 Oct	0	0	51	120	Parkhurst	Aldine

In the discussions that follow, frequency distributions of ozone, nitrogen dioxide, and peroxyacetylnitrate (PAN) are presented. The frequency distributions were calculated using the hourly averaged concentrations including nighttime observations, measured at each fixed monitoring location. Concentrations measured by mobile monitors were not included. On occasion, two monitoring instruments using different measurement methods were used to measure the same pollutant at the same location. For these cases, the concentrations measured by the instrument most commonly used throughout the monitoring network were used in calculating the frequency distributions.

Ozone

Ozone was measured at 23 of the 24 stations used in the HOMS. Mobile monitors were used at 6 of the 23 sites for periods ranging from 3 to 7 days; data from the mobile monitors are not included in the frequency distributions. The frequency distributions for the remaining 17 sites are presented in Figure 4. The order of the frequency distributions is from high to low mean ozone concentrations.

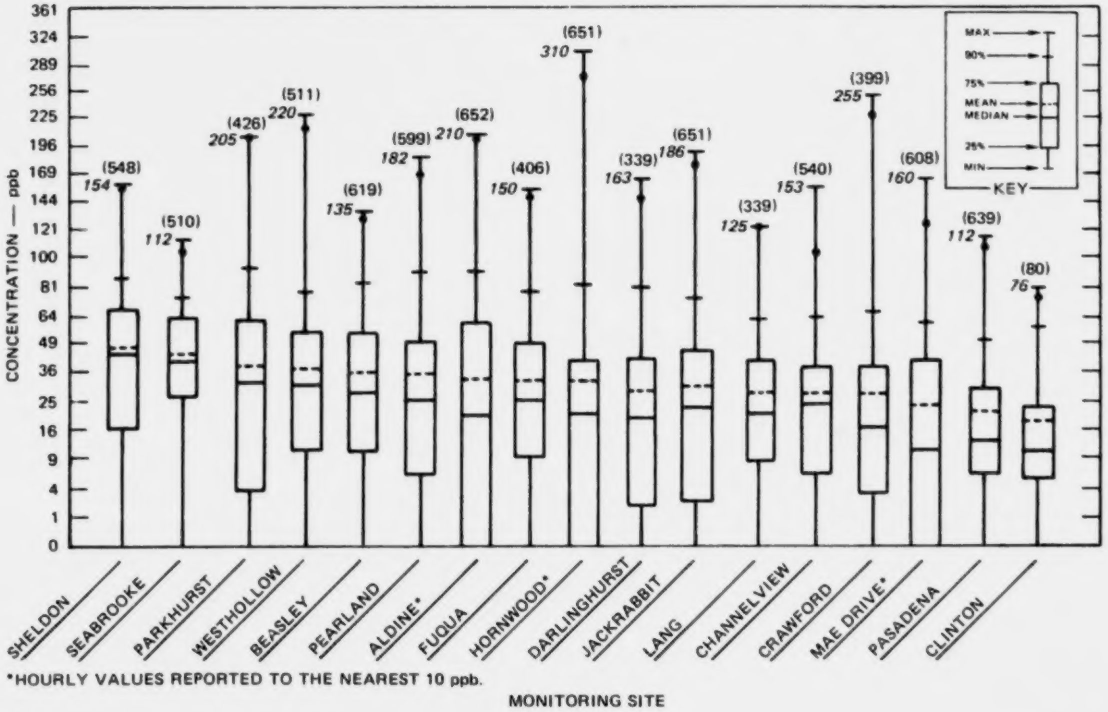

Figure 4. Ozone frequency distributions for the HOMS data base.

Values in parentheses indicate number of observations; values in italics indicate peak concentrations and the symbol • indicates second highest concentrations.

Examination of the spatial distribution of the mean ozone concentrations shows that the monitoring locations with the three lowest mean concentrations were located within and just east of the city limits of Houston: Mae Drive, Pasadena, and Clinton (Figure 5). The remaining mean concentrations show no apparent pattern except that along any radial, the mean concentrations increase with increasing distance from Houston. If the highest ozone concentrations monitored at each site during HOMS are examined (Figure 6), it is found that the three highest peaks occur at Crawford in downtown Houston, and west of downtown at Hornwood and Westhollow. The second three highest ozone concentrations were observed northwest of Houston (Aldine, Parkhurst, and Jackrabbit) and the three lowest peaks were observed southeast of the downtown area at Clinton, Pasadena, and Seabrooke. An examination of the surface wind directions at Pearland and Sheldon showed that the prevailing surface wind directions during HOMS were from the east through south. Thus, the locations

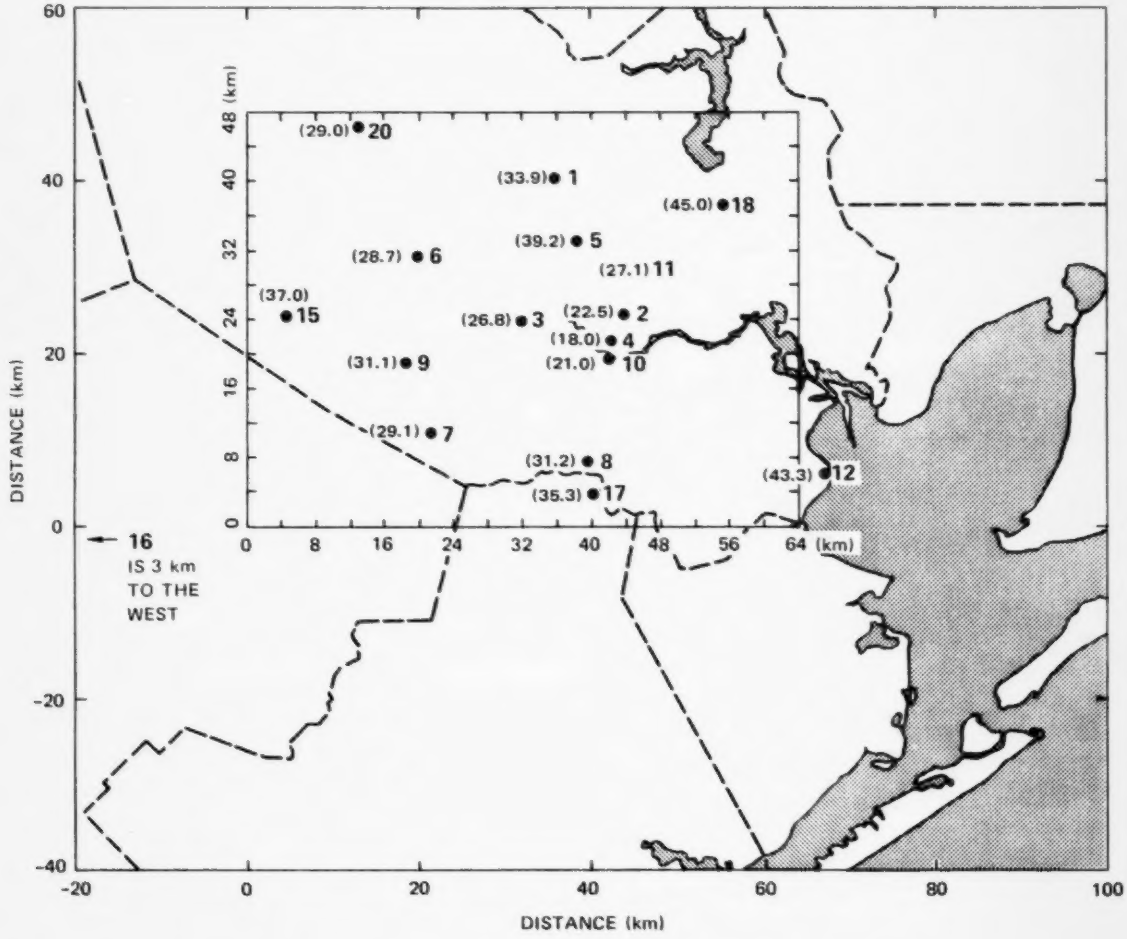

Figure 5. Mean hourly ozone concentrations (ppb) during the HOMS monitoring period. Site numbers are keyed to Table 1.

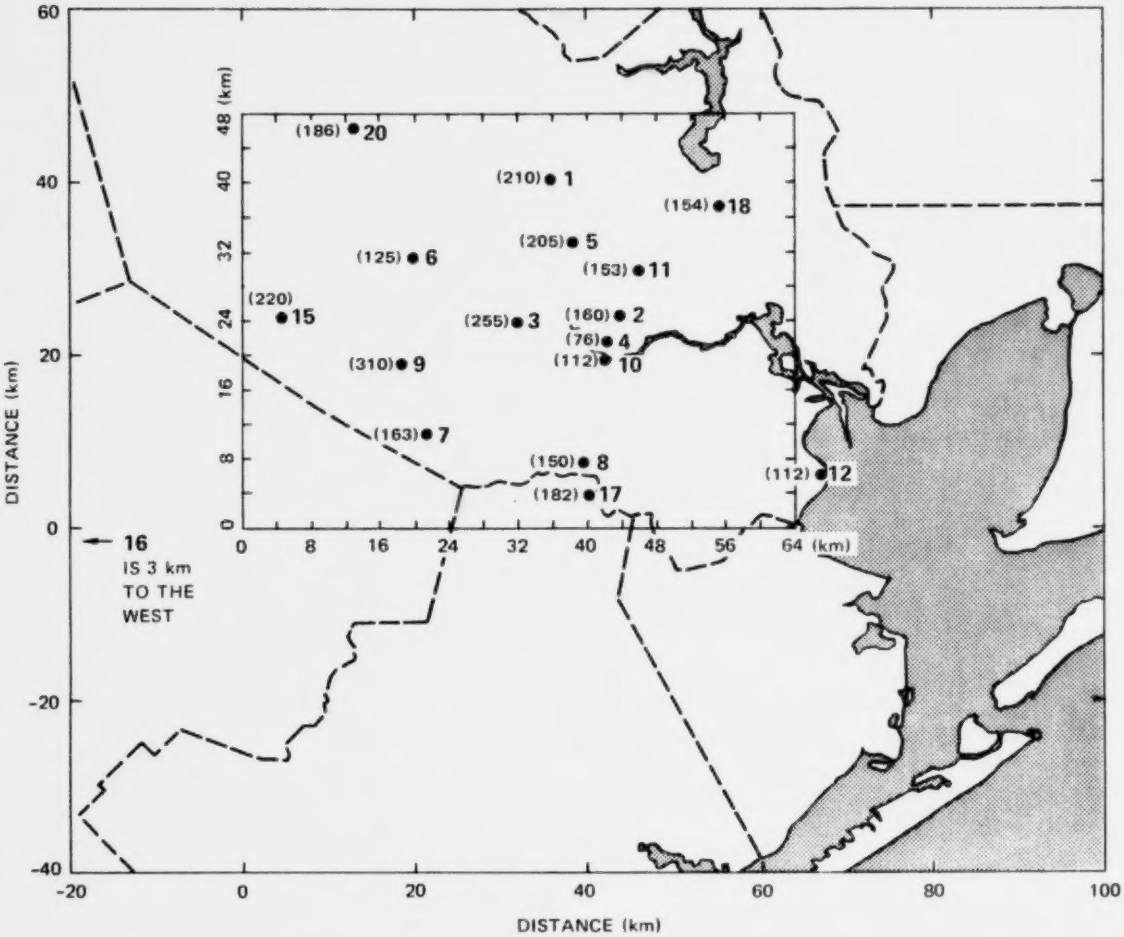

Figure 6. Peak hourly ozone concentrations (ppb) during the HOMS monitoring period. Site numbers are keyed to Table 1.

of the low mean, low peak, and high peak ozone concentrations indicate that local transport of ozone in the region was significant during HOMS. Analyses of local transport for individual days are presented later in this report.

The National Ambient Air Quality Standard (NAAQS) for ozone is 120 ppb for an hourly average. The frequency distributions suggest that 11 of the monitoring sites could be violating the standard since both their highest and second highest concentrations exceed 120 ppb. After examining the daily ozone records of these 11 sites, we found 9 to be in violation of the ozone NAAQS. The remaining two sites, Lang and Beasley, recorded their highest and second highest peaks on the same day, and neither site recorded ozone concentrations on other days in excess of 120 ppb. Thus, both Lang and Beasley might be in compliance with the NAAQS ozone standard, but this conclusion is based only on the short reporting period of HOMS.

Nitrogen Dioxide NO_2

During the HOMS, 17 of the 24 monitoring locations monitored NO_2. Six of these 17 sites monitored NO_2 with mobile monitors for periods ranging from 3 to 7 days total and are not included in the frequency distributions. The frequency distributions for the remaining 11 sites are given in Figure 7. As with the ozone data, the frequency distributions of the monitoring sites are ranked in descending order of their mean hourly NO_2 concentrations.

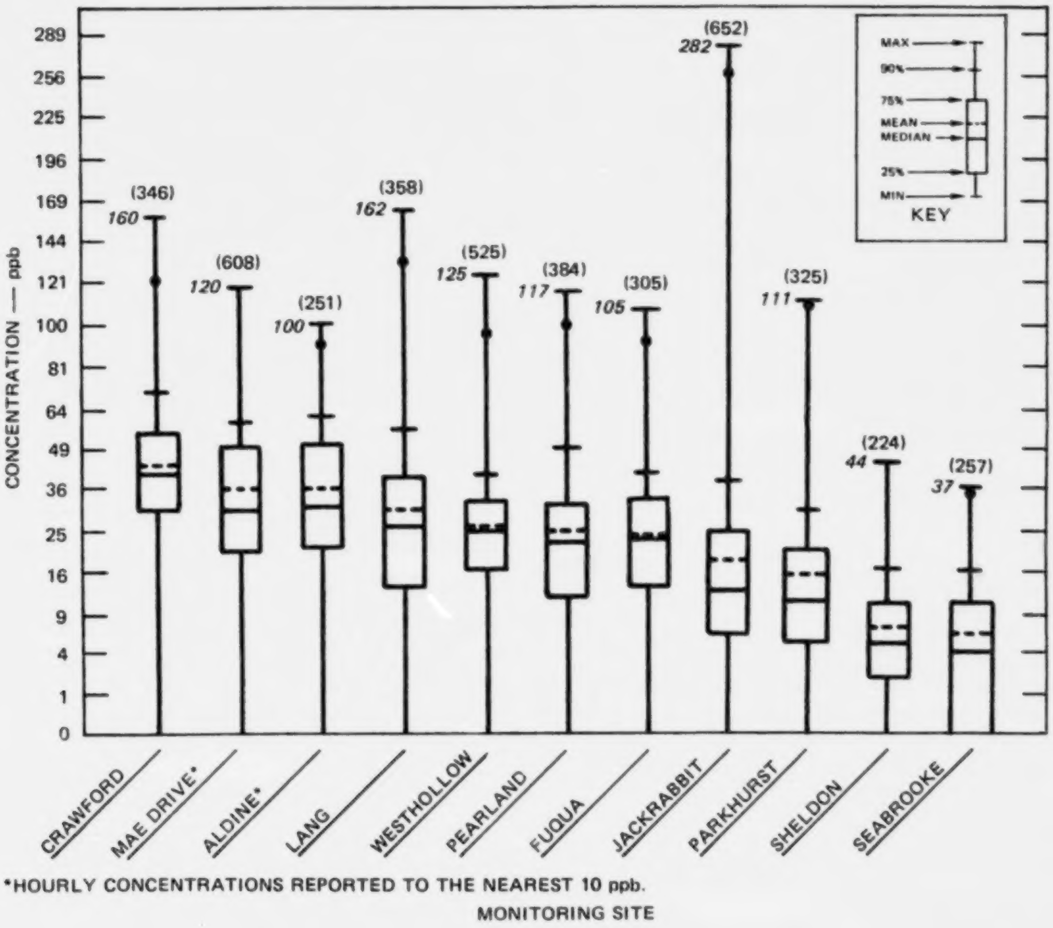

Figure 7. Nitrogen dioxide frequency distributions for the HOMS data base

Values in parentheses indicate number of observations; values in italics indicate peak concentrations and the symbol ● indicates second highest concentrations.

No apparent pattern was discerned from the spatial distribution of the mean hourly NO_2 concentrations (Figure 8). However, as with the ozone mean hourly concentrations, the lowest mean hourly NO_2 concentrations are east of Houston. Sheldon is northeast of Houston and had a mean NO_2 concentration of 6.9 ppb, while Seabrooke is southeast of Houston and had a mean of 5.9 ppb. These concentrations are less than half the next lowest mean hourly NO_2 concentration. However, both sites had a relatively low number of data points compared to most of the other sites.

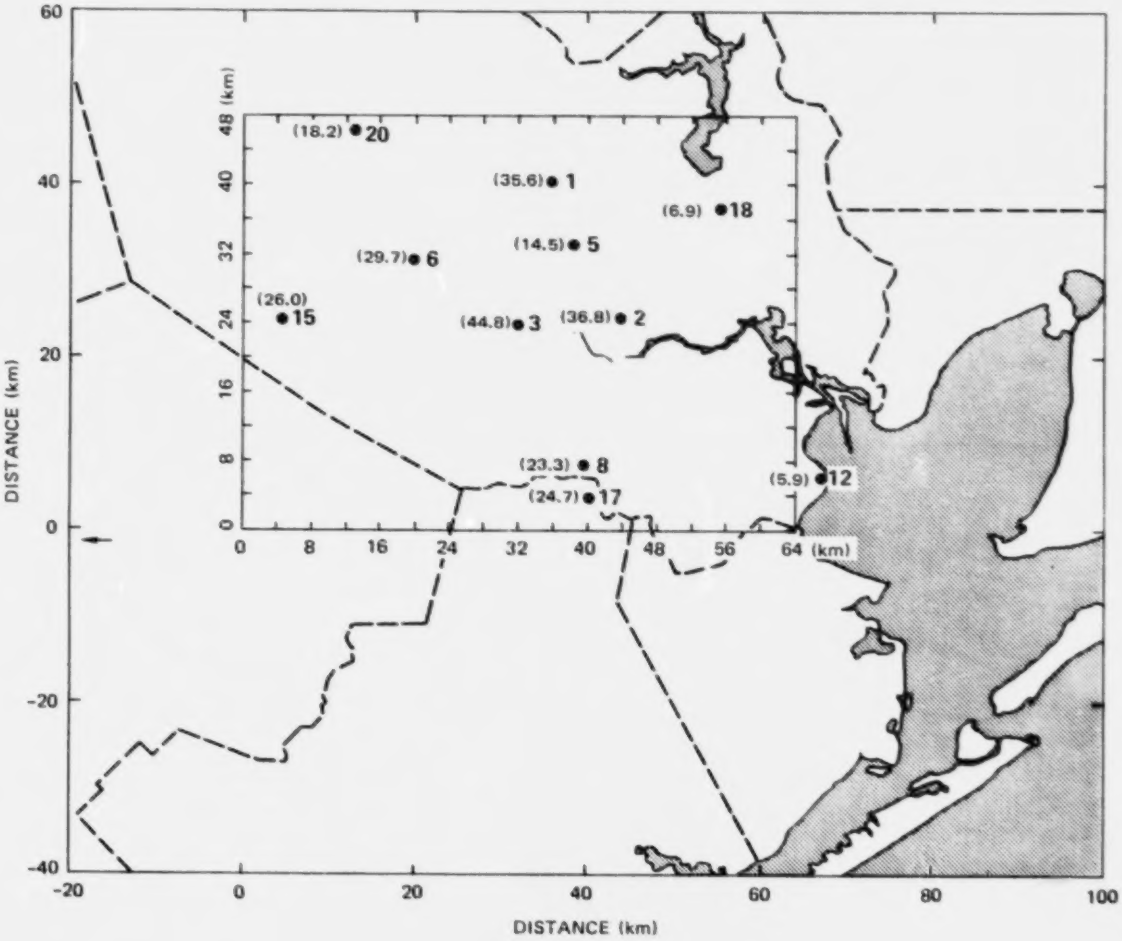

Figure 8. Mean hourly NO_2 concentrations (ppb) during the HOMS monitoring period. Site numbers are keyed to Table 1.

Figure 9 shows the spatial distribution of the peak hourly NO_2 concentrations. Again, the lowest peaks are east of Houston at Sheldon and Seabrooke. The highest peaks are at Crawford, which is downtown, and west and northwest of downtown at Jackrabbit, Lang, and Westhollow.

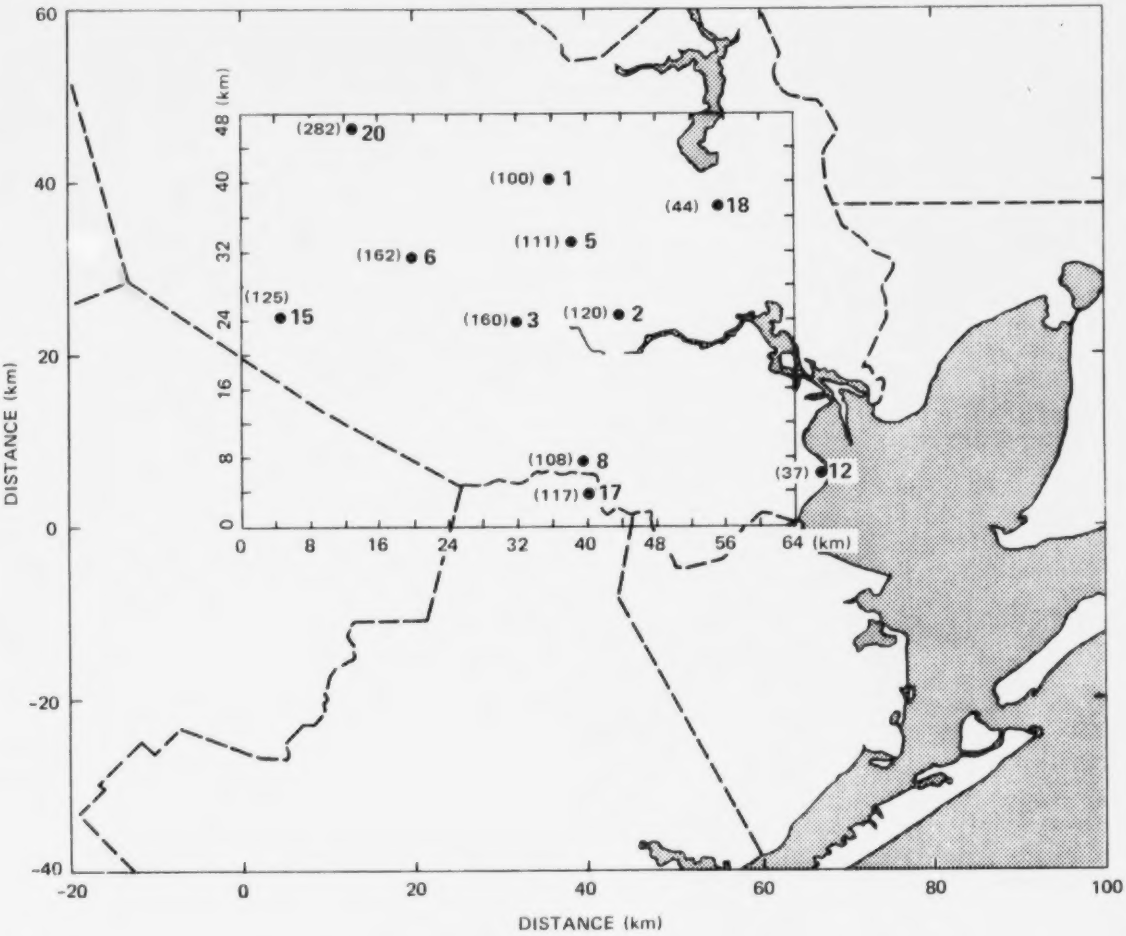

Figure 9. Peak hourly NO_2 concentrations (ppb) during the HOMS monitoring period. Site numbers are keyed to Table 1.

The NAAQS for NO_2 is 50 ppb for annual average concentrations. No violation is expected, but this expectation is based solely on the HOMS data. However, higher NO_2 concentrations are more common during winter months than during the late summer and early fall.

Peroxyacetylnitrate (PAN)

PAN concentrations were monitored at two sites, Sheldon and Jackrabbit. The frequency distributions of PAN at the two sites are presented in Figure 10. The mean concentrations are 0.79 ppb at Sheldon and 0.75 ppb at Jackrabbit. The frequency distribution at Jackrabbit is skewed toward zero because many values (49 percent) were reported to be below detectable limits and were assumed to be zero. At Sheldon, no values below detectable limits were reported. In fact, the lowest PAN concentration reported at Sheldon was 0.2 ppb.

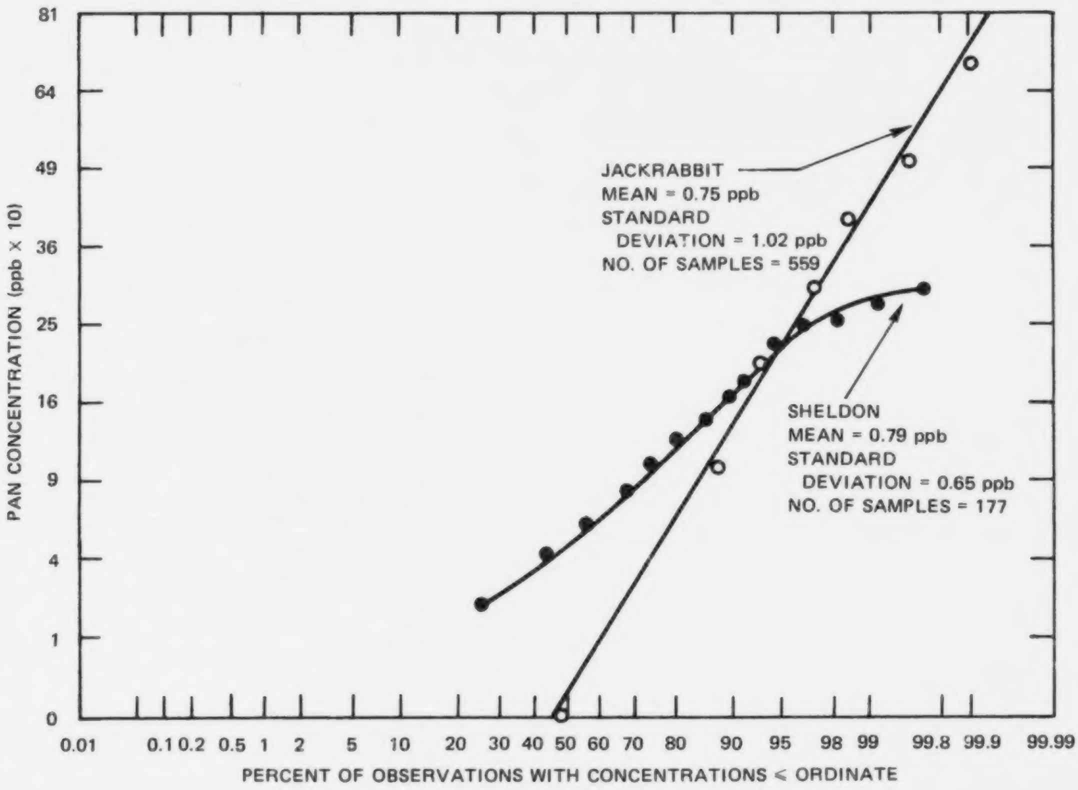

Figure 10. PAN frequency distributions for the HOMS data base.

In 1977, as part of the HAOS program, PAN data were collected at Fuqua, Crawford, Aldine, and Westhollow (Ludwig and Martinez, 1979). At Fuqua, Crawford, and Aldine, instantaneous measurements were taken every half hour from June through October. At Westhollow, hourly averaged concentrations were measured during September. The maximum observed PAN concentrations at Fuqua, Crawford, and Aldine were approximately 12.5 ppb, 10.5 ppb, and 15.5 ppb, respectively. These peaks were observed during September and October. At Westhollow, the maximum value was 9 ppb. In addition, at Westhollow, 86 percent of the observations were below the detection limit, while at Fuqua, Crawford, and Aldine 81 to 86 percent of the observations taken during September were below detectable limits. Ludwig and Martinez (1979) reported that the PAN concentrations observed during HAOS were significantly lower than values previously observed in Los Angeles, St. Louis, and Hoboken, New Jersey.

The frequency distributions of PAN data collected during HOMS are similar to those of the HAOS data, particularly at Jackrabbit. The peak PAN concentrations observed during HOMS (3.0 ppb and 7.0 ppb at Sheldon and Jackrabbit, respectively) are lower than the maxima observed during HAOS. However, the Jackrabbit peak is similar to the Westhollow peak observed during HAOS, and a large percentage of the Jackrabbit data were below detectable limits. The PAN data collected during HOMS substantiates the relatively low PAN concentrations observed during HAOS when compared with data collected in Los Angeles, St. Louis, and Hoboken, New Jersey.

ATMOSPHERIC HYDROCARBONS

Ground-Level Hydrocarbons and Their Sources

The hydrocarbon sampling program conducted during the HOMS was introduced in Section 2. In this section we investigate the patterns of hydrocarbon concentrations for the interval 0600-0900 (CDT), which is the prime period for the emission of ozone-precursor hydrocarbons and other pollutants. The analysis will focus on a group of individual hydrocarbons and includes efforts to identify their sources.

Site Classifications and Nonmethane Hydrocarbons

Table 7 classifies the sampling sites used in the HOMS. It is apparent that the monitoring locations cover a variety of environments in the Houston area. The Pasadena site is located in the neighborhood of the heavily industrialized ship channel. Mae Drive is about 4 km north of Pasadena and is influenced by both traffic and industrial sources. The Crawford station is in downtown Houston and should be strongly influenced by mobile sources, as is the Washburn Tunnel. The suburban stations are located on the periphery of the city and are susceptible to the influence of both traffic and stationary sources. Sheldon was the only rural site monitored; it is located in a state park about 25 km northeast of downtown Houston.

Figure 11 displays the daily fluctuations of nonmethane hydrocarbons (NMHC) at Crawford, Mae Drive, Parkhurst and Clinton; the plots were previously produced for the HAOS data analysis (Ludwig and Martinez, 1979). The graphs show that Crawford, Mae Drive, and Parkhurst are influenced by mobile sources, as evidenced by the distinctive peak in NMHC that is associated with the morning traffic rush.

Even though detailed laboratory analyses of hydrocarbons were not made at Clinton for the HOMS, we have included this site in Figure 11 because it can be considered as a surrogate for Pasadena. As shown in Figure 1, the Clinton and Pasadena sites are very close; thus, we expect Pasadena to display NMHC variations similar to Clinton's. Figure 11 shows that the NMHC fluctuations for Clinton differ significantly from the other three. It is evident that any

TABLE 7. CLASSIFICATION OF HYDROCARBON MONITORING STATIONS IN THE HOMS

Site Name	Site Type
Crawford	Urban
Washburn Tunnel	Urban
Pasadena	Industrial
Mae Drive	Suburban/Industrial
Parkhurst	Suburban
Lang	Suburban
Westhollow	Suburban
Seabrooke	Suburban (Coastal)
Jackrabbit	Suburban
Pearland	Suburban
Sheldon	Rural

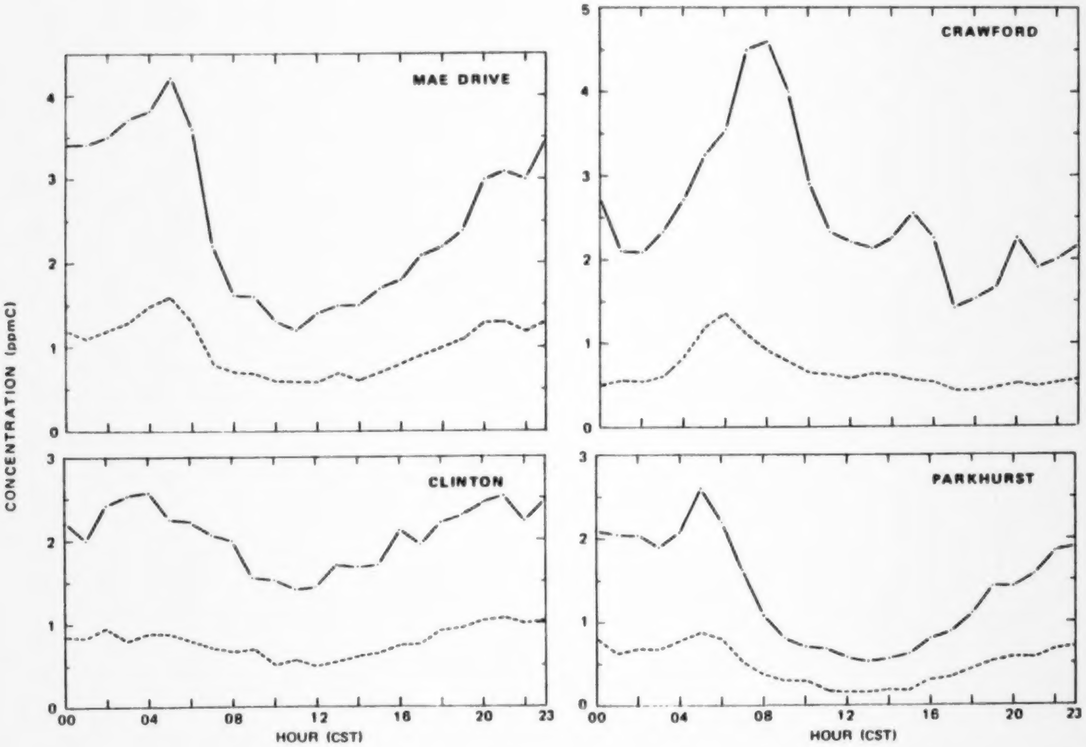

Figure 11. Average diurnal variation in NMHC concentrations at selected sites in the Houston area, May-October 1977.

Top curve (—) is the mean of the top 25% and the lower curve (- - -) is the midmean of the concentration distribution for each hour. Midmean is the average of values between 25th and 75th percentiles. (Adapted from Ludwig and Martinez, 1979.)

mobile source effects at Clinton are masked by the impact of other sources. The lack of a pronounced morning peak at Clinton and the relatively small hourly variations reflect the presence of steady sources of hydrocarbons, which is to be expected for a site located in the industrial ship channel area. We will examine later the composition of the hydrocarbon mixture at the various sites to identify compositional differences between industrial locations and sites where other sources predominate.

The laboratory analysis of the Pearland and Sheldon samples was performed by WSU, and the EPA analyzed the samples for the other nine locations. The EPA analyses identified 64 compounds, listed in Table 8, whereas WSU

TABLE 8. HYDROCARBON COMPOUNDS IDENTIFIED BY THE U.S. ENVIRONMENTAL PROTECTION AGENCY

Ethane
Ethylene
Propane
Acetylene
Isobutane
n-Butane
Propylene
Isopentane
n-Pentane
Isobutylene
t-Butene-2
c-But-2 + Butadiene
Pentene
2-Methylbutene-1
t-Pentene-2
c-Pentene-2
2-Methylbutene-2
Acetaldehyde
Cyclopentane
2-Methylpentane
3-Methylpentane
4-Methylpentene-2
n-Hexane
Hexene-1
t-Hexene-3
2,4-Dimethylpentane
Methylcyclopentane
cis-Hexene-2
Propionaldehyde
Acetone
3,3-Dimethylpentane
Cyclohexane
2-Methylhexane
2,3-Dimethylpentane
3-Methylhexane
1-cis-3-Dimethylcyclopentane
2,2,4-Trimethylpentane
1-tris-3-Dimethylcyclopentane
n-Heptane
Methylcyclohexane
Benzene
Trans-Octene-4 + Thiophene
4,4-Dimethylheptane
Toluene
Nonane
Ethylbenzene
p-Xylene
m-Xylene
n-Decane
o-Xylene
n-Propylbenzene + i-Propylbenzene
n-Propylbenzene
m- and p-Ethyltoluene
i-Butylbenzene
1,3,5-Trimethylbenzene
o-Ethyltoluene
sec-Butylbenzene + Undecane
1,2,4-Trimethylbenzene
Isopropyltoluene
1,4-Diethylbenzene
1,2,3-Trimethylbenzene
1,3-Diethylbenzene
1,2-Diethylbenzene
m-Butylbenzene

identified 59 species, shown in Table 9. It is apparent that the two sets of compounds in Tables 8 and 9 are not identical, although they overlap considerably. Thus, it is inappropriate to compare the NMHC concentration, which is the sum of the compounds identified, at the EPA and WSU sites. In what follows we first examine NMHC at the EPA sites and then focus our attention on 11 individual hydrocarbons, which process will allow us to compare all the sites on an equal basis.

TABLE 9. HYDROCARBON COMPOUNDS IDENTIFIED
BY WASHINGTON STATE UNIVERSITY

Ethane
Ethylene
Acetylene
Propane
Propene
i-Butane
n-Butane
I-Butene
i-Butene
t-2-Butene
c-2-Butene
i-Pentane
n-Pentane
I-Pentene
t-2-Pentene
c-2-Pentene
Cyclopentene
Cyclopentane
2,3-Dimethylbutane
2-Methylpentane
c-4-Methyl-2-pentene
3-Metylpentane
1-Hexene
n-Hexane
t-2-Hexene
c-2-Hexene
Methylcyclopentane
2,4-Dimethylpentane
Benzene
Cyclohexane
2,3-Dimethylpentane
3-Methylhexane
2,2,3-Trimethylpentane
n-Heptane
Methylcyclohexane
2,4-Dimethylhexane
2,3,4-Trimethylpentane
Toluene
2,3-Dimethylhexane
2-Metylheptane
3-Ethylhexane
n-Octane
Ethylcyclohexane
Ethylbenzene
p & m-Xylene
Styrene
o-Xylene
n-Nonane
i-Propylbenzene
n-Propylbenzene
p-Ethyltoluene
m-Ethyltoluene
o-Ethyltoluene
1,3,5-Trimethylbenzene
1,2,4-Trimethylbenzene
1,2,3-Trimethylbenzene
Methylstyrene
1,3-Diethylbenzene
1,4-Diethylbenzene

Table 10 shows the mean NMHC measured at the EPA sites during 0600-0900 CDT; the NMHC is the sum of the concentrations of the 64 compounds listed in Table 8. (The Washburn Tunnel is not included in Table 10 because its samples are essentially instantaneous and were not obtained during the 0600-0900 period.)

TABLE 10. 0600-0900 (CDT) NONMETHANE HYDROCARBONS

Site	Mean Concentration ± Standard Deviation (ppbC)	Number of Samples
Crawford	2098 ± 1099	19
Pasadena	896 ± 927	19
Mae Drive	1449 ± 1236	17
Parkhurst	1125 ± 846	17
Lang	1417 ± 824	16
Westhollow	1100 ± 370	11
Seabrooke	452 ± 355	17
Jackrabbit	474 ± 295	23

Apparent differences in mean NMHC levels at the various sites are evident in Table 10. Crawford, in downtown Houston, has the highest concentration, indicative of a high emissions density. As has been shown, Mae Drive and Parkhurst are influenced by traffic during 0600-0900 and show relatively high NMHC. Lang and Westhollow are located in areas of moderate emissions density that are mostly traffic-related at this time of day; their mean NMHC appears to be similar to those at Mae Drive and Parkhurst. The Pasadena site shows mean NMHC that seems to be lower than at the urban and suburban stations. Seabrooke and Jackrabbit are located on the edge of the urban area (see Figure 1), and show the lowest mean NMHC. The density of hydrocarbon sources in the vicinity of these two stations is known to be relatively low (Ludwig and Martinez, 1979).

Table 10 shows that the standard deviations can be rather large compared to the mean, which raises questions about the statistical significance of the apparent differences in mean NMHC between the various sites. To answer this question, we performed a statistical analysis of the NMHC data that included re-expressing the data via a square-root transformation to stabilize the variance, performing an analysis of variance, and testing statistically the differences between the means of pairs of sites as well as between the means of groups of sites. In the statistical tests, differences were deemed to be significant if the significance level was 0.05 or better.

The analysis revealed that the sites cluster into the following three groups:

- Crawford
- Mae Drive, Pasadena, Parkhurst, Lang and Westhollow
- Seabrooke and Jackrabbit.

The mean NMHC at Crawford is significantly different not only from each of the other individual sites, but also from the mean of the two other groups, as tested by the method of linear contrasts (Scheffe, 1959). This suggests that during 0600-0900 the source strength at Crawford is quantitatively different from that prevailing at the other sites.

The stations in the five-site cluster, i.e., Mae Drive, Pasadena, Parkhurst, Lang, and Westhollow, show no statistically significant differences among themselves, which indicates that these sites are located in areas with similar emissions strength. Based on the ratio of the means, the 0600-0900 source strength at these five stations is about 60 percent of that at Crawford. Although Pasadena is expected to be influenced by industrial sources, its NMHC levels do not differ significantly from those at Mae Drive, Parkhurst, Lang, and Westhollow, where mobile sources predominate at this time of day.

Seabrooke and Jackrabbit have statistically indistinguishable mean NMHCs that are substantially lower than at the other six locations. Mean NMHC at each of these two sites differs significantly (in a statistical sense) from the corresponding NMHC at each of the other six sites considered individually. Considered as a group, NMHC at Seabrooke and Jackrabbit also differs significantly from the mean NMHC of the other two groups of sites. This is consistent with the fact that these two stations are located on the fringes of the urban envelope in areas of relatively low source strength. Judging by the ratio of the means, we find the emissions strength at these two locations to be about 20 percent that at Crawford.

Analysis of Selected Hydrocarbons

The previous analysis examined quantitative differences in NMHC levels at eight of the HOMS sites. Below we investigate qualitative as well as quantitative differences at all ten sites by examining individual hydrocarbons. The analysis will consider 11 hydrocarbons: ethane (C_2H_6), propane (C_3H_8), acetylene (C_2H_2), propylene (C_3H_6), isopentane ($i\text{-}C_5H_{12}$), isobutane ($i\text{-}C_4H_{10}$), n-butane ($n\text{-}C_4H_{10}$), benzene, toluene, m+p-xylene, and o-xylene. The principal sources of these compounds are shown in Table 11.

The eleven hydrocarbons selected for study include five alkanes (C_2H_6, C_3H_8, $i\text{-}C_5H_{12}$, $i\text{-}C_4H_{10}$, and $n\text{-}C_4H_{10}$), one alkene (C_3H_6), four aromatics (benzene, toluene, m+p-xylene, and o-xylene) and one alkyne (C_2H_2). Based on the rate of reaction with the hydroxyl radical, C_3H_6 is the most reactive of these compounds, and is known to play an important role in ozone formation. The xylenes are the next most reactive hydrocarbons, followed by toluene, which is about half as reactive as the xylenes. The reactivity of C_3H_8, $i\text{-}C_4H_{10}$, $n\text{-}C_4H_{10}$, and $i\text{-}C_5H_{12}$ is approximately the same, and is between one-third to one-half that of toluene. Benzene, C_2H_6, and C_2H_2 are the least reactive compounds, benzene being somewhat more reactive than the other two. C_2H_2 is considered to be essentially inert over a span of several hours and will be used as a normalizing factor to account for dilution effects.

TABLE 11. PRINCIPAL SOURCES OF SELECTED HYDROCARBONS*

Compound	Source
Ethane	Commercial natural gas
Propane	Liquefied petroleum gas
Acetylene	Automotive exhaust
Propylene	Automotive exhaust
i-Pentane	Gasoline vapor
i-Butane	Gasoline vapor
n-Butane	Gasoline vapor, geogenic natural gas
Benzene	Auto exhaust, solvents, gasoline vapor, petroleum processing
Toluene	Auto exhaust, solvents, gasoline vapor, petroleum processing
m-Xylene	Auto exhaust, solvents, gasoline vapor
p-Xylene	Auto exhaust, gasoline vapor
o-Xylene	Auto exhaust, gasoline vapor

*Mayrsohn and Crabtree, 1976; Graedel, 1978.

Hydrocarbon levels measured during 0600-0900 (CDT) are shown in Table 12, which contains the mean and standard deviation of the concentration of the selected compounds. Using the data in Table 12, we investigated concentration patterns, using statistical procedures similar to those previously employed in connection with NMHC; the results are displayed in Table 13. Table 13 shows that the sites have been divided into clusters for each hydrocarbon. Each cluster is composed of sites with mean concentrations that are statistically indistinguishable from each other (with a significance level of 0.05 or better). Conversely, concentration differences between sites in different clusters are statistically significant. Clusters are labeled 1, 2, 3, 4, with the sites assigned to Cluster 1 having the highest concentration, those in Cluster 2 the next highest, and so on. It is emphasized that the clusters are defined for each individual hydrocarbon and are displayed in the rows of Table 13. Thus, the columns of Table 13 are not to be interpreted as clusters.

Table 13 shows that C_2H_6 and C_3H_8, which are emitted primarily by stationary sources, have a relatively high degree of spatial uniformity. For C_2H_6, the sites form three clusters, with three sites in Cluster 1, six in Cluster 2, and one in Cluster 3. Sheldon, a rural location, has the lowest concentration, and Crawford, Parkhurst, and Pearland the highest levels of C_2H_6. C_3H_8 is more evenly distributed than C_2H_6: it shows only two clusters, and one contains all the sites except Pearland. The spatial uniformity of C_2H_6 and C_3H_8 suggests that they are produced mainly by well-dispersed area-type sources. The high concentrations observed at Pearland indicate that

TABLE 12. 0600-0900 (CDT) HYDROCARBON CONCENTRATIONS IN HOUSTON
(mean ± standard deviation—ppbC)

Hydrocarbon	Crawford	Pasadena	Mae Drive	Parkhurst	Lang	Westhollow	Seabrooke	Jackrabbit	Pearland	Sheldon
C_2H_6	93 ± 59	50 ± 38	66 ± 43	92 ± 85	66 ± 49	54 ± 35	54 ± 37	63 ± 45	138 ± 147	28 ± 17
C_3H_8	74 ± 46	96 ± 142	116 ± 135	78 ± 63	61 ± 40	50 ± 30	52 ± 34	51 ± 33	135 ± 112	56 ± 38
C_2H_2	59 ± 44	16 ± 17	50 ± 89	28 ± 27	41 ± 24	13 ± 6	9 ± 10	12 ± 11	13 ± 9	5 ± 5
C_3H_6	31 ± 23	18 ± 20	23 ± 20	14 ± 13	19 ± 15	6 ± 5	13 ± 21	6 ± 8	45 ± 78	7 ± 7
$i\text{-}C_5H_{12}$	203 ± 141	85 ± 154	183 ± 188	94 ± 96	109 ± 76	46 ± 35	26 ± 18	36 ± 26	110 ± 76	22 ± 22
$i\text{-}C_4H_{10}$	54 ± 33	39 ± 53	79 ± 87	45 ± 40	32 ± 26	20 ± 16	25 ± 19	21 ± 17	102 ± 79	21 ± 20
$n\text{-}C_4H_{10}$	123 ± 66	31 ± 23	83 ± 43	84 ± 82	79 ± 39	44 ± 36	30 ± 20	38 ± 27	105 ± 56	27 ± 23
Benzene	69 ± 48	46 ± 39	41 ± 26	41 ± 33	47 ± 29	18 ± 8	14 ± 14	15 ± 10	19 ± 11	–
Toluene	103 ± 72	27 ± 29	53 ± 41	52 ± 45	63 ± 42	30 ± 18	25 ± 42	21 ± 14	41 ± 20	–
m+p-Xylene	78 ± 59	19 ± 21	36 ± 26	40 ± 38	44 ± 31	18 ± 11	9 ± 7	16 ± 11	31 ± 44	–
o-Xylene	30 ± 20	6 ± 7	12 ± 7	16 ± 15	18 ± 12	6 ± 5	4 ± 3	6 ± 4	14 ± 15	–

TABLE 13. CLUSTERING OF HOUSTON MONITORING SITES ACCORDING
TO HYDROCARBON CONCENTRATIONS*

Hydrocarbon	Crawford	Pasadena	Mae Drive	Parkhurst	Lang	Westhollow	Seabrooke	Jackrabbit	Pearland	Sheldon
C_2H_6	1	2	2	1	2	2	2	2	1	3
C_3H_8	2	2	2	2	2	2	2	2	1	2
C_2H_2	1	2	1	1	1	2	2	2	2	3
C_3H_6	1	1	1	2	1	2	2	2	1	2
$i\text{-}C_5H_{12}$	1	2	1	2	2	3	3	3	2	3
$i\text{-}C_4H_{10}$	2	3	2	2	3	4	4	4	1	4
$n\text{-}C_4H_{10}$	1	2	1	1	1	2	2	2	1	2
Benzene	1	1	1	1	1	2	2	2	2	–
Toluene	1	4	2	2	2	3	4	4	3	–
m+p-Xylene	1	3	2	2	2	3	4	3	2	–
o-Xylene	1	3	2	2	2	3	3	3	2	–

*NOTE: Clusters are defined only for each individual hydrocarbon; sites belonging to the same cluster display identical numbers. Clusters are ranked by concentration: 1 denotes the highest and 4 the lowest.

local sources affect this neighborhood. This result is consistent with the findings of the HAOS (Ludwig and Martinez, 1979), which showed a preponderance of C_2H_6 and C_3H_8 at Fuqua, which is near Pearland (see Figure 1).

C_2H_2, C_3H_6, and the aromatics are linked to mobile sources. However, C_2H_2 is also reputed to be emitted by some industries in Houston. Tables 12 and 13 show that mean C_2H_2 at Pasadena, the industrial site, is significantly lower than at Crawford, Mae Drive, Parkhurst, and Lang. Moreover, for C_2H_2, Pasadena is in the same cluster with four suburban sites that are not expected to be heavily impacted by stationary sources. Consequently, even if all the C_2H_2 at Pasadena were due to industrial sources, the evidence suggests that such sources would not be substantial contributors to the overall C_2H_2 burden during 0600-0900 CDT. Tables 12 and 13 also show that Sheldon has the lowest mean C_2H_2, which is expected for a rural site.

The spatial distribution of C_3H_6 displays two clusters, each with five sites. The cluster with the highest mean concentrations includes Crawford, Pasadena, Mae Drive, Lang, and Pearland. This includes the downtown area (Crawford) as well as industrial locations (Pasadena, Mae Drive). The five sites in the other cluster are located on the fringes of the urban envelope and exhibit lower mean concentrations. The sources of C_3H_6 affecting the various sites will be discussed below when the C_3H_6/C_2H_2 ratio is examined.

Considerable spatial variability is evident in Table 13 for i-C_5H_{12} and i-C_4H_{10}, both of which are linked primarily to gasoline-vapor emissions. The table shows that there are three clusters of sites for i-C_5H_{12} and four for i-C_4H_{10}. Note that the pattern of clusters for i-C_5H_{12} is similar to that for i-C_4H_{10}. Thus, Table 13 shows that except for Pearland and Parkhurst, all the other sites appear in the same clusters for both compounds. This suggests that the two compounds have a common source. Relative to the other sites, Pearland appears to be a "hot spot" for i-C_4H_{10} but not for i-C_5H_{12}.

The spatial variability of n-C_4H_{10} is much less pronounced than for i-C_4H_{10}. This is evident in Table 13, which shows only two clusters for n-C_4H_{10}, but four for i-C_4H_{10}. The relative spatial uniformity of n-C_4H_{10} may be induced by the geogenic natural-gas source. Such a source would be diffuse and continuous, and would produce a relatively smooth background. This could explain the fact that the rural site (Sheldon) is in the same cluster as four nonrural locations. The influence of anthropogenic sources is evident in Cluster 1, which contains those sites that are located in more urban areas; the mean level of n-C_4H_{10} in Cluster 1 is between two and five times higher than in Cluster 2. Although Pearland continues to exhibit high concentrations, this time (in contrast to i-C_4H_{10}), its mean level does not differ significantly from that of four other sites.

The sites also form two clusters in the case of benzene. The two-cluster pattern reflects a sharp variation in spatial concentration. The highest levels occur in the sites located within the urban envelope, which are assigned to Cluster 1. Cluster 2, by contrast, contains all the sites located on the periphery of the urban area, and its mean levels of benzene are at least two times lower than for the sites in Cluster 1.

Toluene and the xylenes exhibit a substantial degree of spatial inhomogeneity. Toluene and m+p-xylene each show four clusters in Table 13, and o-xylene has three. For all three compounds, the Crawford site has mean concentrations that are significantly higher than at any other site. This indicates that mobile sources are major contributors of these aromatics. The lack of uniformity in the spatial distribution suggests that these aromatics are associated with a variety of localized sources. This is consistent with the fact that these compounds are emitted by several different types of sources (see Table 11).

Compositional differences in the hydrocarbon mixture are displayed in Table 14, which shows the mean hydrocarbon/acetylene ratio of each compound at the various sites. There is no statistically significant difference between the mean ratio for C_2H_6 and C_3H_8 at all the sites except Pasadena. Thus, essentially the same proportion of C_2H_6 and C_3H_8, relative to C_2H_2, is present at all but one site. This is consistent with the earlier finding about the relatively high degree of spatial uniformity exhibited by these two compounds.

TABLE 14. 0600-0900 (CDT) RATIOS OF HYDROCARBON/ACETYLENE CONCENTRATIONS (ppbC) IN HOUSTON
(mean ratio ± standard deviation)

Hydrocarbon	Crawford	Pasadena	Mae Drive	Parkhurst	Lang	Westhollow	Seabrooke	Jackrabbit	Pearland	Sheldon
C_2H_6	1.8 ± 1.1	3.6 ± 1.7	3.0 ± 1.9	4.2 ± 2.3	1.9 ± 1.1	4.2 ± 1.7	10.7 ± 7.2	7.1 ± 4.8	13.1 ± 14.6	7.6 ± 4.8
C_3H_8	1.5 ± 0.87	5.8 ± 3.9	5.6 ± 7.2	3.8 ± 2.1	1.9 ± 1.1	4.1 ± 1.7	10.3 ± 7.0	5.9 ± 3.6	12.7 ± 11.0	20.5 ± 31.4
C_3H_6	0.51 ± 0.097	1.4 ± 1.5	1.1 ± 1.1	0.48 ± 0.25	0.48 ± 0.20	0.41 ± 0.25	1.7 ± 1.6	0.48 ± 0.32	4.3 ± 4.4	1.3 ± 0.98
i-C_5H_{12}	3.8 ± 1.1	5.6 ± 5.7	9.6 ± 14.1	3.6 ± 1.5	3.0 ± 1.4	3.5 ± 1.6	4.8 ± 3.2	3.5 ± 1.7	9.8 ± 4.4	5.7 ± 5.2
i-C_4H_{10}	1.0 ± 0.48	2.6 ± 2.2	3.9 ± 4.8	1.8 ± 0.94	0.88 ± 0.38	1.5 ± 0.65	4.9 ± 4.1	2.1 ± 1.0	9.8 ± 7.8	5.3 ± 4.3
n-C_4H_{10}	3.0 ± 1.1	5.9 ± 6.9	10.9 ± 18.4	3.2 ± 1.2	2.6 ± 1.1	3.3 ± 1.4	6.1 ± 4.9	3.9 ± 1.6	11.4 ± 6.7	7.6 ± 6.1
Benzene	1.3 ± 0.39	4.6 ± 4.0	2.0 ± 1.8	1.7 ± 0.62	1.3 ± 0.49	1.3 ± 0.41	2.6 ± 1.6	1.5 ± 0.68	2.3 ± 2.2	–
Toluene	1.8 ± 0.32	1.8 ± 0.91	2.3 ± 1.9	2.0 ± 0.42	1.7 ± 0.57	2.2 ± 1.0	3.5 ± 3.2	2.1 ± 0.96	4.7 ± 4.5	–
m+p-Xylene	1.4 ± 0.29	1.4 ± 0.85	1.5 ± 0.97	1.5 ± 0.41	1.1 ± 0.40	1.3 ± 0.59	1.5 ± 0.82	1.7 ± 0.91	2.5 ± 1.3	–
o-Xylene	0.55 ± 0.12	0.46 ± 0.28	0.63 ± 0.44	0.58 ± 0.20	0.48 ± 0.17	0.38 ± 0.19	0.61 ± 0.43	0.56 ± 0.36	1.2 ± 0.87	–

The spatial distribution of the ratios of C_2H_6 and C_3H_8 is less uniform than for the concentration, and is a consequence of the distribution of C_2H_2. Thus, the lowest ratios occur at Crawford and Lang, which have some of the highest levels of C_2H_2. Likewise, the highest ratios are found at Seabrooke, Jackrabbit, Pearland, and Sheldon, where low levels of C_2H_2 occur.

For some hydrocarbons, the fraction contributed by mobile sources at a particular site can be estimated by comparing the hydrocarbon/acetylene ratio observed at the site with the corresponding ratio characteristic of mobile sources. Ratios associated with mobile sources are given in Table 15, which contains hydrocarbon/acetylene ratios measured in roadway tunnels in Los Angeles, New York, and Houston. The ratios for New York are based on 30-minute integrated samples; the others are derived from instantaneous samples. These ratios are compared with ambient ratios observed at the Houston monitoring sites.

TABLE 15. ESTIMATED AMBIENT RATIOS OF HYDROCARBON/ACETYLENE CONCENTRATIONS (ppbC) IN ROADWAY TUNNELS IN LOS ANGELES, NEW YORK, AND HOUSTON (mean ratio ± standard deviation)

Hydrocarbon	Sepulveda Street Tunnel, Los Angeles*	Lincoln Tunnel, New York†	Washburn Tunnel, Houston‡	Washburn Tunnel, Houston§
C_2H_6	0.21	—	—	0.21 ± 0.01
C_3H_8	0.15	—	—	0.078 ± 0.008
C_3H_6	0.66	0.61 ± 0.07	—	0.69 ± 0.03
$i-C_5H_{12}$	0.81	1.25 ± 0.14	1.34	1.44 ± 0.66
$i-C_4H_{10}$	0.12	0.34 ± 0.05	0.30	0.25 ± 0.02
$n-C_4H_{10}$	0.44	0.97 ± 0.12	1.25	1.21 ± 0.22
Benzene	—	—	—	1.27 ± 0.13
Toluene	—	—	—	1.39 ± 0.17
m+p-Xylene	—	—	—	0.91 ± 0.19
o-Xylene	—	—	—	0.35 ± 0.07

*Calculated from data in Mayrsohn et al. (1975).
†Lonneman et al. (1974).
‡Siddiqi and Worley (1977).
§This report.

In Table 14, the sites form three clusters for C_3H_6, each being composed of sites with mean ratios that do not differ significantly in a statistical sense. One cluster includes Crawford, Parkhurst, Lang, Westhollow, and

Jackrabbit (CPLWJ), and has mean ratios ranging from 0.41 to 0.51. These ratios are close to, but lower than, the C_3H_6/C_2H_2 ratios for mobile sources given in Table 15, which range from 0.61 to 0.69. In fact, if C_3H_6 were emitted primarily by mobile sources, we would expect the C_3H_6/C_2H_2 ratio in Table 14 to be lower than those in Table 15. The reason is that the ratios in Table 14 are derived from 3-hr samples, and chemical reactions during this period would lower the concentration of C_3H_6 but not of C_2H_2, thereby lowering the C_3H_6/C_2H_2 ratio. Since the tunnel samples were obtained over a relatively short period, C_3H_6 reacts less, and the ratio would be higher. We conclude that C_3H_6 at these five sites is due to mobile sources.

The influence of stationary sources of C_3H_6 is evident in Table 14 at Pasadena, Mae Drive, Seabrooke, Pearland, and Sheldon, all of which have C_3H_6/C_2H_2 ratios greater than those in Table 15. Pearland has the highest mean ratio and it differs significantly from all the others. The high ratio suggests that stationary sources contribute at least 90 percent of the C_3H_6 observed at Pearland. Pasadena, Mae Drive, Seabrooke, and Sheldon form a cluster (PMSS) since their mean ratios, which range from 1.1 to 1.7, do not differ significantly from each other. Comparing these ratios with those for the CPLWJ cluster, we estimate that stationary sources contribute at least 60 percent of the C_3H_6 at PMSS.

The ratios for $i\text{-}C_5H_{12}$, $i\text{-}C_4H_{10}$, and $n\text{-}C_4H_{10}$ given in Table 14 are higher than the corresponding ratios for mobile sources in Table 15. Therefore, it appears that stationary sources account for a significant fraction of the atmospheric burden of these compounds in the Houston area. The fraction of these three hydrocarbons due to stationary sources can be estimated using the ratios in Table 15, if we assume that C_2H_2 is due entirely to mobile sources. Using the mean ratio 1.44 for mobile sources, we estimate that stationary-source contributions of $i\text{-}C_5H_{12}$ range from at least 50 percent at Lang to 85 percent at Pearland. Applying a similar procedure to the two butanes yields estimates of stationary source impacts ranging from 30 percent at Lang to 97 percent at Pearland for $i\text{-}C_4H_{10}$. For $n\text{-}C_4H_{10}$, the estimates vary from 50 percent at Lang to 90 percent at Pearland. Thus, for these three compounds, the impact of stationary sources is smallest, but still substantial, at Lang, and largest at Pearland.

Table 14 shows that the benzene/acetylene ratios at Crawford, Parkhurst, Lang, Westhollow, and Jackrabbit approximate the ratios given in Table 15. Thus, it appears that mobile sources are the principal emitters of benzene at these sites. The predominance of mobile sources at these five locations is consistent with the earlier finding for C_3H_6. The mean benzene/C_2H_2 ratios at Pasadena, Mae Drive, Seabrooke, and Pearland suggest that part of the benzene burden at these sites originated in stationary sources.

For toluene and the xylenes, the differences in the ratios at the eight sites from Crawford through Jackrabbit are not statistically significant. Only the ratio at Pearland differs significantly from the rest. Thus, even though these compounds exhibit a noticeable variability in spatial concentration (see Table 13), the spatial distribution of the ratios is more homogeneous. The weighted mean ratios for the eight sites from Crawford through Jackrabbit are 2.2 for toluene, 1.4 for m+p-xylene, and 0.54 for o-xylene.

Comparing these ratios with those in Table 15 indicates that the ratio of mobile- to stationary-source contributions at these eight sites is approximately 3:2 for each of the three hydrocarbons. The condition is reversed at Pearland, where the mobile/stationary source split is approximately 3:7 for toluene and o-xylene and 2:3 for m+p-xylene.

Comparison of HOMS and HAOS Hydrocarbon Data

Table 16 shows mean concentrations of selected hydrocarbons sampled during the HAOS in the summer of 1977. Crawford is the only hydrocarbon-sampling site that was used in both the HOMS and the HAOS. The HAOS site at Clinton may be compared with the HOMS sites at Mae Drive and Pasadena, because of their proximity (see Figure 1). Similarly, Aldine (HAOS) may be paired with Parkhurst (HOMS), and Fuqua (HAOS) with Pearland (HOMS).

TABLE 16. 0600-0900 (CDT) CONCENTRATIONS OF SELECTED HYDROCARBONS MEASURED DURING THE HAOS, JUNE-OCTOBER 1977
(mean ± standard deviation—ppbC)

Hydrocarbon	Aldine	Crawford	Clinton	Fuqua
C_2H_6	73 ± 84	67 ± 21	87 ± 73	94 ± 92
C_3H_8	72 ± 88	70 ± 33	85 ± 62	100 ± 99
C_2H_2	30 ± 26	75 ± 32	30 ± 35	23 ± 20
C_3H_6	21 ± 14	37 ± 10	27 ± 14	23 ± 28
$i-C_5H_{12}$	84 ± 81	157 ± 54	88 ± 63	79 ± 62
$i-C_4H_{10}$	40 ± 46	42 ± 10	51 ± 34	54 ± 53
$n-C_4H_{10}$	74 ± 78	119 ± 31	80 ± 55	75 ± 65

Comparing Tables 12 and 16 shows that mean levels at Crawford are in general agreement for both HOMS and HAOS. In fact, the apparent differences in mean concentration are not statistically significant for any compound. The same is true when comparing Aldine with Parkhurst and Clinton with Mae Drive. The comparison of mean concentrations for Clinton and Pasadena shows that C_2H_6 and $n-C_4H_{10}$ differ significantly between sites, but the other compounds do not. For Fuqua and Pearland, only $n-C_4H_{10}$ shows a statistically significant difference in mean concentration. Localized sources are undoubtedly responsible for these differences since the sites are not collocated. Therefore, we conclude that the HAOS measurements of these seven hydrocarbons are consistent with the HOMS data.

Mean hydrocarbon/acetylene ratios for the HAOS are shown in Table 17; those for the HOMS were presented in Table 14. It is evident that the mean C_3H_6/C_2H_2 ratio at Crawford is essentially identical in both tables. However, for the other compounds, the mean ratios observed at Crawford in the HOMS are statistically different from the HAOS ratios. It is unlikely that this discrepancy is caused by differences in measurement techniques since, as

TABLE 17. 0600-0900 (CDT) RATIOS OF HYDROCARBON/ACETYLENE CONCENTRATIONS (ppbC) MEASURED DURING THE HAOS, JUNE-OCTOBER 1977
(mean ratio ± standard deviation)

Hydrocarbon	Aldine	Crawford	Clinton	Fuqua
C_2H_6	2.6 ± 1.3	0.96 ± 0.28	3.9 ± 3.0	6.0 ± 6.1
C_3H_8	2.5 ± 1.6	0.96 ± 0.36	3.8 ± 2.4	6.1 ± 6.2
C_3H_6	0.82 ± 0.32	0.52 ± 0.12	1.2 ± 0.60	1.3 ± 0.92
$i\text{-}C_5H_{12}$	2.9 ± 0.92	2.2 ± 0.61	3.8 ± 2.0	4.4 ± 2.7
$i\text{-}C_4H_{10}$	1.3 ± 0.76	0.62 ± 0.20	2.5 ± 2.0	2.8 ± 2.5
$n\text{-}C_4H_{10}$	2.4 ± 0.91	1.7 ± 0.45	3.6 ± 2.4	4.0 ± 2.8

previously noted, mean concentrations observed at Crawford in the HOMS are consistent with those in the HAOS. Moreover, if the experimental methods were different, then the two C_3H_6/C_2H_2 ratios would not match so well. The apparent discrepancy is probably the result of stationary source effects. Since stationary sources account for practically all the C_2H_6 and C_3H_8, and can contribute substantial amounts of $i\text{-}C_5H_{12}$, $i\text{-}C_4H_{10}$, and $n\text{-}C_4H_{10}$, the ratio of these compounds to acetylene would vary in proportion to the influence of stationary sources. Consequently, larger contributions from stationary sources may be responsible for the higher ratios that appear in the HOMS data.

In contrast to the situation at Crawford, ratios for the HOMS sites at Pasadena and Mae Drive do not differ significantly from the ratios at Clinton, an HAOS site. Hence, these three sites are impacted by hydrocarbon sources that appear to be qualitatively similar. Comparing Parkhurst (HOMS) and Aldine (HAOS) shows that there is no statistical difference between the sites for $i\text{-}C_5H_{12}$ and $i\text{-}C_4H_{10}$, and that the remaining four ratios differ significantly. The ratio for C_3H_6 at Aldine is greater than Parkhurst's. The magnitude of the C_3H_6/C_2H_2 ratio suggests that stationary sources of C_3H_6 may be impacting Aldine (see Table 15 for the magnitude of the mobile-source ratio). The ratios for C_2H_6, C_3H_8, and $n\text{-}C_4H_{10}$ at Parkhurst are greater than Aldine's, which is similar to the condition previously seen in connection with the Crawford site. All the ratios for Pearland and Fuqua differ significantly, Pearland's being consistently greater than Fuqua's. Both sites show evidence of substantial stationary-source effects, and the differences in the ratios are probably due to the impact of local sources.

There appears to be a discrepancy in the benzene and toluene measurements in the HOMS and HAOS. Table 18 compares the ratios for the two data sets. All but one of the HOMS ratios are less than 1, whereas the four HAOS ratios are greater than 1. The difference between the two Crawford ratios is statistically significant, as is that between the ratios at Mae Drive and Clinton, Parkhurst and Aldine, and Pearland and Fuqua. There is no statistical difference between the ratios at Pasadena and Clinton. Each data set seems to be internally consistent, so it is difficult to find a reason for the discrepancy. A review of 1974-1975 data for the Los Angeles area shows that

TABLE 18. 0600-0900 (CDT) RATIOS OF BENZENE/TOLUENE CONCENTRATIONS (ppbC) IN THE HOUSTON AREA DURING THE HAOS, JUNE-OCTOBER 1977
(mean ratio ± standard deviation)

Site	HOMS	HAOS
Mae Drive	0.86 ± 0.13	—
Crawford	0.72 ± 0.17	1.2 ± 0.56
Parkhurst	0.85 ± 0.12	—
Lang	0.78 ± 0.077	—
Pasadena	2.50 ± 2.1	—
Seabrooke	0.86 ± 0.36	—
Westhollow	0.67 ± 0.16	—
Jackrabbit	0.78 ± 0.28	—
Pearland	0.54 ± 0.40	—
Aldine	—	2.7 ± 2.1
Clinton	—	1.8 ± 0.92
Fuqua	—	2.1 ± 1.5

downtown Los Angeles has a mean benzene/toluene ratio of 0.25. Four other locations near Los Angeles have mean ratios ranging from 0.30 to 0.64. Measurements made in an industrial section of Denver in 1973 (Ferman et al., 1977) have a mean ratio of 0.31. Thus, except for the Pasadena ratio, the HOMS ratios are consistent with benzene/toluene ratios in Los Angeles and Denver. The HAOS ratios for Crawford, Aldine, and Fuqua, on the other hand, appear to be out of line. However, the higher ratios for Clinton and Pasadena are consistent, and are probably caused by stationary sources of benzene at these two industrial sites.

Comparison of Hydrocarbons in Houston, Southern California, and Denver

In this section, the 0600-0900 HOMS hydrocarbon measurements will be compared with similar data for Denver (Ferman et al., 1977) and for five locations in southern California (Mayrsohn et al., 1975). Our aim is to identify differences and similarities between Houston's hydrocarbon mixture and that of the other areas. The analysis will focus on the 11 selected hydrocarbons previously identified.

Table 19 shows the monitoring locations in Denver and southern California, including the site type, number of samples collected, and the monitoring period. Instantaneous samples were collected every hour at Denver, and the samples for the hours 0600, 0700, 0800, and 0900 were used to obtain the 0600-0900 average. The southern California data consist of integrated three-hour samples collected during the period 0600-0900.

TABLE 19. 0600-0900 (LT) HYDROCARBON MONITORING IN DENVER AND SOUTHERN CALIFORNIA

Site Name	Site Type	Number of Samples	Monitoring Period
Denver	Industrial	19	4 Nov-14 Dec 1973
Long Beach	Urban/Industrial	41	18 Jun-5 Sep 1974
Downtown Los Angeles	Urban	13	18 Jun-18 Jul 1974
Azusa	Suburban	39	18 Jun-5 Sep 1974
El Monte	Suburban	34	1 Jul-5 Sep 1974
Upland	Suburban	36	18 Jun-5 Sep 1974

The Denver sampling site was located in an industrial section about 6 km northeast of downtown Denver. Within 3 km of the site are found three freeways, a power plant, oil refineries, and a sewage disposal plant (Ferman et al., 1977). Therefore, it is of interest to compare the hydrocarbon mixture of the Denver site with those of Pasadena and Mae Drive in Houston.

The Long Beach site in southern California is in a densely populated urban area that is heavily industrialized. Two major freeways is within 2 km, and a variety of industrial sources are within 8 km of the site. We expect both mobile and stationary sources to affect this site. Thus, we compare Long Beach with the Mae Drive site in Houston.

Downtown Los Angeles is dominated by mobile sources, and is compared with the Crawford site in downtown Houston. The three suburban sites, Azusa, El Monte, and Upland, are located in the eastern part of the Los Angeles Basin and are primarily receptors of pollution transported from the western and central portions of the Basin. Typically, they experience some of the highest ozone levels in the area. Mobile sources are the principal local emitters at these three sites. Thus, these sites may be comparable to Parkhurst, Jackrabbit, Westhollow, and Lang in Houston.

Table 20 shows the mean hydrocarbon concentrations in Denver and southern California. Comparing Tables 12 and 20 shows that there is no statistical difference (significance $\leq$ 0.05) between the mean concentrations of all but four of the hydrocarbons at Mae Drive (Table 12) and Denver. The exceptions are n-C_4H_{10}, benzene, and the two xylenes, with Denver's mean levels being higher than at Mae Drive for n-C_4H_{10} and the xylenes, but lower for benzene. Comparing Denver with Pasadena (see Table 12) shows that significant differences exist for six species: C_2H_2, n-C_4H_{10}, and the four aromatics. The mean level of benzene is lower in Denver than in Pasadena, but is higher for the other five hydrocarbons.

Long Beach (see Table 20) and Mae Drive (see Table 12) show significant differences in mean i-C_5H_{12}, toluene, and the xylenes. Mae Drive has higher

TABLE 20. 0600-0900 (LT) HYDROCARBON CONCENTRATIONS IN DENVER AND SOUTHERN CALIFORNIA
(mean ± standard deviation—ppbC)

Hydrocarbon	Denver	Long Beach	Downtown Los Angeles	Azusa	El Monte	Upland
C_2H_6	66 ± 37	97 ± 61	110 ± 61	85 ± 32	94 ± 48	62 ± 23
C_3H_8	85 ± 50	123 ± 71	102 ± 57	71 ± 27	87 ± 45	48 ± 19
C_2H_2	78 ± 54	31 ± 15	95 ± 50	51 ± 25	48 ± 29	47 ± 20
C_3H_6	30 ± 20	20 ± 10	36 ± 18	20 ± 8	22 ± 12	16 ± 4
$i-C_5H_{12}$	159 ± 106	102 ± 55	175 ± 93	107 ± 48	123 ± 72	85 ± 36
$i-C_4H_{10}$	61 ± 40	52 ± 30	50 ± 26	33 ± 14	40 ± 20	25 ± 9
$n-C_4H_{10}$	134 ± 78	115 ± 69	121 ± 65	78 ± 34	99 ± 59	59 ± 24
Benzene	22 ± 15	49 ± 12	77 ± 24	66 ± 22	77 ± 21	55 ± 28
Toluene	82 ± 51	88 ± 33	316 ± 113	200 ± 105	141 ± 69	154 ± 111
m+p-Xylene	60 ± 38	106 ± 35	224 ± 75	152 ± 59	138 ± 61	103 ± 67
o-Xylene	28 ± 17	60 ± 23	103 ± 33	83 ± 33	71 ± 28	49 ± 34

$i-C_5H_{12}$ than Long Beach, but toluene and the xylenes are higher at Long Beach. Comparing Long Beach and Pasadena (see Table 12) shows significant differences not only for toluene and the xylenes, but also for benzene, C_2H_6, and C_2H_2. In general, the mean levels of the four aromatics at Long Beach are higher than at Mae Drive or Pasadena, but the difference for benzene is small.

Mean C_2H_2, toluene, and the xylenes in downtown Los Angeles (see Table 20) differ significantly from Crawford's (see Table 12). There is no statistical difference between the sites with respect to the other compounds. As with Long Beach, the mean concentration of the aromatics is higher in downtown Los Angeles than in downtown Houston, with only a slight difference for benzene. Toluene and the xylenes are about three times higher in Los Angeles than in Houston, and mean C_2H_2 is about 60 percent higher. The latter figure suggests that mobile-source emissions are stronger in Los Angeles than in Houston. But this cannot account for the factor-of-three difference in toluene and the xylenes. Thus, stationary sources must be invoked as the likely cause of the higher levels of these aromatics observed in downtown Los Angeles.

The sites at Azusa, El Monte, and Upland in southern California (see Table 20) have mean hydrocarbon levels similar to those found at the Lang site in Houston (see Table 12), with some exceptions. Comparing Lang with both Azusa and El Monte shows significant differences only in the aromatics, which are higher at the two California sites (benzene is 40 and 60 percent higher at Azusa and El Monte, respectively), and toluene and the xylenes are more than twice as high. Upland and Lang have statistically different $n-C_4H_{10}$, toluene, and the xylenes, but not benzene. Thus, these three suburban southern California sites continue the pattern of high levels of aromatics seen at Long Beach and downtown Los Angeles.

Hydrocarbon/acetylene ratios in Denver and southern California are shown in Table 21. Comparing these ratios with those in Table 15 indicates that mobile sources are the primary contributors of C_3H_6 at all six locations. This contrasts with Houston, where Pasadena and Mae Drive show evidence of stationary-source contributions of C_3H_6 (see Table 14). Comparing Denver with Pasadena shows that the ratios are significantly different for all the compounds except the xylenes. The same pattern holds for Denver and Mae Drive, except that o-xylene also is statistically different. In general, the ratios at Pasadena and Mae Drive are higher than Denver's. Thus, Denver's hydrocarbon mixture appears to be qualitatively different from Pasadena's and Mae Drive's. In fact, Denver's ratios resemble those at the Lang site in Houston, which suggests that the mixture at the Denver location is similar to that found in suburban Houston.

TABLE 21. 0600-0900 (CDT) RATIOS OF HYDROCARBON/ACETYLENE CONCENTRATIONS (ppbC) IN DENVER AND SOUTHERN CALIFORNIA
(mean ratio ± standard deviation)

Hydrocarbon	Denver	Long Beach	Downtown Los Angeles	Azusa	El Monte	Upland
C_2H_6	1.1 ± 0.61	3.2 ± 1.7	1.2 ± 0.55	1.9 ± 1.1	2.1 ± 0.61	1.4 ± 0.40
C_3H_8	1.3 ± 0.74	4.3 ± 2.7	1.1 ± 0.44	1.6 ± 0.76	1.9 ± 0.63	1.1 ± 0.40
C_3H_6	0.36 ± 0.11	0.66 ± 0.29	0.38 ± 0.03	0.44 ± 0.16	0.49 ± 0.18	0.37 ± 0.15
$i\text{-}C_5H_{12}$	2.0 ± 1.1	3.3 ± 1.1	1.8 ± 0.26	2.2 ± 0.59	2.6 ± 0.55	1.9 ± 0.29
$i\text{-}C_4H_{10}$	0.81 ± 0.60	1.8 ± 0.87	0.54 ± 0.16	0.74 ± 0.37	0.91 ± 0.28	0.58 ± 0.21
$n\text{-}C_4H_{10}$	2.0 ± 1.0	3.9 ± 1.9	1.3 ± 0.34	1.7 ± 0.60	2.1 ± 0.75	1.3 ± 0.33
Benzene	0.34 ± 0.24	1.8 ± 0.85	0.78 ± 0.19	1.5 ± 0.74	2.0 ± 0.86	1.1 ± 0.44
Toluene	1.2 ± 0.51	3.0 ± 0.85	3.2 ± 1.2	4.1 ± 1.5	3.3 ± 0.99	3.0 ± 1.6
m+p-Xylene	1.2 ± 1.8	3.7 ± 1.5	2.2 ± 0.37	3.3 ± 1.3	3.4 ± 1.4	2.0 ± 0.84
o-Xylene	0.39 ± 0.13	2.1 ± 1.1	1.0 ± 0.23	1.8 ± 0.87	1.8 ± 0.97	0.93 ± 0.46

Long Beach and Pasadena show significant differences in the ratios for C_3H_6 and the aromatics, but not for the others. Thus, the proportion of C_3H_6 is greater at Pasadena than at Long Beach, and the opposite is true with respect to the aromatics. The relationship between Long Beach and Mae Drive is similar. Thus, Long Beach has an excess of aromatics, while the two Houston sites have more C_3H_6 relative to C_2H_2.

The ratios for downtown Los Angeles and Crawford are similar for C_2H_6, C_3H_8, and C_3H_6, and differ significantly for the others. The influence of motor vehicles is indicated by the ratio for C_3H_6. Crawford's mixture has more alkanes and benzene (relative to C_2H_2), while Los Angeles has more toluene and xylenes.

Compared to Azusa, El Monte, and Upland, the ratios for Lang differ significantly only for toluene and the xylenes, the California ratios being substantially higher. Thus, the hydrocarbon mixture of suburban Houston, as exemplified by Lang's, is similar to that of suburban southern California's in its alkane and propylene components. The ratios show that propylene is mainly contributed by mobile sources at these locations.

The compounds C_3H_6 and n-C_4H_{10} have been used as surrogates to characterize the reactivity of urban hydrocarbon mixtures (Hendry et al., 1978; Whitten and Hogo, 1978). In this approach, C_3H_6 and n-C_4H_{10} are considered to typify the high- and low-reactive components of the mixture, respectively. The Empirical Kinetic Modeling Approach (EKMA) is an example of a method that uses C_3H_6 and n-C_4H_{10} in this manner (Whitten and Hogo, 1978; EPA, 1977; 1978). The EKMA computer code defines the initial reactivity of the mixture by specifying the initial ratio n-C_4H_{10}/C_3H_6, and uses a ratio of 3:1 (Whitten and Hogo, 1978). Thus, it is of interest to compare the n-C_4H_{10}/C_3H_6 ratios for the various sites in Houston, Denver, and California. These ratios are shown in Table 22.

TABLE 22. 0600-0900 (LT) RATIOS OF n-C_4H_{10}/C_3H_6 CONCENTRATIONS (ppbC) IN HOUSTON, DENVER, AND SOUTHERN CALIFORNIA

Site Name	Range	Median	Mean	Standard Deviation	Number of Ratios
Houston					
Crawford	2.6-10.4	5.5	5.8	2.0	20
Pasadena	0.8-39.0	3.8	6.4	8.9	19
Mae Drive	0.8-30.8	6.1	9.4	8.8	19
Parkhurst	2.8-22.0	7.7	8.0	4.5	17
Lang	3.3-11.7	4.8	5.5	2.3	16
Westhollow	3.6-21.0	9.0	11.0	5.5	13
Seabrooke	0.8-10.5	5.0	4.9	2.8	17
Jackrabbit	3.4-22.0	7.5	9.1	5.2	21
Pearland	0.6-33.6	4.1	6.6	7.5	28
Sheldon	0.5-14.0	6.4	6.0	3.6	21
Denver	2.6-11.4	4.1	5.0	2.4	18
Southern California					
Long Beach	2.3-13.1	5.7	6.1	2.5	41
Downtown Los Angeles	2.4-5.2	3.2	3.3	0.73	13
Azusa	2.4-5.7	3.8	3.9	0.84	39
El Monte	2.7-10.1	4.5	4.6	1.3	34
Upland	2.1-7.2	3.5	3.8	1.2	36

Table 22 shows that, as a group, the ratios in Houston range from very low (0.5) to very high (39.0). Thus, when the n-C_4H_{10}/C_3H_6 ratio is used as an indicator of reactivity, Houston's hydrocarbon mixture fluctuates from very reactive to very unreactive. The widest excursions of the ratio occur at Pasadena, Mae Drive, Pearland, Seabrooke, and Sheldon. As we have seen, the first three sites are impacted by stationary sources and the last two are located on the edges of the urban area. The hydrocarbon mixture at these sites would be affected by sources whose influence is conditioned on the vagaries of wind direction, so that large fluctuations in reactivity are to be expected.

The other Houston sites are located within the urban envelope, are more heavily influenced by area sources, and thus display a narrower range of ratios, from 2.6 to 22.0. The same condition is evident at the Denver and California sites, whose ratios vary from 2.1 to 13.1. Note that the median ratio for downtown Los Angeles approximates the default ratio of 3:1 used in the EKMA. The range of ratios in Denver and in El Monte is similar to those at Crawford and Lang in Houston. However, the median ratios at Crawford and Lang are somewhat higher, suggesting a slightly less reactive mixture than in Denver and El Monte. Crawford and Long Beach have similar median ratios, which indicates that their respective reactivities are alike. Azusa in California and Pasadena in Houston have equal median ratios, but the reactivity of Azusa's hydrocarbon mixture is much more steady than Pasadena's. The lowest median ratios occur in downtown Los Angeles and Upland, but the difference between these ratios and Pasadena's is small. Judging by the median n-C_4H_{10}/C_3H_6 ratio, it seems that the reactivity in downtown Los Angeles tends to be higher than at Crawford in downtown Houston. In fact, the difference between the medians at these two sites is statistically significant.

Aldehydes in the Houston Area

The HOMS included a program that measured total aldehydes and formaldehyde at Fuqua, Crawford, Parkhurst, and Clinton. The sampling program and experimental procedures have been described by Joshi (1979). Below, we examine the pattern of aldehydes in Houston.

Table 23 shows the concentrations of formaldehyde and total aldehydes at each site. [The table omits three questionable concentrations of total aldehydes (Joshi, 1979).] Clinton, which is an industrial site, has the lowest median formaldehyde, but the second lowest median total aldehydes, while Parkhurst reverses this sequence. Crawford, in downtown Houston, has the highest median levels of both species, and Fuqua the second highest. However, these spatial differences are somewhat misleading, because the measurements were made on different days at the four sites. Thus, all the high concentrations at Fuqua and Crawford occurred during the ozone episode that took place between 1 and 4 October (see Table 6). In general, the high concentrations at all the sites occurred on days with elevated ozone levels, but the converse is not necessarily true.

The sequence of formaldehyde measurements is shown in Figure 12. The figure plots formaldehyde as a function of time, and shows the daily ozone maximum as well as the location of formaldehyde monitoring. Since each formaldehyde sample was collected over several hours, the points in Figure 12 are plotted at the midpoint of the sampling interval. Figure 12 shows that levels of formaldehyde greater than 20 ppb occur only when the maximum ozone is at least 100 ppb. However, it is apparent that the occurrence of high ozone levels does not guarantee high formaldehyde. Figure 12 also shows that

TABLE 23. ALDEHYDES IN THE HOUSTON AREA

Site Name	Formaldehyde			Total Aldehydes		
	Range (ppb)	Median (ppb)	Number of Samples	Range (ppb)	Median (ppb)	Number of Samples
Fuqua	1.04–27.27	10.27	17	4.8–36.33	15.59	14
Crawford	3.42–24.73	14.19	20	4.69–34.48	22.38	19
Parkhurst	2.76–14.35	7.73	19	4.34–16.25	8.54	14
Clinton	1.10–27.60	6.40	21	4.36–40.40	11.80	21

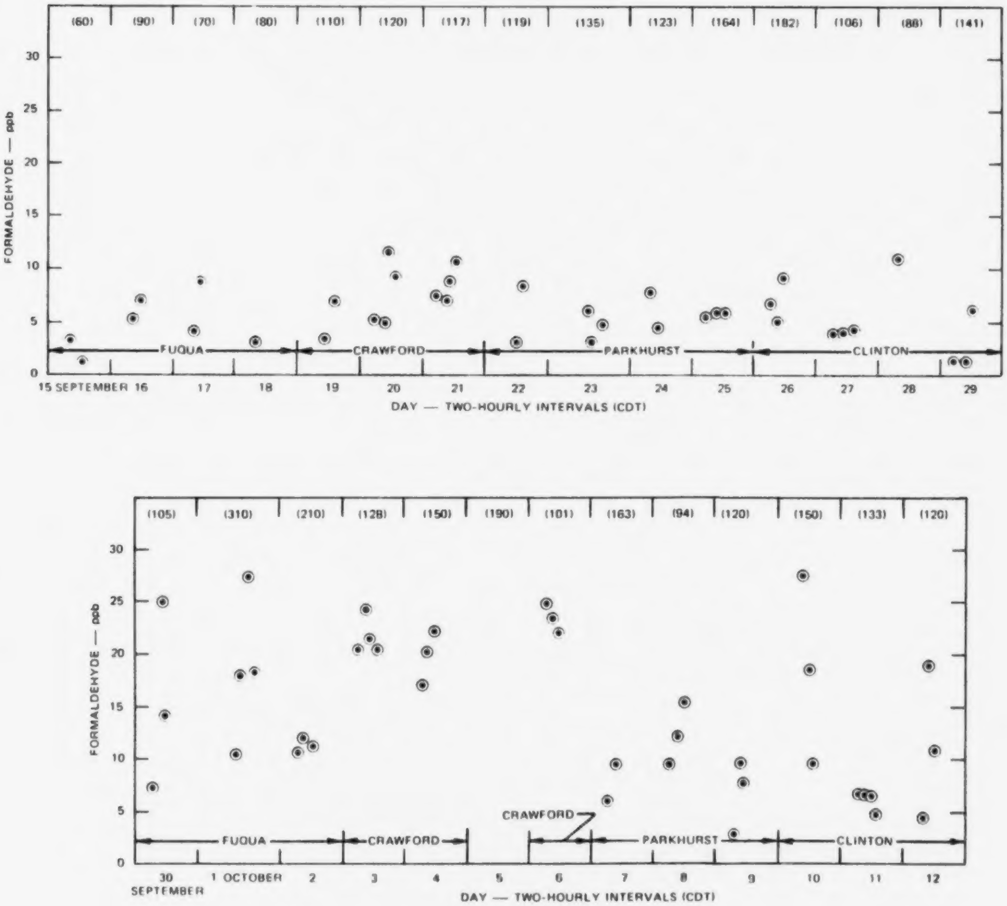

Figure 12. Time series of formaldehyde concentrations.
Daily maximum ozone concentrations (ppb) are shown in parentheses.

formaldehyde follows a daily cycle that increases in the morning, peaks around noon, and decreases thereafter. This is, of course, the typical cycle followed by photochemical smog.

One of the input requirements for photochemical models is the initial concentration of aldehydes. A typical modeling run begins in the early morning, and requires aldehyde levels for that time period. The HOMS data provide guidance for estimating early-morning aldehyde levels. Six samples collected during the period 0600-0800 (including two samples obtained during 0610-0810 and 0617-0812) had total aldehydes ranging from 7 to 22 ppb, with a mean of 11 ppb, while formaldehyde ranged from 1 to 7 ppb, with a mean of 4 ppb.

NMHC/NO_x RATIOS

Ratios of NMHC to NO_x for the period 0600-0900 (CDT) were computed for six HOMS sites. Table 24 shows the range, median, and number of ratios for each site. Of the 75 ratios, 69 are in the range 1 to 82. The six ratios greater than 82 occurred at Mae Drive (ratio = 151) and at Parkhurst (ratios of 105, 138, 159, 163, and 210). These six large ratios are unusual, but the data on which they are based seem to be valid. Examination of the data shows that the high ratios are caused by low NO_x rather than by high NMHC.

TABLE 24. 0600-0900 (CDT) NMHC/NO_x RATIOS
IN THE HOUSTON AREA, 15 SEPTEMBER–12 OCTOBER 1978

Site Name	Range	Median	Number of Ratios
Aldine	5-16	10.9	10
Mae Drive	4-151	9.7	23
Crawford	23-48	37.0	11
Parkhurst	69-210	137.8	7
Fuqua	50-51	50.5	2
Jackrabbit	1-66	7.0	22

Summer 1977 NMHC/NO_x ratios for 0600-0900 were estimated using HAOS data for five sites, of which four coincide with the HOMS monitoring stations. Table 25 lists the HAOS ratios and shows that all are in the range 1 to 85. This highlights the unusual nature of the high ratios present in the HOMS data. Comparing Tables 24 and 25 shows that Aldine has the same lower bound in both cases, but that the upper limit and the median ratio are higher in the HAOS. The difference may be the result of the disparity in the number of ratios corresponding to the HOMS and HAOS. Except for the ratio equal to 151, the range of the ratios at Mae Drive is comparable in the HOMS and HAOS, with the HOMS data having a somewhat higher incidence of low ratios, as evidenced by its lower median. The range of ratios estimated at Crawford during HOMS is well within the range observed during HAOS, but the frequency of large ratios

TABLE 25. 0600-0900 (CDT) $NMHC/NO_x$ RATIOS IN THE HOUSTON AREA, 1 MAY—31 OCTOBER 1977

Site Name	Range	Median	Number of Ratios
Aldine	5-53	18.0	113
Mae Drive	3-71	12.0	36
Crawford	2-85	13.5	18
Parkhurst	1-48	12.0	49
Clinton	3-59	9.5	26

in HOMS is higher. These larger ratios at Crawford are also attributed to low NO_x instead of to high NMHC. In general, the HAOS data (Table 25) show less spatial variability than the HOMS ratios (Table 24).

Figure 13 compares the cumulative frequency distribution of the HOMS and HAOS ratios. Both distributions have comparable median ratios, 14 and 12,

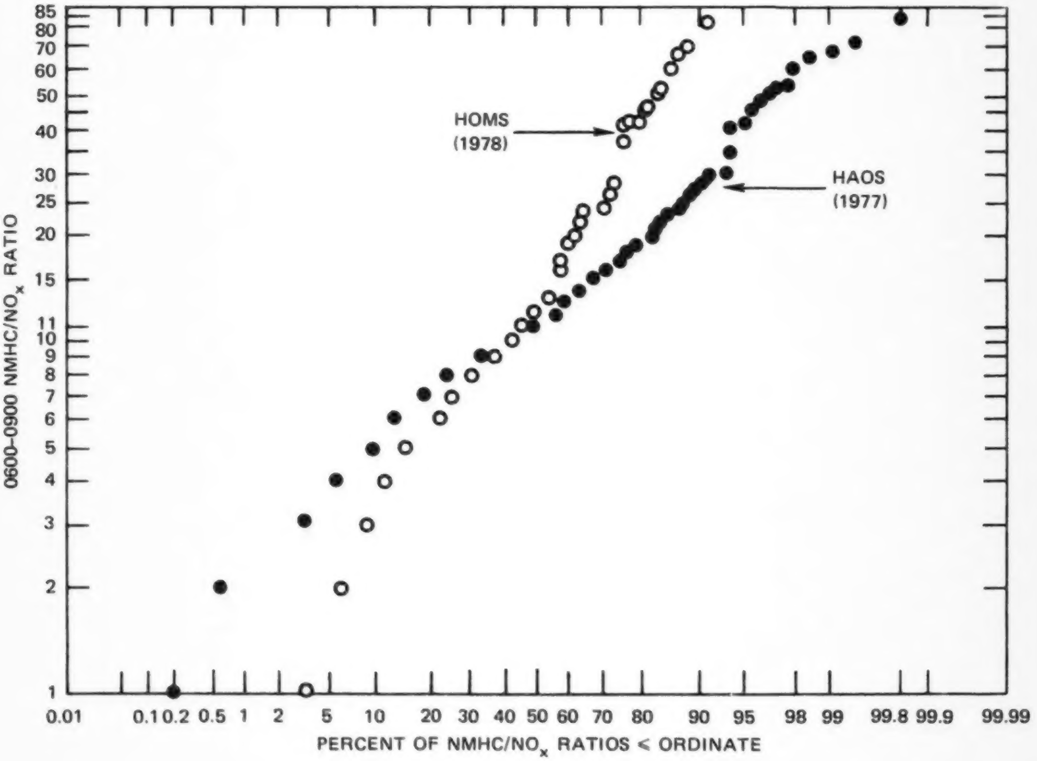

Figure 13. Cumulative frequency distributions of $NMHC/NO_x$ ratios for the HOMS and HAOS.

respectively, but diverge substantially on both sides of the median. The figure suggests that the median ratio is insensitive to divergence in the tails of the distribution. Thus, using the median as the sole descriptor of the distribution of ratios, as is sometimes done (EPA, 1977), can be misleading, since this can mask substantial differences, as shown in Figure 13.

The six high ratios observed in the HOMS are similar to ratios estimated at Clute, Bayport, and Texas City in the HAOS. These three sites are located well beyond Houston's urban envelope and their ratios range from 1 to 185, with a median of 29 (Ludwig and Martinez, 1979). Low NO_x was also responsible for the high ratios at Clute, Bayport, and Texas City. Thus, although HOMS data exhibit ratios that are unusually high for the urban monitoring stations, such ratios have been observed at other sites in the Houston area.

SPATIAL PATTERNS IN THE POLLUTANT DATA

Method of Analysis

In a data set that consists of observations taken at different locations over a period of time, there frequently will be considerable redundancy of information. The observations at one site will be correlated significantly with those at other sites; there are important patterns in the variations of observations about their means. For example, there may be tendencies for increases (or decreases) of observed values at one site to be a fraction of those at some nearby site. In some cases, the changes may tend to be in opposite directions, with an increase at one site accompanied by a decrease at another.

Lorenz (1956) used principles of factor analysis to identify patterns of variability in atmospheric pressure. We have adopted his techniques, which are described in Appendix B, and used them to identify patterns of variability in the ozone, NMHC, and NO_x data from Houston. Lorenz (1956) uses the term "empirical orthogonal function" for the technique used to describe the patterns of variability. The patterns observed can be reproduced reasonably well by a sum of the mean values and multiples of a few of the most important empirical orthogonal functions. Typically, a few functions will account for more than 80 percent of the variance in the data set. Lorenz (1956) points out that the remaining variance, which can be accounted for by considering more empirical orthogonal functions, is frequently of smaller spatial scale and might be noise or unrepresentative of the larger scale patterns of variability.

In the following discussions, we present the mean values of the concentrations at the various observing sites and the values for the empirical orthogonal functions at each observing site. It is necessary to have a complete data set (that is, data from each of the observing sites) for a particular hour, to be included in the calculation of the empirical orthogonal functions. Because there are a considerable number of missing data at many of the sites, it has been necessary to reduce the number of sites considered and use only those with the most complete data sets, otherwise the number of hours with simultaneous observations at all sites would have been too few to give reliable empirical orthogonal functions. In the case of the ozone-monitoring sites, we used data from six locations: Sites 1, 2, 9, 10, 11, and 16 in Figure 1. For NMHC, the sites used were 1, 2, 3, and 4, and for NO_x, Sites 2, 5, 15, and 20.

We begin by presenting the mean patterns and the patterns associated with the most important empirical orthogonal functions. The significance of the mean pattern and the empirical orthogonal functions is discussed. This is followed by discussions of the mean values for the coefficients [q_1 and q_2, see Eq. (9) in Appendix B] for each hour of the day and for different wind directions. As can be seen, the empirical orthogonal functions and the variations in their coefficients with wind direction and time of day provide some very interesting information about the nature of pollutant patterns and pollutant sources in the Houston area.

Ozone Patterns

Figure 14(a) and 14(b) shows the mean concentration pattern derived from the data and the pattern associated with the first empirical orthogonal function, which explains 82 percent of the variance in the data set. Both the mean and the first empirical orthogonal function are characterized by relatively uniform gradients, increasing from southeast toward northwest. Inasmuch as the one pattern represented by the first empirical orthogonal function accounts for most of the variance, there must be considerable redundancy in the data. This in turn means that it should be possible to represent the major features of the ozone field with relatively few sites, provided they are representative of their surroundings. Certainly the number of ozone sites used in the HOMS should be more than adequate for describing the distributions of ozone with a level of detail consistent with the requirements of most simulation models.

If we refer to Eq. (9) in Appendix B, we see that when the coefficients of the most important orthogonal function are near zero, the observed pattern will be similar to the mean. In the case of ozone, when the coefficient for the first empirical orthogonal function is large and positive, the observed ozone concentrations will be higher than average and the gradient more pronounced. With large positive coefficients, we would expect to see concentrations increasing rapidly to rather high values toward the inland locations northwest of the city. For negative coefficients, some multiple of the pattern shown in Figure 14(b) would be subtracted from the mean, leading to generally lower ozone values and a weaker gradient.

Figure 15 shows the average hourly values of the coefficient for the first empirical orthogonal function for ozone. The coefficients tend to be quite large and positive during the daytime and negative (but with smaller absolute values) at night. Around 0600, the average coefficient is about -50. The values of the empirical orthogonal functions at Sites 1 and 10 are 0.54 and 0.24, respectively. The means are 31 and 20 ppb. With these values, the ozone concentrations would decrease from about 7 or 8 ppb [20 - (50 x 0.24)] near Site 10 to about 4 ppb [31 - (50 x 0.54)] near Site 1. In other words, the interpretation that can be given to the average 0600 coefficient is that the night and early morning ozone patterns tend to be relatively uniform (with perhaps a gradient opposite to the mean gradient) and the absolute

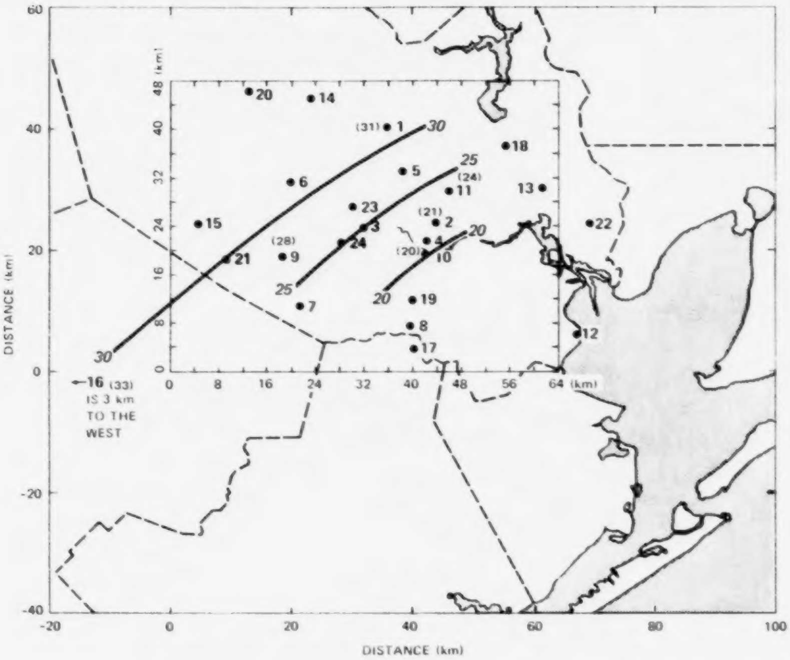

(a) MEAN OZONE (ppb)

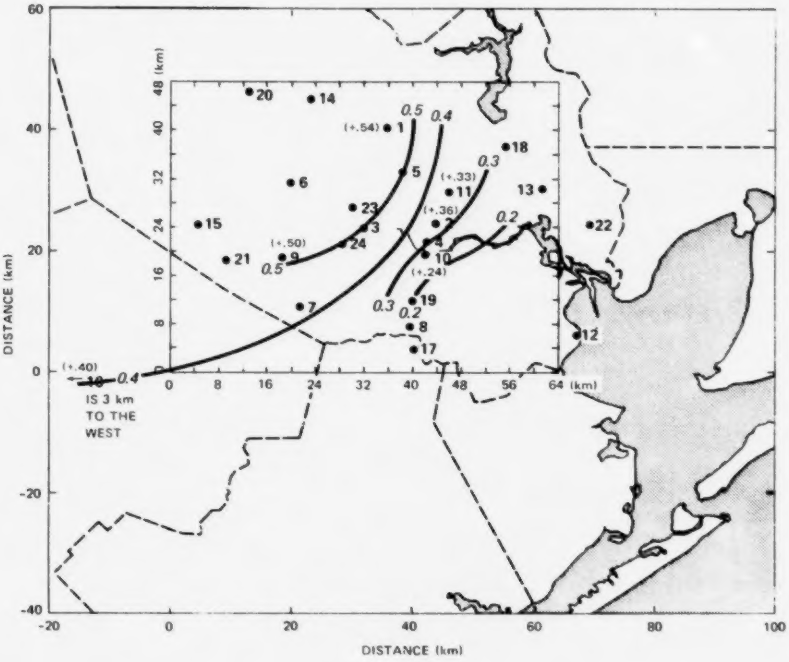

(b) 82% VARIANCE

Figure 14. Mean ozone concentrations (ppb) and the most important empirical orthogonal functions.

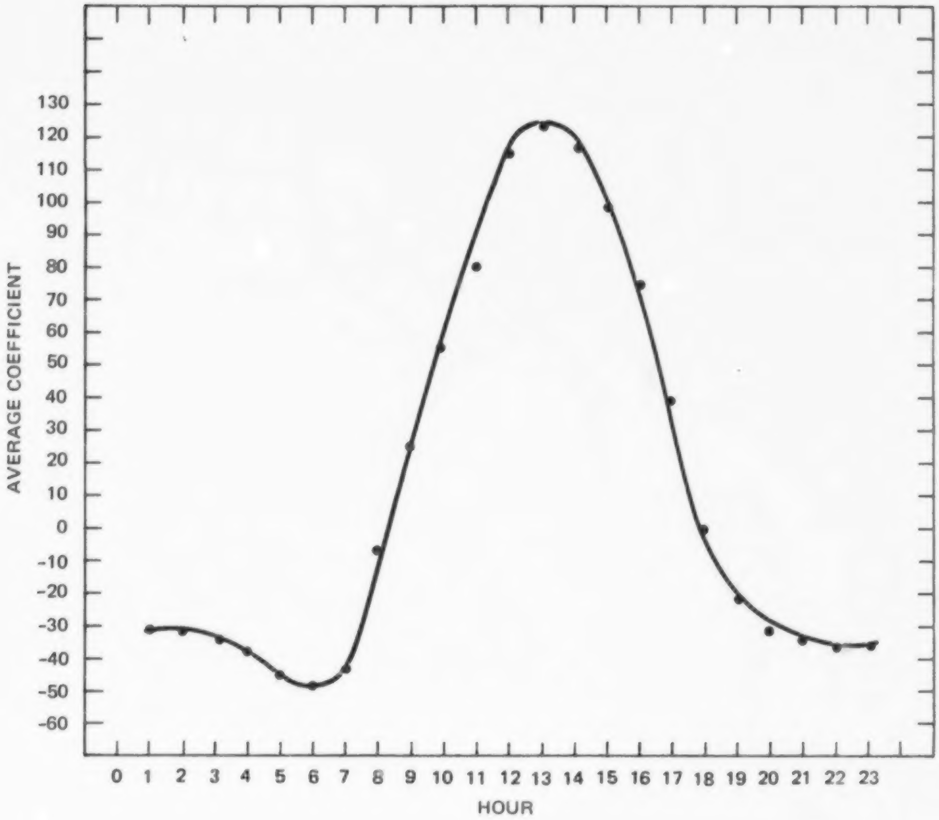

Figure 15. Average hourly values of the coefficient for the first empirical orthogonal function for ozone.

concentrations fairly low. By contrast, the midday average coefficient of 120 leads to much higher values and much stronger gradients. For a coefficient of 120, concentrations would increase from about 50 ppb near Site 10 to about 100 ppb near Site 1.

When so much of the variance is explained by a single empirical orthogonal function, it allows us to infer the behavior of the whole pattern from the behavior of a single descriptor, i.e., the coefficient for the most important empirical orthogonal function. Thus, from Figure 15 it can be determined that the typical diurnal behavior of ozone patterns in the Houston area proceeds from relatively flat, low concentration fields at night to much higher concentrations in the daytime, peaking around 1300. Figure 15 shows that the peak gradient will on average occur at that time and then fall rather irregularly to the nighttime weak gradients by early evening. There seems to be some tendency for concentrations to drop and gradients to reverse between 0400 and 0600. Otherwise, conditions seem to remain relatively constant through most of the night.

Figure 16 shows the average coefficients for the first empirical orthogonal function for ozone for each of 16 wind directions (measured at Mae Drive). There is considerable scatter to the points because not all wind directions are equally represented in the sample. Nevertheless, there is clear evidence that concentrations tend to be highest and gradients sharpest when winds are from directions between southeast and south-southwest. Northwest winds are associated with weaker gradients and lower concentrations of ozone.

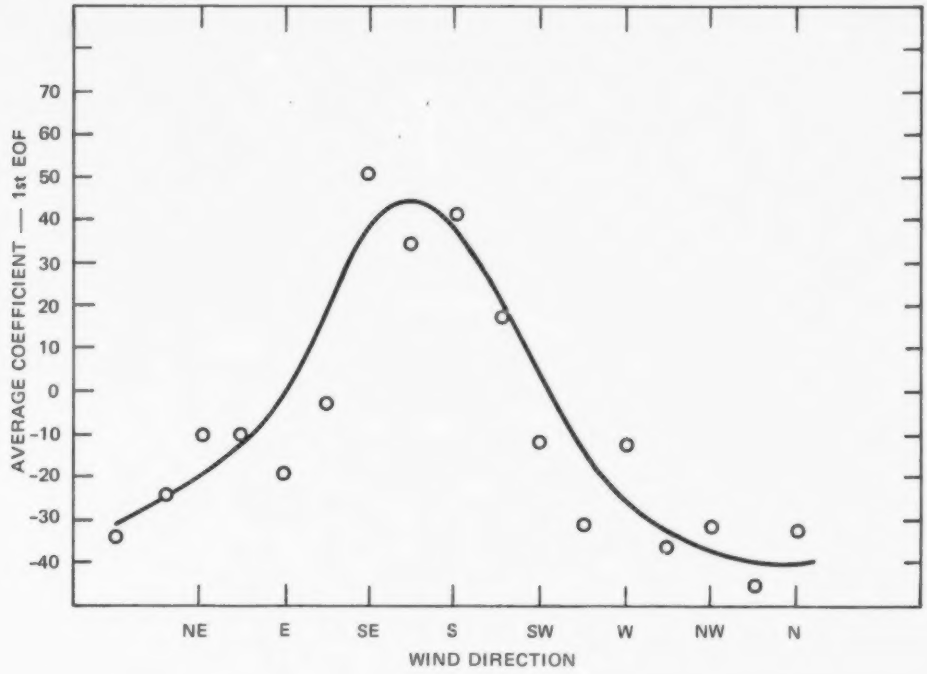

Figure 16. Average values of the coefficient for the first empirical orthogonal function for ozone according to wind direction at Mae Drive.

Hydrocarbons

Figure 17(a), (b), and (c) shows the mean concentration pattern for nonmethane hydrocarbons and the first and second most important empirical orthogonal functions, based on observations at four sites. The differences between the patterns for NMHC and ozone are striking. First, 82 percent of the variance is explained by one empirical orthogonal function for ozone; the most important empirical orthogonal function for NMHC explains 61 percent of the variance and the second most important 34 percent of the variance. Thus, we can infer that there is more regularity in the behavior of the ozone concentration patterns than in those for NMHC. This is apparent in the patterns themselves, which show relatively small scale features compared to the rather general smooth shape for the mean ozone field and its first empirical orthogonal function.

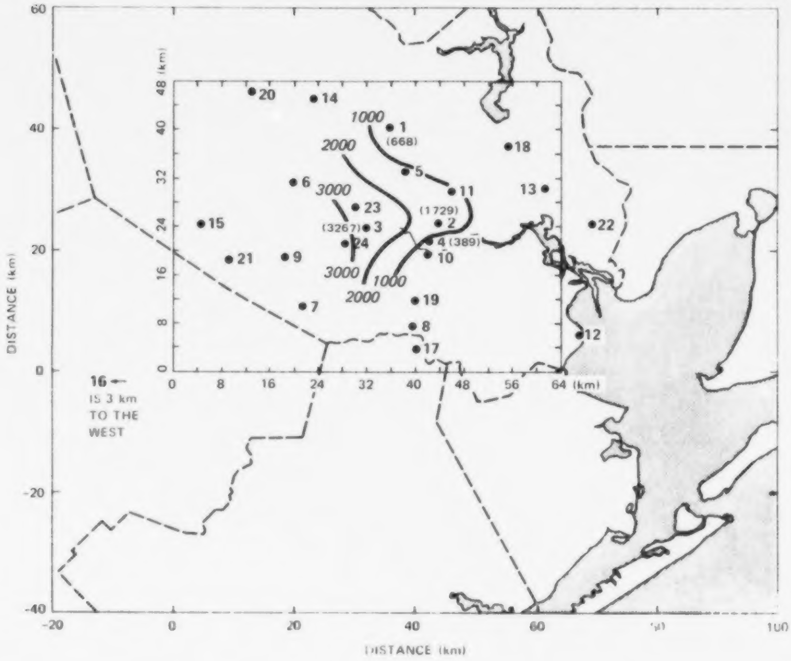

(a) MEAN NMHC

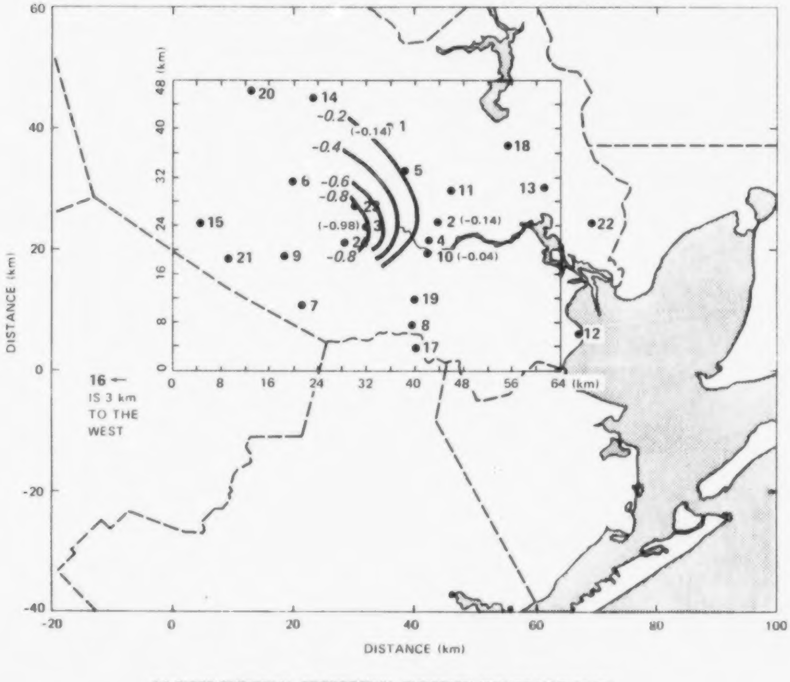

(b) FIRST EMPIRICAL ORTHOGONAL FUNCTION (61% OF VARIANCE)

Figure 17. Mean NMHC concentrations (ppbC) and the two most important empirical orthogonal functions.

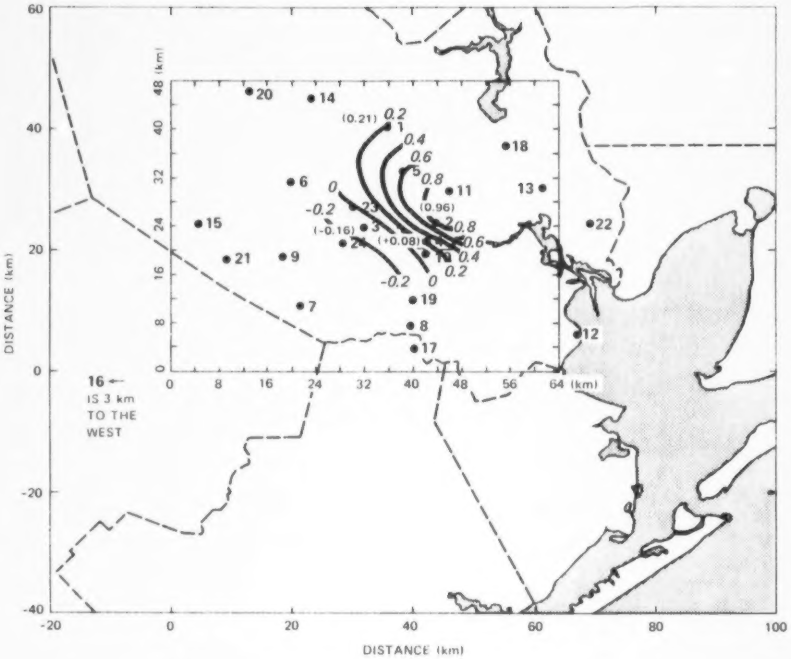

(c) SECOND EMPIRICAL ORTHOGONAL FUNCTION (34% OF VARIANCE)

Figure 17. Mean NMHC concentrations (ppbC) and the two most important empirical orthogonal functions. (Concluded)

As expected, the mean NMHC pattern shown in Figure 17(a) tends to reflect the source distribution in the area, with a ridge of high concentration extending over the area just north of the ship channel out from the peak concentration near central Houston. An examination of the most important empirical orthogonal function, shown in Figure 17(b), shows that most of the variability accounted for by this function arises from observations at Site 3, which is in downtown Houston. The empirical orthogonal functions have been normalized (i.e., the sum of the squares of the four values plotted equals 1), so that the value of -0.98 at Site 3 means that variations in the coefficients for this function translate almost directly into variations in concentration at that site; concentration variations at the other sites will be considerably smaller. Similarly, Figure 17(c) shows that most of the variance accounted for by the second empirical orthogonal function arises from variations in concentrations at Site 2 (Mae Drive).

Examination of the mean and the first empirical orthogonal function patterns shows that large negative coefficients for the first function will tend to make the mean pattern more pronounced, i.e., raise the ridge and the high values in the mean pattern. Large positive coefficients for the first function will tend to do the opposite and weaken the pattern. Large positive coefficients for the second empirical orthogonal function will tend to shift the location of the maximum values toward Site 2, east of the position of the mean field.

Figure 18 shows the diurnal variation in the coefficient for the first two empirical orthogonal functions in NMHC. The curves are shown by dashed lines during the forenoon hours because during these hours considerable data were missing, so the averages are based on fewer cases than for other hours of the day. Remembering that large negative coefficients for the first empirical orthogonal function will cause an accentuation of the mean pattern, we see that this should happen during the hours around 0600-0700. This is probably caused by the morning traffic peak in combination with meteorological conditions that inhibit dilution of emissions. After the morning traffic peak, there is a rapid change from large negative to large positive values for the average coefficient of the first function. This suggests reduced concentrations and a more nearly uniform distribution of those concentrations. This behavior is consistent with the change in mixing that would accompany the onset of solar heating.

The average coefficients of the second pattern reach a minimum during midday and are reasonably uniform at higher values during the night. This suggests that the influence of the second pattern is governed primarily by diurnal changes in meteorological factors. Increased mixing and consequent

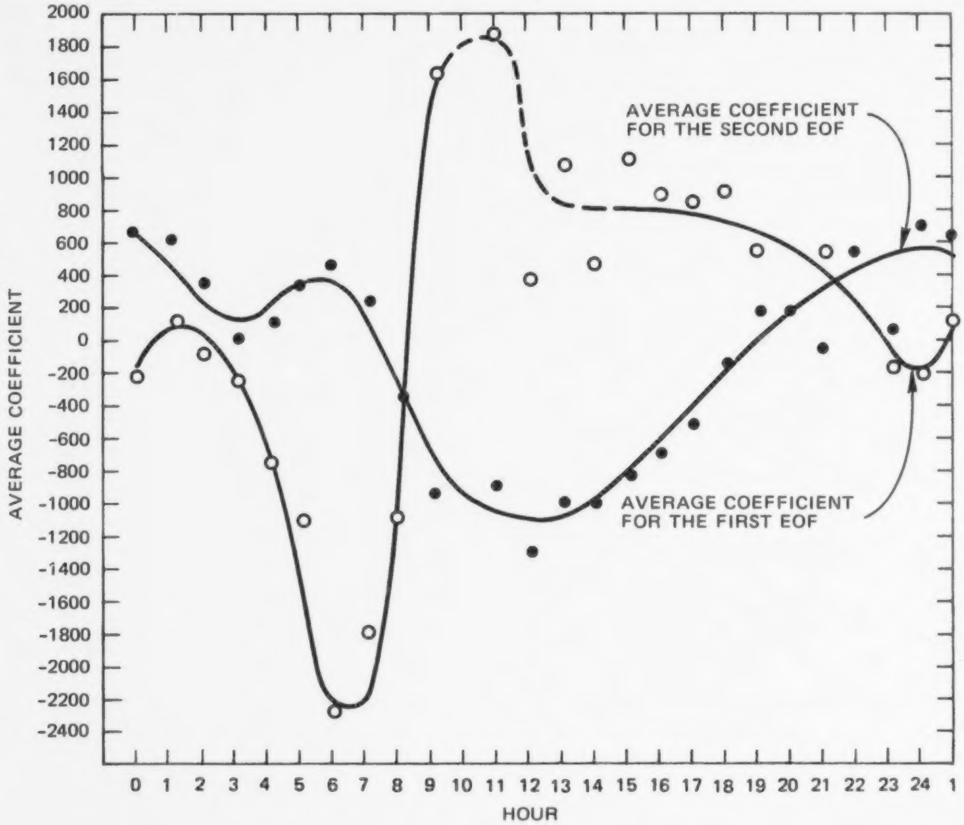

Figure 18. Average hourly values of the coefficients for the first two empirical orthogonal functions for NMHC.

dilution decreases the coefficient during the daytime relative to the night. Since this second pattern largely reflects the behavior of concentrations at Site 2, this suggests that the emissions that govern the concentrations at that site remain relatively uniform during the day, but the resulting NMHC concentrations are reduced by daytime mixing. By contrast, the first empirical orthogonal function for NMHC shows not only the influence of diurnal changes in meteorological factors, but also a pronounced influence from diurnal cycles in emissions.

Figure 19 shows the average coefficient for the first two empirical orthogonal functions for NMHC according to the wind direction measured at Mae Drive (Site 2). As before, there is considerable scatter in the data, arising

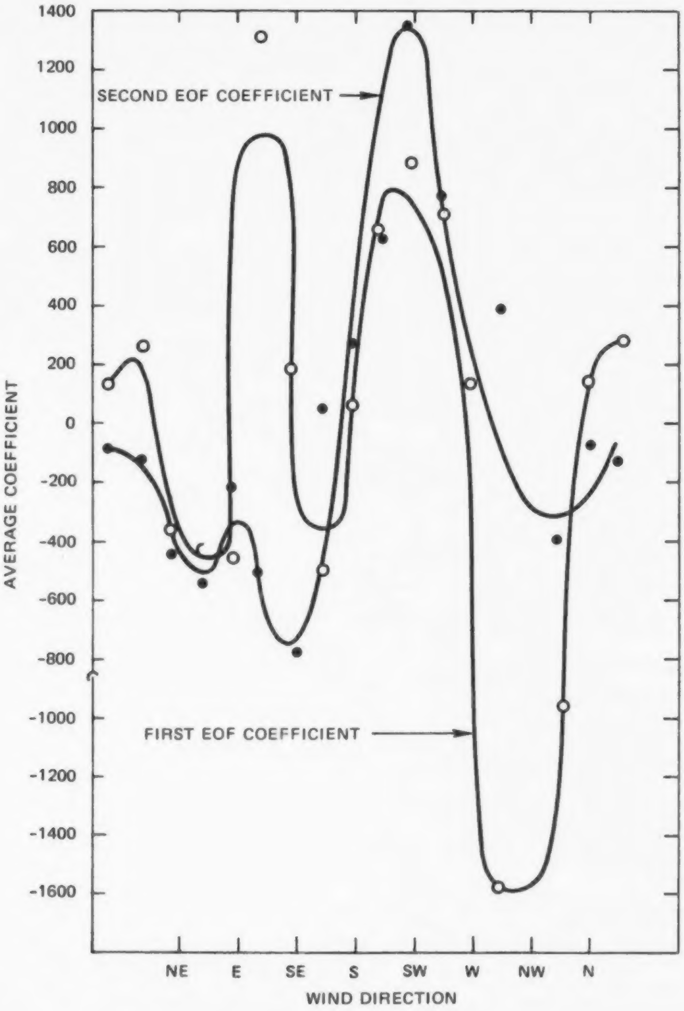

Figure 19. Average values of the coefficients for the first two empirical orthogonal functions for NMHC according to wind direction at Mae Drive.

from differences in wind directions. This is especially apparent in the coefficients for the first empirical orthogonal function; most pronounced are the large negative values associated with winds from the northwest. This may be a consequence of two different effects. First, the wind may have been from the northwest more frequently during the morning hours when, as discussed above, the higher emissions lead to higher concentrations near Site 3. The second factor is of course that major sources of hydrocarbons are located northwest of the site.

The behavior of the coefficients for the second empirical orthogonal function is more easily explainable. As noted before, this function chiefly reflects influences on concentration at Site 2. Thus, the peak coefficient values associated with winds from the southwest suggest that important hydrocarbon sources southwest of Site 2 are major contributors to the observed NMHC concentration at that site.

Oxides of Nitrogen

Figure 20(a), (b), and (c) shows the mean NO_x concentration pattern and those for the two most important empirical orthogonal functions. As with the hydrocarbons, the patterns are based on data from four stations, but they are a different four. The highest mean values occur near the center of the region and fall off toward the north, northwest, and west; no data were used in these analyses that would describe gradients in other directions. The most important empirical orthogonal function (which explains 65 percent of the variance) is generally similar in pattern to the mean. Therefore, high positive values of the coefficient for that function will increase concentrations in the central part of the region and result in steeper gradients as one moves away from it.

As was the case with the NMHC, the two most important empirical orthogonal functions for the NO_x data tend to be associated with observations from individual sites. The first empirical orthogonal function is strongly reflective of conditions at Site 2, while the second (which explains 23 percent of the variance) is almost exclusively the result of observations at Site 20. A large negative coefficient for the second function indicates a large increase in concentration at Site 20, with relatively little change at the other sites. This is the pattern that one might expect if concentrations at a given location were very heavily influenced by emissions from a single source. Figure 21 tends to support this interpretation. This figure shows average coefficients for the different wind directions measured at Aldine. For the second most important empirical orthogonal function, which primarily governs concentration changes at Site 20, the average coefficient remains relatively constant for all directions except those from south to southwest. We have been unable to identify a major NO_x source in that direction from Site 20, although there is considerable directional dependence of the observed NO_x concentrations at Site 20.

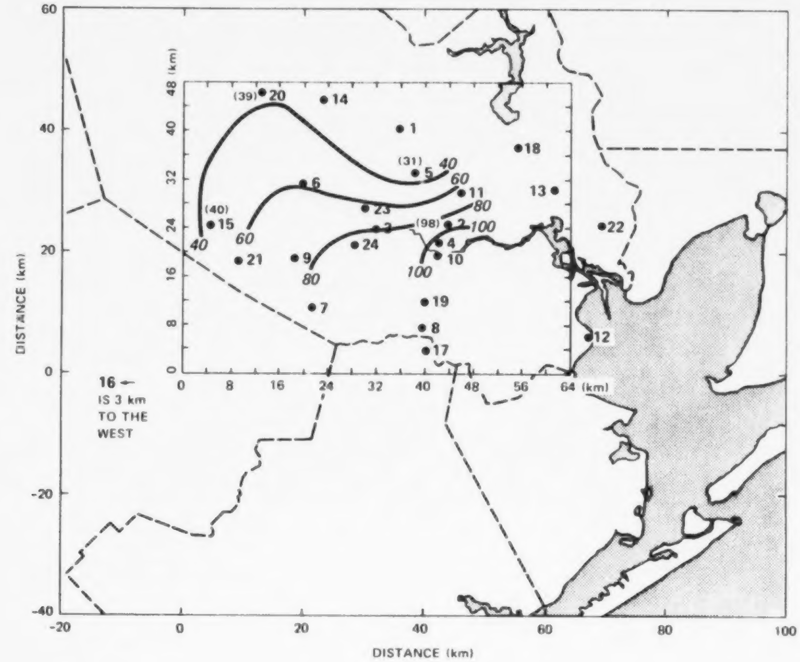

(a) MEAN NO_X

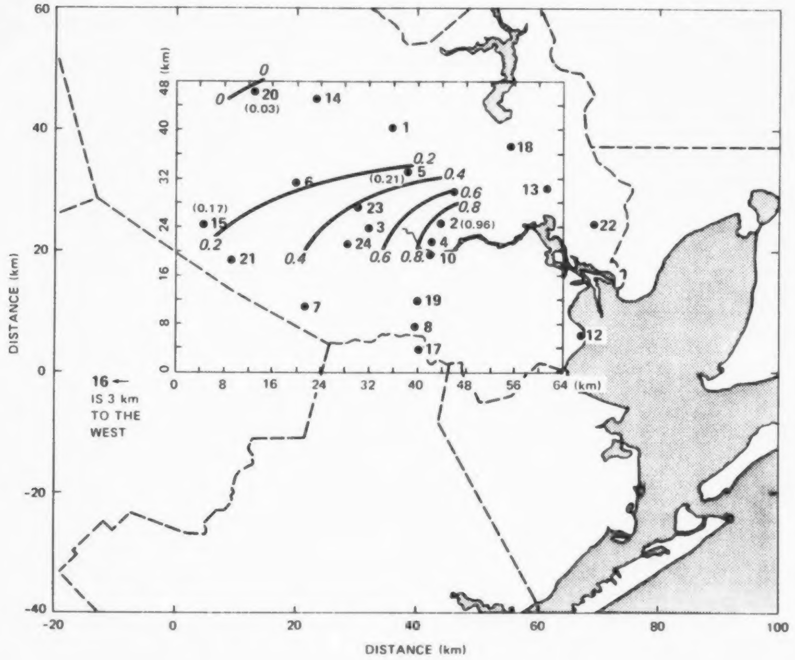

(b) FIRST EMPIRICAL ORTHOGONAL FUNCTION (65% OF VARIANCE)

Figure 20. Mean NO_x concentrations (ppb) and the two most important empirical orthogonal functions.

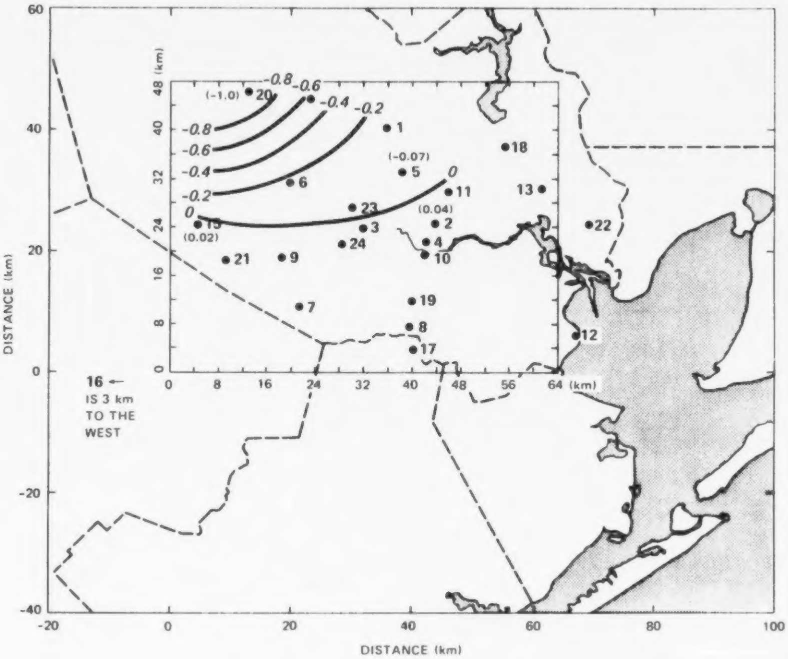

(c) SECOND EMPIRICAL ORTHOGONAL FUNCTION (23% OF VARIANCE)

Figure 20. Mean NO_x concentrations (ppb) and the two most important empirical orthogonal functions. (Concluded)

The curve shown in Figure 21 indicates that high positive values for the most important empirical orthogonal function are generally associated with winds from the southwest to west. Since this function is most characteristic of concentrations at Site 2, the results suggest that concentrations of NO_x observed at that site are heavily influenced by emissions in the central Houston area. The secondary peak associated with winds from the east-northeast may reflect more localized influences, but again we have not been able to identify just what those influences are.

Figure 22 shows the diurnal behavior of the coefficients for the two most important NO_x empirical orthogonal functions. The influence of the morning traffic peak is clearly evident in the coefficient for the first function. This supports the earlier contention that the major influence on the coefficient for this function was to be found in the emissions from central Houston. There are also counterbalancing effects from the diurnal cycles of mixing and dilution, as was discussed earlier in connection with the most important function for the NMHC.

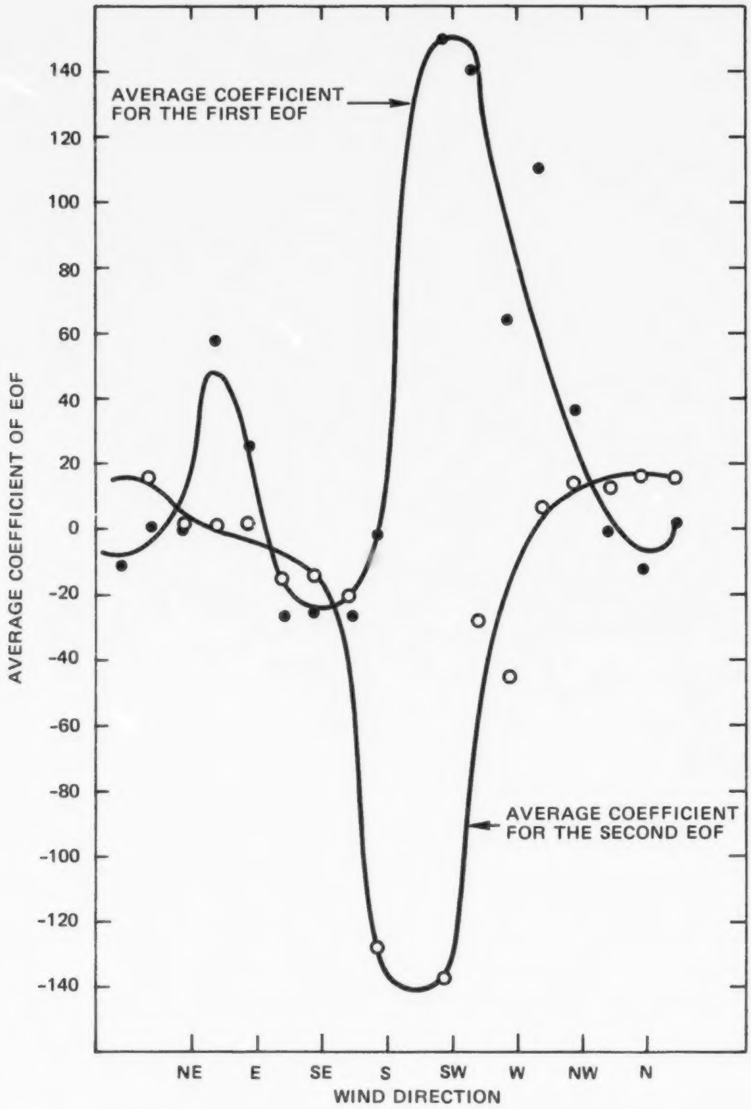

Figure 21. Average values of the coefficients for the first two empirical orthogonal functions for NO_x according to wind direction at Aldine.

The large negative values of the average coefficients for the second empirical orthogonal function at 1100 indicate increases in concentration at Site 20 at that time. This is puzzling, because there is no obvious meteorological or emissions cycle that will explain such behavior. There appears to be some localized influence that plays a strong role in determining the NO_x concentrations that were observed at Site 20.

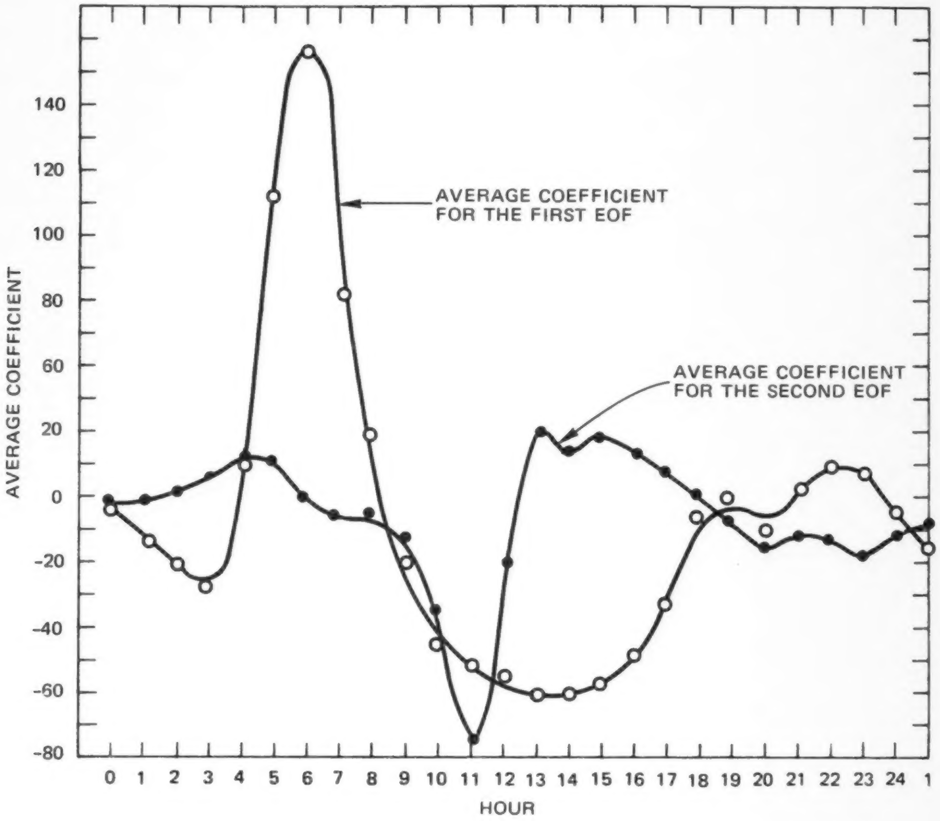

Figure 22. Average hourly values of the coefficients for the first two empirical orthogonal functions for NO_x.

Discussion

Results presented above show that empirical orthogonal functions are useful tools for interpreting air-quality data. The results show that the ozone patterns tend to be much more uniform and are characterized by larger-scale features than are the patterns for NMHC and NO_x. Therefore, the observational networks for ozone would probably not need to be quite so dense as those for the other two pollutants, to provide the kind of spatial resolution required for modeling efforts. The results show that there are important small-scale features and local influences on the NMHC and NO_x, so that more measurements of these parameters would probably be required than of the ozone concentrations. This is contrary to the design of the HOMS, the HAOS, and most other networks where ozone measurements are emphasized over those of the other pollutants. However, the distributions of NO_x and NMHC are critically important for modeling purposes because they are required initial and boundary conditions, and thus play an important role in determining ozone concentrations.

Before concluding this discussion, it is worth noting that the use of empirical orthogonal functions could provide an objective method for interpolating observed concentrations of the various pollutants. The most important of the empirical orthogonal functions (those that explain the greatest amount of variance) identify the major recurring features of the patterns, and hence can be used to smooth out some of the less important noise. Such smoothing could be very valuable for modeling purposes because it would tend to eliminate some sub-grid-size anomalies in the observations. This should make integration of the equations somewhat easier and more representative of the major processes.

CASE STUDIES OF POTENTIAL MODELING DAYS

General

Four days have been chosen from among those available to illustrate some of the effects observed in the Houston area, which might have to be treated through modeling. Two of the days are in sequence and are days when high ozone concentrations were observed in the Houston area, namely, 1 and 2 October 1978. Concentrations reached only 120 ppb at the surface during the third day selected (20 September 1978), so it is somewhat more normal in that respect, but it does have some interesting characteristics. For example, the wind direction at the surface was quite different from the wind direction at the 850-mb level (about 1500 m). The day finally chosen, 29 September 1978, also had peak observed ozone concentrations of 120 ppb at the surface. The winds at the surface also differed from those aloft in the morning, but were similar in direction during the early afternoon.

In the discussions of these four days, four types of data displays have been used. They are:

- Isopleth maps of ozone concentrations at the surface
- Isopleth maps of ozone concentrations aloft
- Isopleth mappings of ozone concentrations in a vertical plane
- Conventional profiles of ozone, NO_x, and temperature.

The first two displays are used to show differences between patterns of ozone near ground level and those aloft. The vertical cross-section analyses describe different planes on different days. In some instances, the plane was downwind of the city and perpendicular to the wind, so that the analysis provides a view of the cross section of the city's "ozone plume." In other instances, the plane of the analysis passed through the city in an upwind-downwind direction to show how the upwind conditions are modified by passage over the urban area. No attempt has been made to correct for differences in the times at which the different measurements of vertical and horizontal profiles were made, but the data have been selected so that they generally span no more than a period of two hours. It is assumed that the conditions remained the same throughout the period.

Case Studies

20 September 1978--Figure 23 shows a weather map for this day. A cold front was approaching from the northwest with winds at about 1500 meters from the southeast during the morning and from the east-southeast during the early afternoon. During the early morning, surface winds were generally from the north-northeast at the airport and the wind monitoring sites of the HOMS network. However, some of the more inland HOMS sites observed winds from the east-southeast, similar to those aloft in the early afternoon. Figure 24, based on data from Westberg et al. (1979), shows the ozone concentrations at 1500 feet. Obviously, there were very small gradients and relatively low ozone concentrations. Concentrations ranged from around 20 to 25 ppb west of the city to about 50 ppb near the coast. At the same time (0700 CST), the ozone concentrations at the surface did not exceed 15 ppb. Figure 24 shows the locations where three different spirals were taken upwind and Figure 25 shows the ozone, NO_x, and temperature readings for those profiles. The two pollutants are distributed relatively evenly in the vertical. Ozone concentrations increased slightly with height but changed by only 20 ppb at most. The NO_x concentrations are also reasonably uniform in the vertical, but with some evidence in the third profile of elevated NO_x concentrations at about 4500 ft.

The fourth profile, which was taken west of Houston (see Figure 26), shows the NO_x concentrations increasing in the lowest layers, which suggests that there may be some influence from ground-level emissions. The ozone profile does not look very different from those at the other side of the city, except that it exhibits a more pronounced decrease in concentration at the lower levels, consistent with the NO_x profile.

By midday, the situation in the Houston area had changed considerably. Figure 27 shows the ozone concentrations aloft at 1500 feet during the period from around 1100 to 1400 CST. At this altitude, there was an area of higher ozone concentrations, in excess of 190 ppb to the northwest of Houston. Based on the winds aloft, this area is generally in the downwind direction. Figure 28 shows that the conditions at approximately the same time at ground level differ considerably from those aloft. The surface concentrations are generally lower and the pattern is also different, with the highest concentrations found northeast of the city. Neither the surface winds nor the upper-air winds would account for transport from the central city in this direction. If a model is to be successful in accounting for the observations, it will have to treat air flow that is different at different altitudes and different parts of the region.

The straight line in Figure 28 shows the location of the vertical cross section that was constructed in Figure 29. The cross section is generally downwind of the major emissions areas. There is considerable evidence of a plume of ozone northwest of the city at altitudes of 1500 to 2000 feet. The highest concentrations exceed 200 ppb, so there is considerable potential for introducing high concentrations of ozone to ground level from aloft. At the time, the ground-level concentrations were about 75 ppb. It will be an interesting test of the models to see if they can reproduce these vertical and horizontal gradients.

Reproduced from
best available copy.

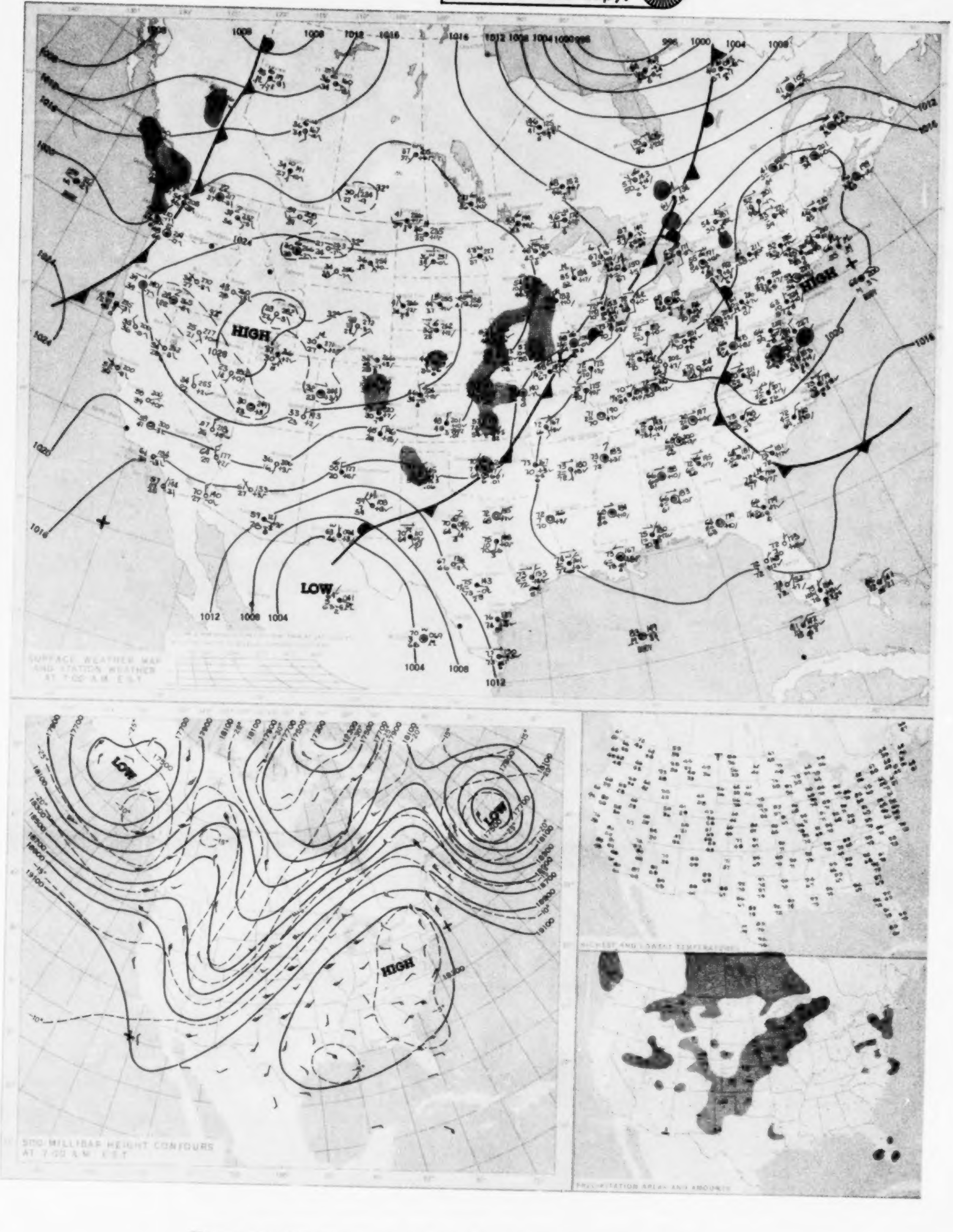
HIGH
LOW
HIGH
1012
1008
1004
SURFACE WEATHER MAP AND STATION WEATHER AT 7:00 A.M. E.S.T.
LOW
LOW
HIGH
500-MILLIBAR HEIGHT CONTOURS AT 7:00 A.M. E.S.T.
HIGHEST AND LOWEST TEMPERATURES
PRECIPITATION AREAS AND AMOUNTS

Figure 23. Weather maps for 0600 CST, 20 September 1978.

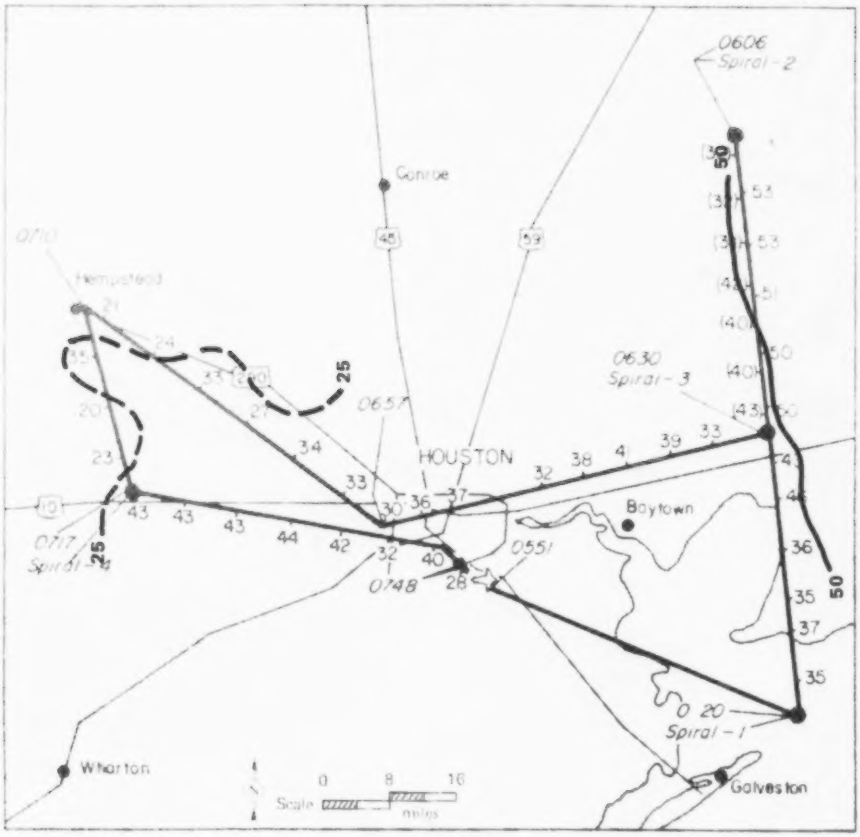

WIND:	HUB 020/6
FLIGHT ALTITUDE:	1500 ft with spirals to 6000 ft
WEATHER:	1800 scattered; 10 miles; 76° F; 29.97 (at landing)

SOURCE: Westberg et al. (1979)

Figure 24. Ozone concentrations (ppb) at 1500 ft msl, 0600–0745 CST, 20 September 1978.

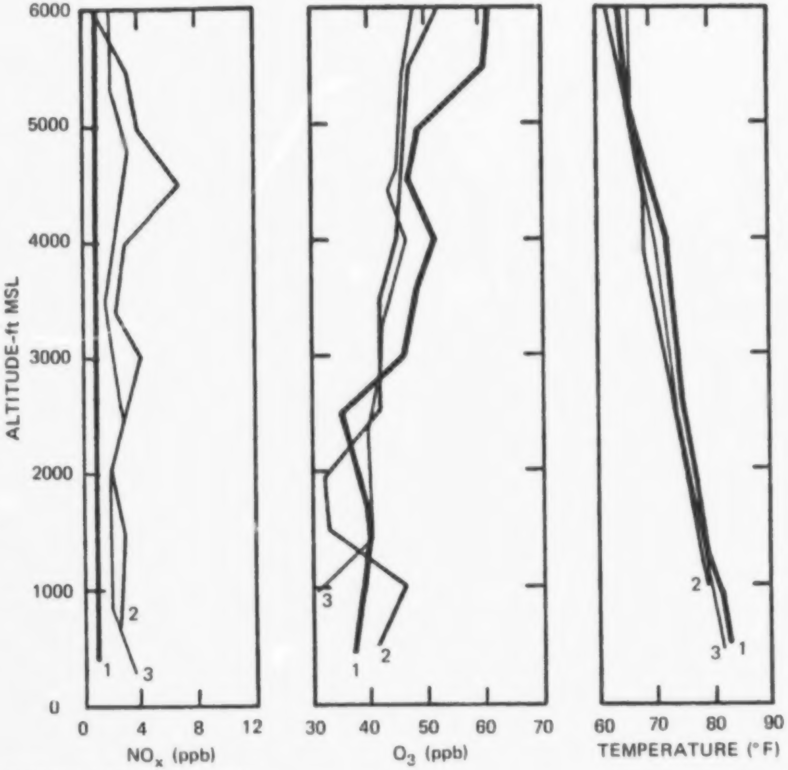

SOURCE: Westberg et al. (1979)

Figure 25. Vertical NO$_x$, O$_3$, and temperature profiles recorded east of Houston during Spirals 1, 2, and 3 on the morning flight of 20 September 1978.

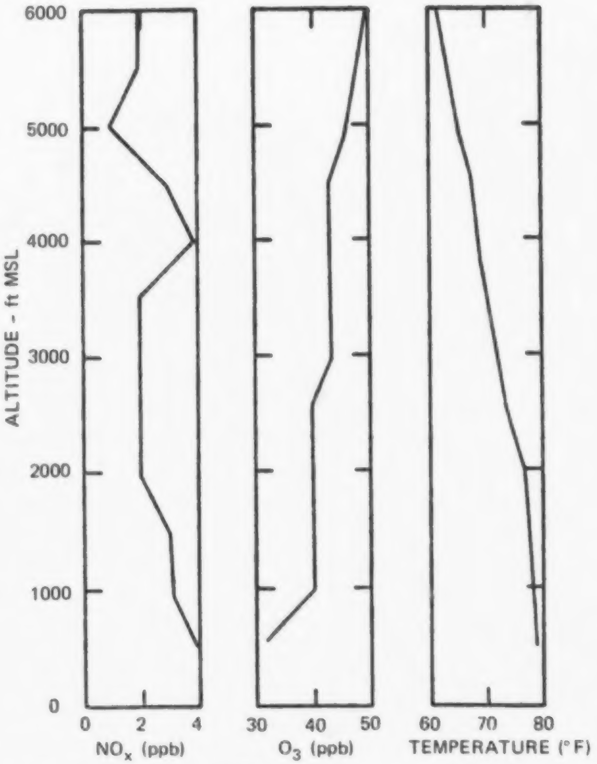

SOURCE: Westberg et al. (1979)

Figure 26. Vertical NO$_x$, O$_3$, and temperature profiles recorded west of Houston during the morning flight of 20 September 1978.

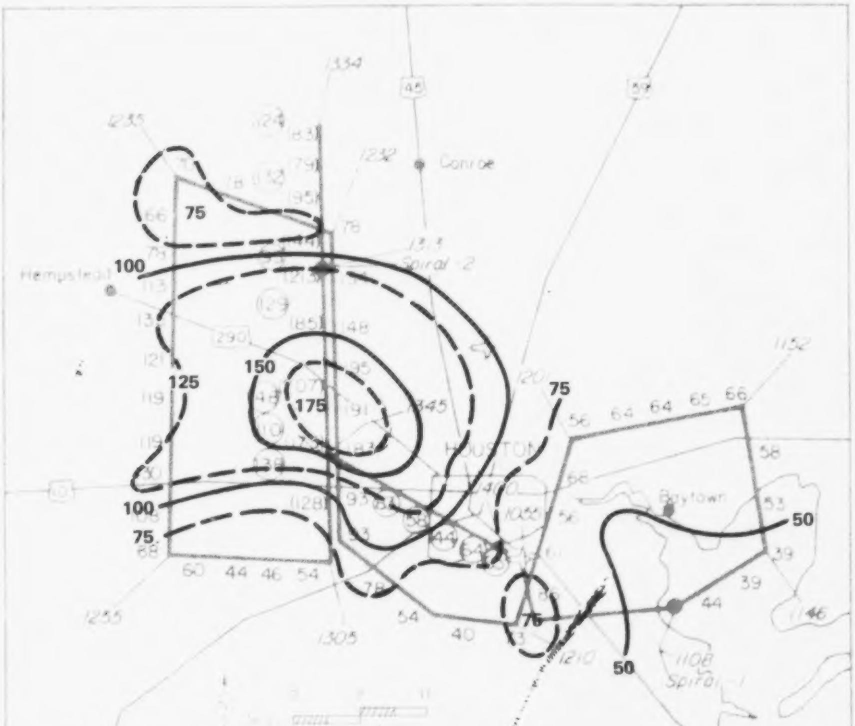

WIND:	HUB 010/5 (take-off); 090/10 (landing)
FLIGHT ALTITUDE:	1500 ft with spirals to 10000 ft; legs with ozone concentrations in parentheses and circles were at 2000 and 3000 ft respectively
WEATHER:	2300 Broken; 8000 Broken; 7 miles; 85°F; 30.00

SOURCE: Westberg et al. (1979)

Figure 27. Ozone concentrations (ppb) at 1500 ft msl from approximately 1100-1400 CST, 20 September 1978.

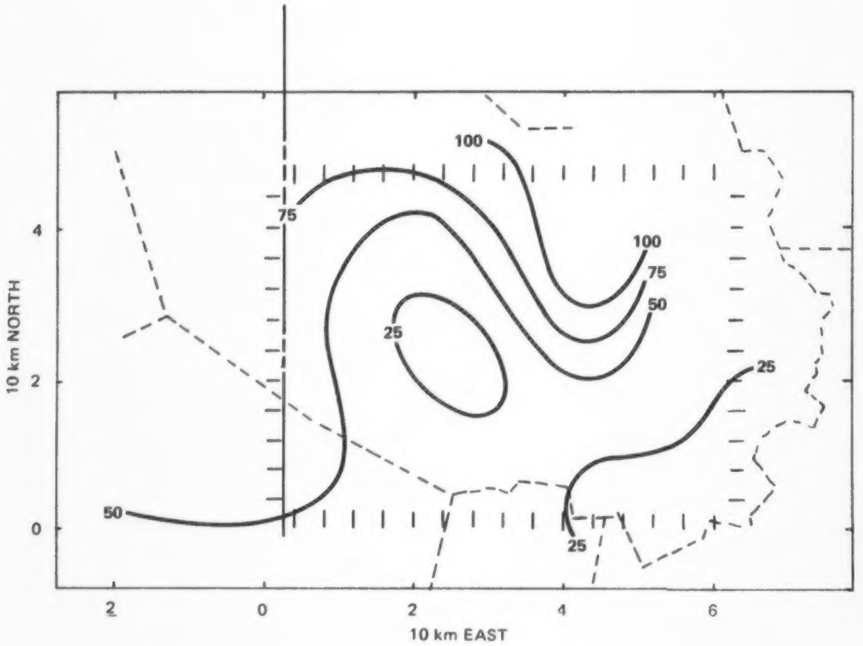

Figure 28. Ozone concentrations (ppb) at ground level, 1300 CST, 20 September 1978.

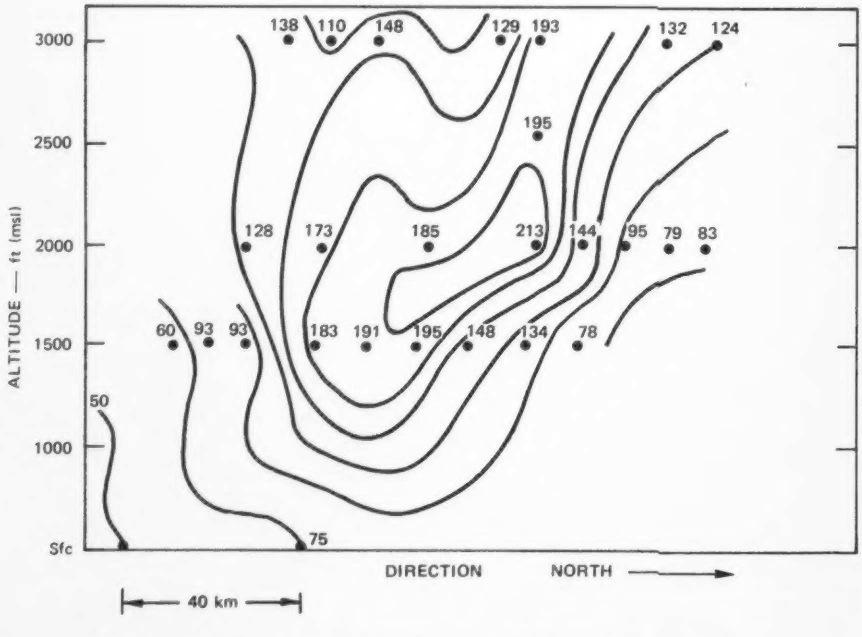

Figure 29. Vertical cross section of ozone concentrations (ppb) downwind of Houston at approximately 1300 CST, 20 September 1978.

29 September 1978--This day is similar to the one just discussed in that it did not show concentrations in excess of 120 ppb at the surface, though such concentrations were found aloft. However, the weather situation was different; the pressure gradients in the area were quite weak, as shown in Figure 30. Figure 31 shows the ozone concentrations at 1500 feet for the late morning hours of 29 September 1978. Winds at the surface and aloft were generally from the north-northeast. The pattern shows the effect of such winds with maximum concentrations south-southwest of central Houston reaching concentrations in excess of 140 ppb at 1500 feet. Figure 32 shows the surface concentrations at about the same time (1000 CST). The gradients are much smaller than they are aloft and the maximum is northwest of the city. It appears that the patterns at the surface are influenced by processes other than transport. Vertical mixing of ozone aloft to ground level may be an important determinant of ground-level concentrations, especially during the morning hours. Figure 33 shows three of the vertical profiles taken to the west of the city. It shows that there are very large vertical gradients of ozone and NO_x in the lowest layers. Of course, the sign of the gradients is different. The ozone increases with height and the NO_x decreases with height. One of the temperature profiles (No. 1) shows a stable layer below a thousand feet.

Figure 34 shows the ozone concentrations at 1500 feet during the early afternoon on 29 September 1980. The pattern was little changed from the morning, but concentrations were somewhat higher (exceeding 175 ppb) and the maximum shifted somewhat further east. The afternoon surface ozone pattern is shown in Figure 35. It shows a maximum to the north-northwest of town, with some indications that there is a maximum toward the south-southwest as well, but there are no data available to support this.

The curved line in Figure 35 shows the location of the vertical cross section in Figure 36. It is obvious from Figure 36 that the higher ozone concentrations were found throughout a deep layer of the atmosphere. The area where concentrations exceed 150 ppb extends from about 1000 feet to 3000 feet, but the vertical gradient in the lowest levels is quite sharp, so the surface concentrations do not reach even 100 ppb beneath this layer of high ozone. This further illustrates the importance of three-dimensional effects in determining ozone.

1 and 2 October 1978--Figure 37 shows the weather map for 1 October 1978. It is apparent that there was almost no pressure gradient in the Houston area, so winds were quite light and allowed the accumulation of precursors. Furthermore, the clear skies promoted strong surface heating, so that vertical mixing was pronounced. As we shall see, this led to reasonably uniform vertical distributions of ozone.

As noted earlier, 1 October was a day of high ozone concentrations and good data coverage. This day also has data from the evening hours, so that examination of the ozone destruction process might be possible. Figures 38 and 39 show the ozone distributions at 1500 feet and at the surface, respectively, around 1400 on 1 October 1978. Greater similarity is seen in the two patterns in this case than in the previous examples. At both altitudes, the highest ozone concentrations are found near the downwind edge of the city; the concentrations aloft are only somewhat higher than they are at the surface.

Reproduced from best available copy.

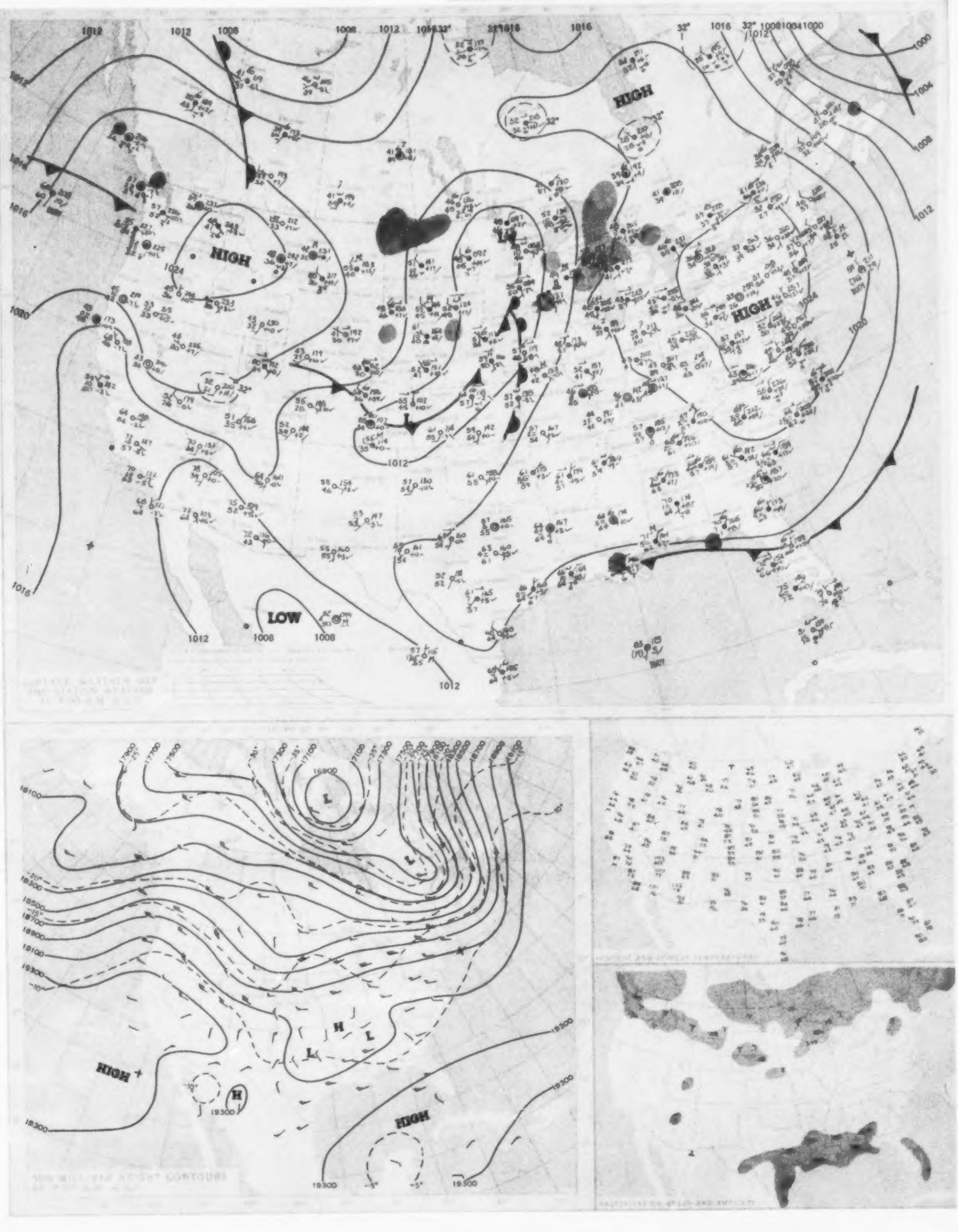

Figure 30. Weather maps for 0600 CST, 29 September 1978.

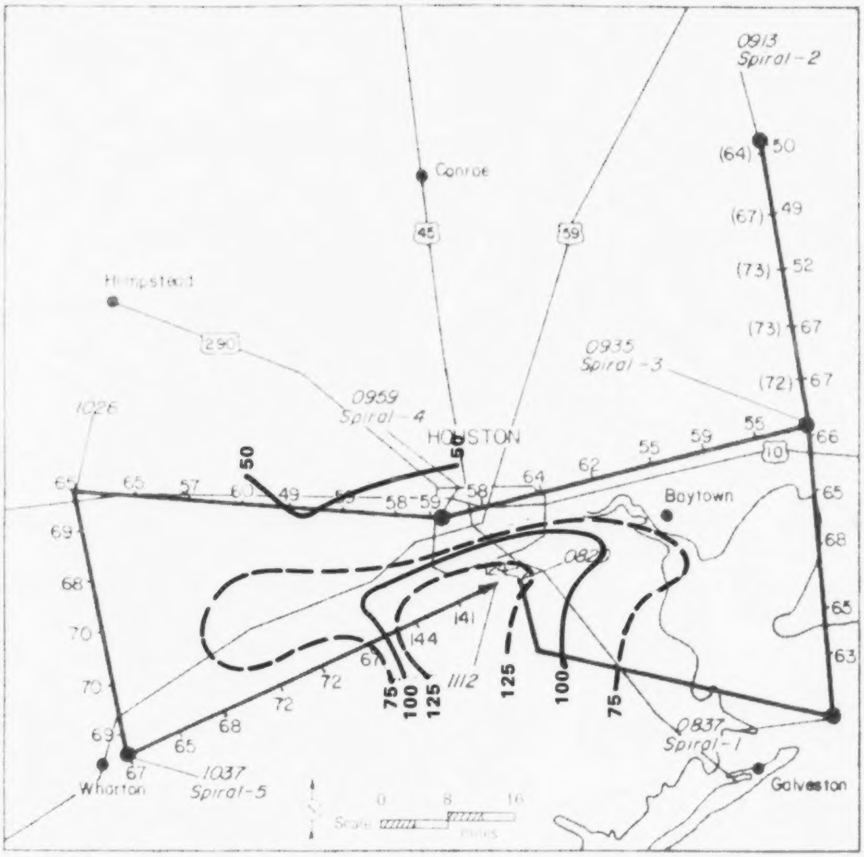

WIND:	HUB 120/10 (take-off) 060/6 (landing)
FLIGHT ALTITUDE:	1500 ft with spirals to 6000 ft; leg with O_3 concentrations in parentheses was at 6000 ft
WEATHER:	5000 scattered; 12000 scattered; 5 miles haze/smoke; 77° F; 30.03

SOURCE: Westberg et al. (1979)

Figure 31. Ozone concentrations (ppb) at 1500 ft msl from approximately 0830-1115 CST, 29 September 1978.

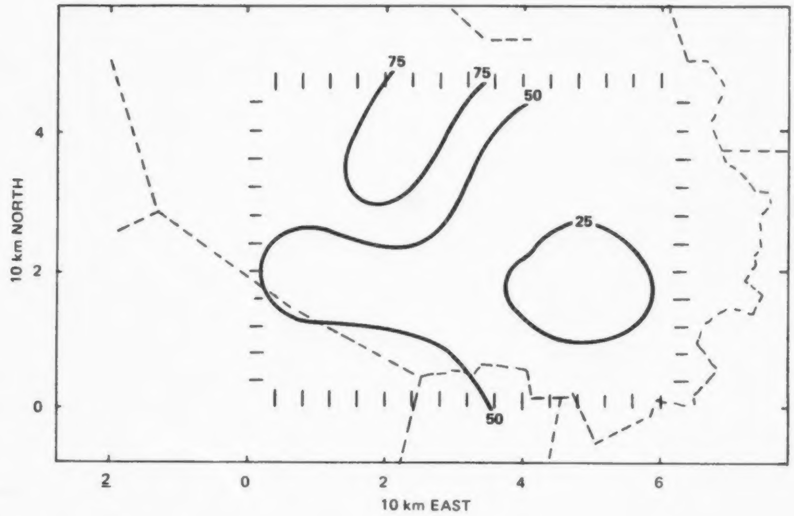

Figure 32. Ozone concentrations (ppb) at ground level, 1000 CST, 29 September 1978.

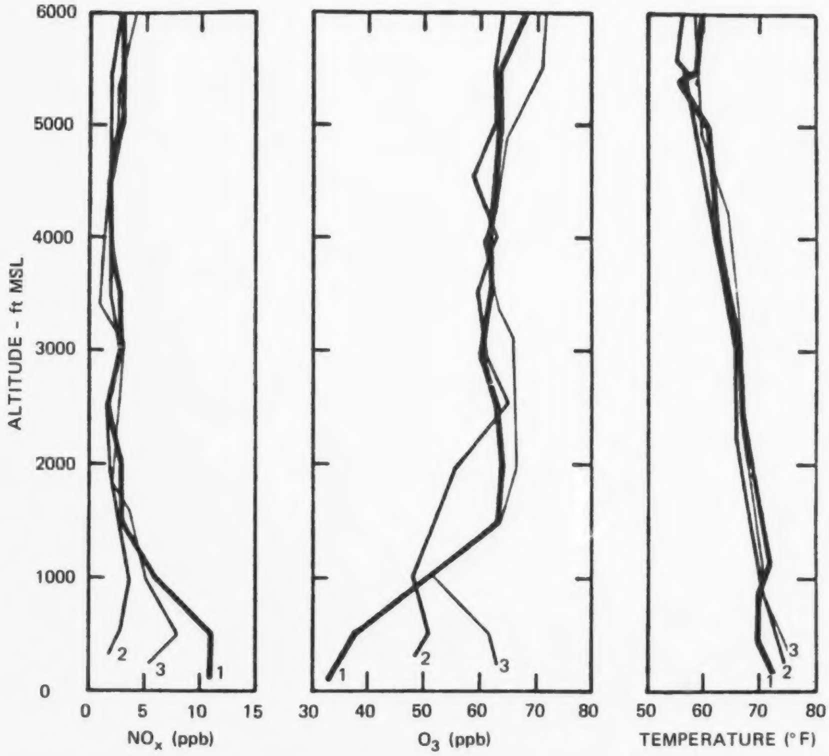

SOURCE: Westberg et al. (1979)

Figure 33. Vertical NO_x, O_3, and temperature profiles recorded east of Houston during Spirals 1, 2, and 3 on the morning flight of 29 September 1978.

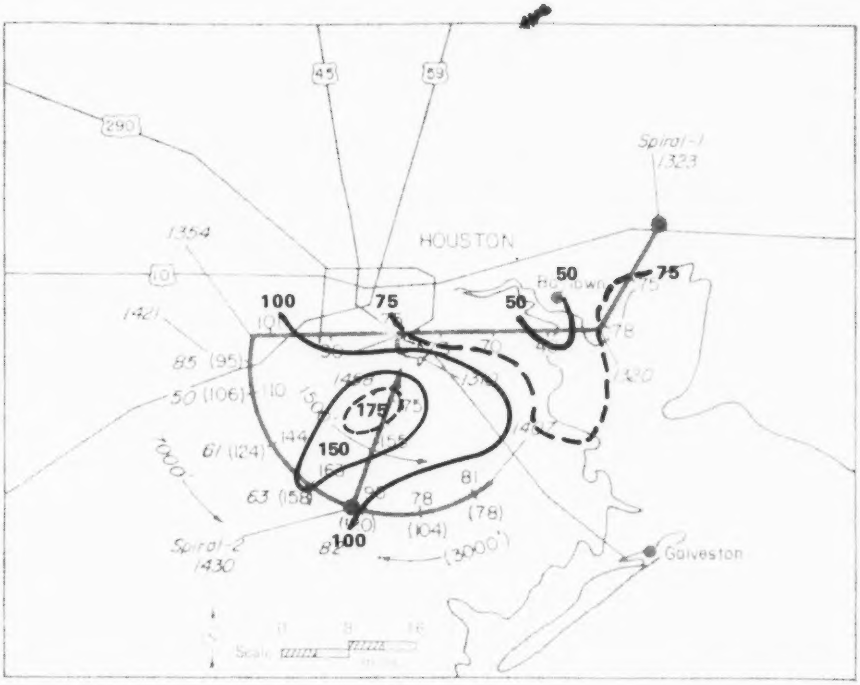

WIND:	050/8
FLIGHT ALTITUDE:	1500 ft with spirals to 7500
WEATHER:	3500 broken 25000 broken; 7 miles; 81° F; 29.97

SOURCE: Westberg, et al. (1979)

Figure 34. Ozone concentration (ppb) at 1500 ft msl from 1320-1500 CST, 29 September 1978.

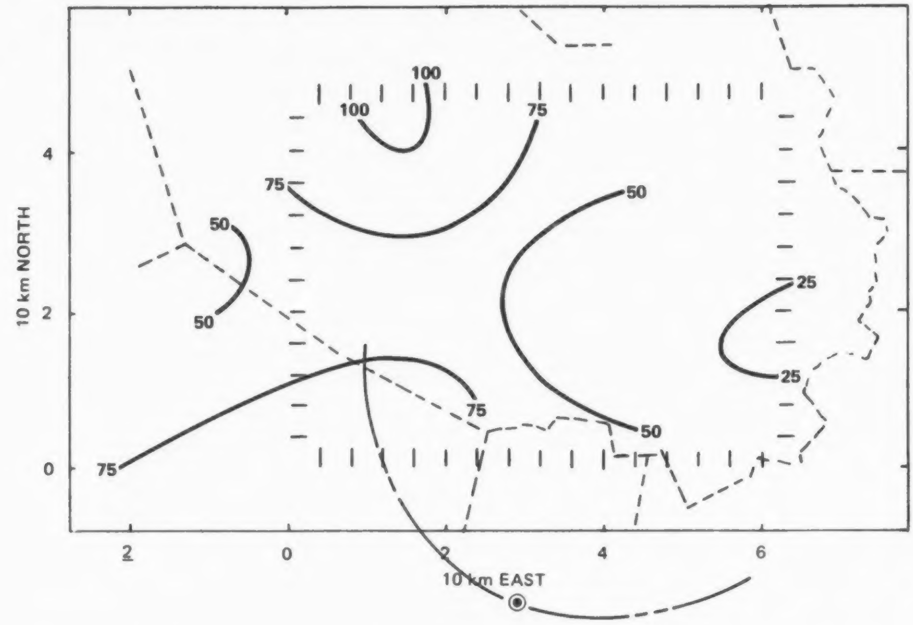

Figure 35. Ozone concentrations (ppb) at ground level, 1400 CST, 29 September 1978.

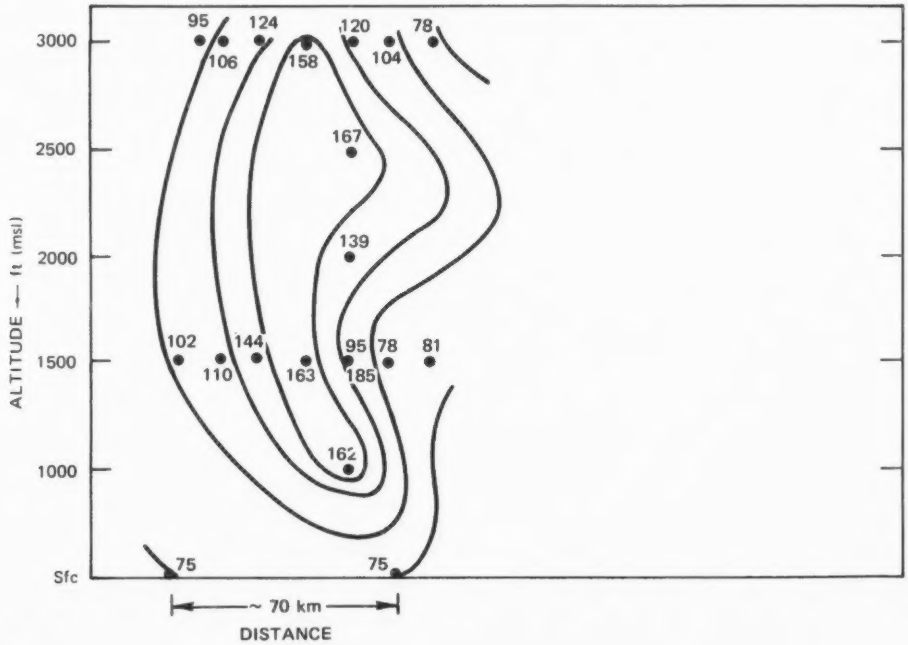

Figure 36. Vertical cross section of ozone downwind of Houston at approximately 1400 CST, 29 September 1978.

Reproduced from best available copy.

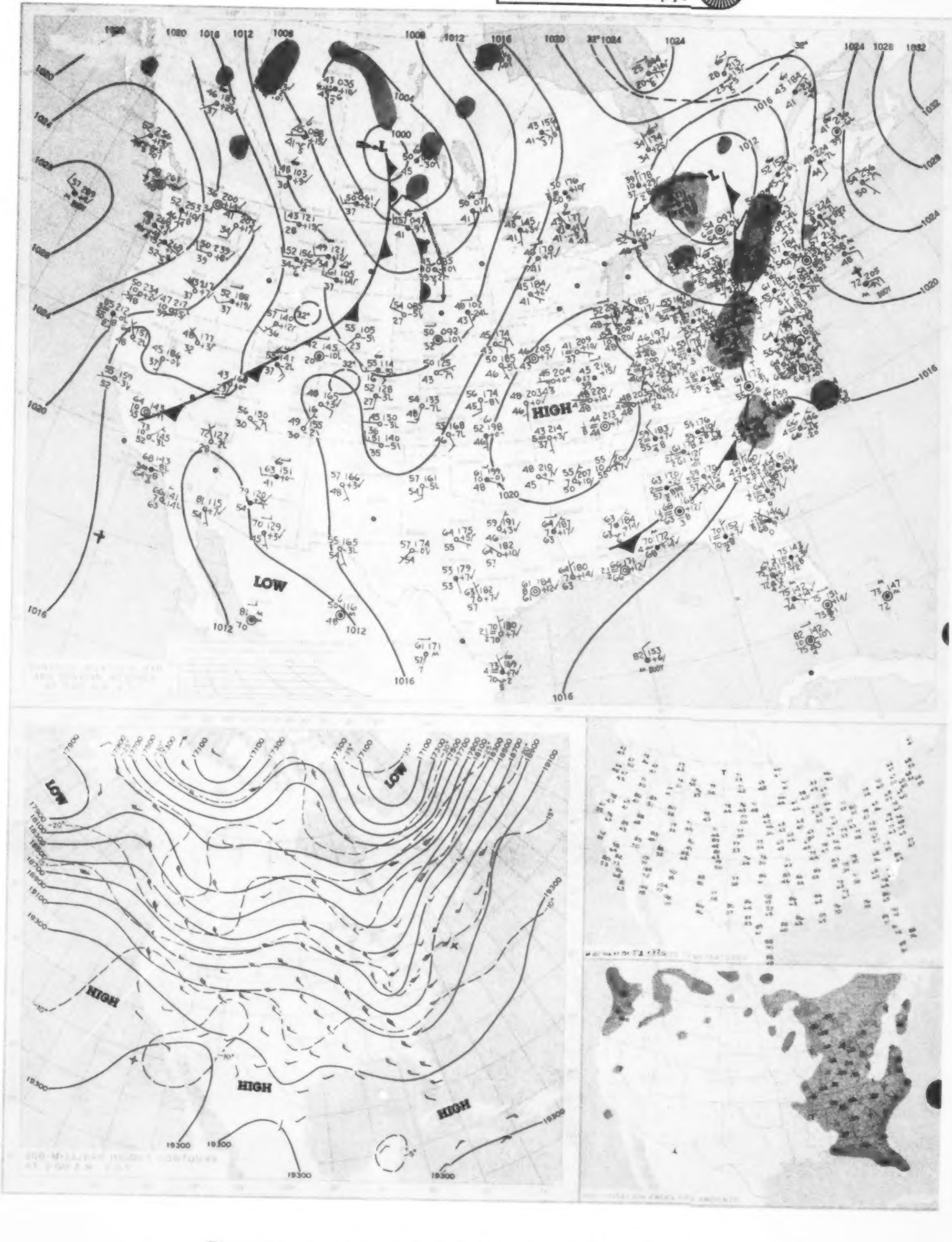

Figure 37. Weather maps for 0600 CST, 1 October 1978.

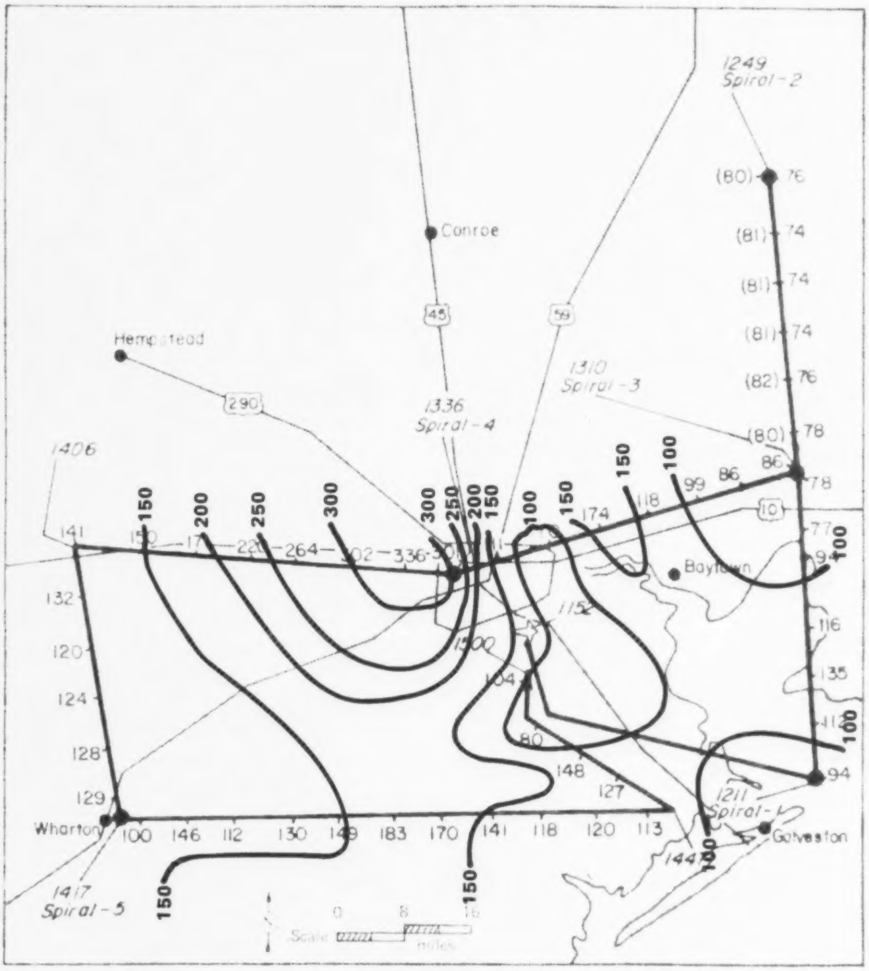

WIND: HUB 310/4 (take-off) 080/8 (landing)

FLIGHT ALTITUDE: 1500 ft with spirals to 6000 ft; leg with O_3 concentrations in parentheses was at 6000 ft

WEATHER: Clear; 6 miles haze/smoke; 86° F; 30.06

SOURCE: **Westberg et al** (1979)

Figure 38. Ozone concentrations (ppb) at 1500 ft msl from approximately 1150 to 1500 CST, 1 October 1978.

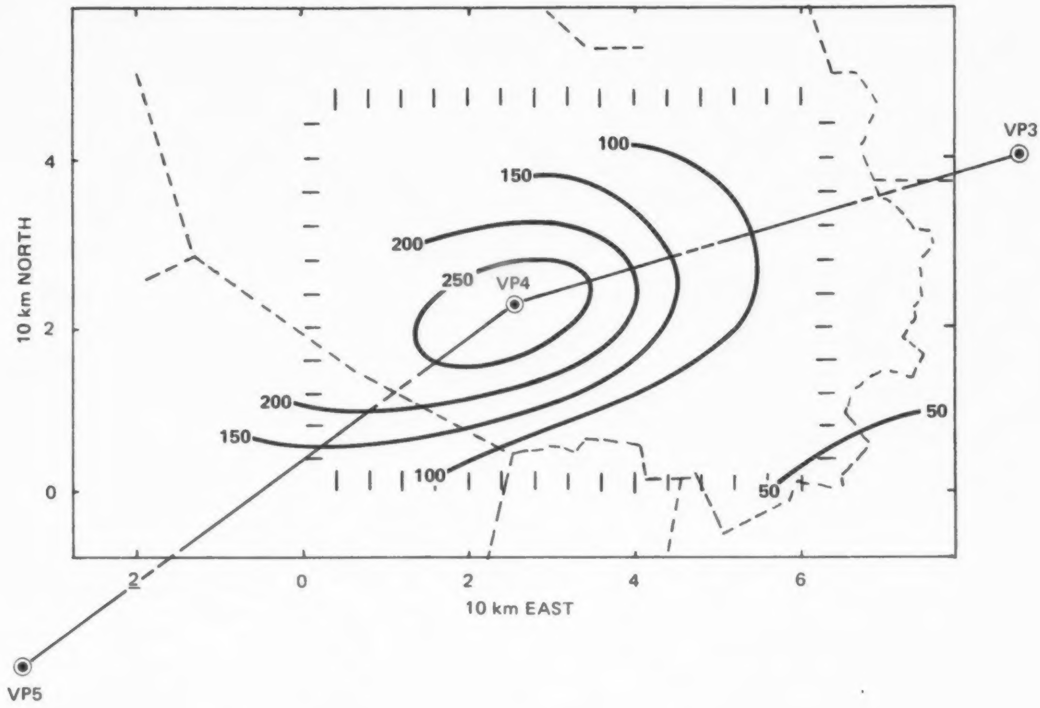

Figure 39. Ozone concentrations (ppb) at ground level, 1400 CST, 1 October 1978.

Aloft, they exceed 330 ppb, while at the surface they reach at least 280 ppb. Upwind concentrations tend to be around 100 ppb aloft and between 50 and 100 ppb at the surface.

The line in Figure 39 shows the position of the vertical cross section in Figure 40. In this instance, the cross-section line runs through the center of the city in a more or less upwind-downwind direction. The nearly vertical orientation of the ozone concentration isopleths in Figure 40 makes it clear why the surface and upper-level patterns are so similar. A vertical isopleth accompanies a zero vertical gradient where the patterns are the same at all altitudes. The isopleths are not perfectly vertical, but in general they slope only slightly upward toward the southwest (the left side of the cross section in Figure 40). Generally, this is the downwind direction, and so the indication is that the pattern has been transported faster and somewhat farther aloft than at the surface. This is not unexpected and it explains the slight downwind displacement of the pattern aloft relative to that at the surface.

Figure 41 shows the ozone concentrations at 1500 feet during the early evening. The peak ozone concentrations are still nearly as great as earlier in the day, but they are considerably farther downwind (toward the northwest). Figure 42 shows that there has been a considerable change in the ozone concentrations near the surface. By 1900, ozone concentrations at the surface were generally 60 ppb or less. Figure 43 is a vertical cross section along the

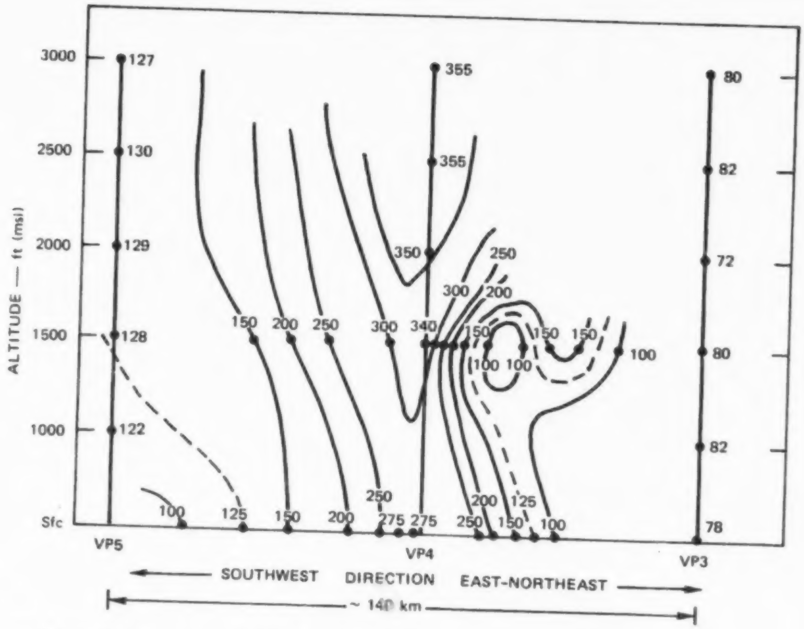

Figure 40. Vertical cross section of ozone concentrations (ppb) in the Houston area at approximately 1400 CST, 1 October 1978.

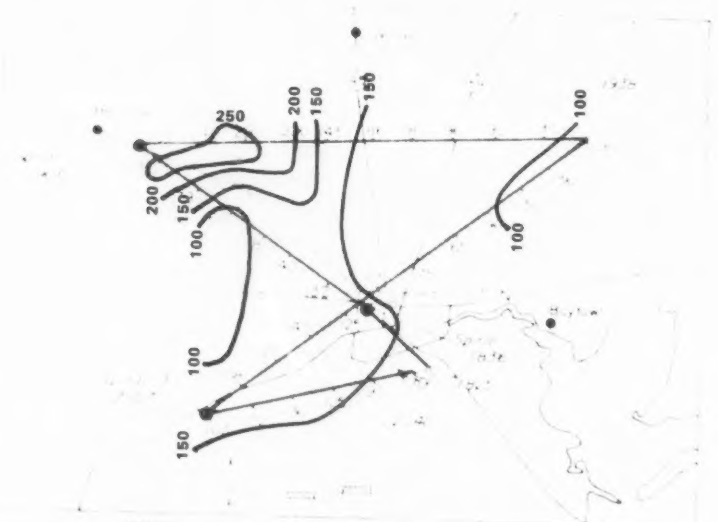

WIND: HUB 150/7

FLIGHT ALTITUDE: 1500 ft with spirals to 6000 ft

WEATHER: Clear; 6 miles haze/smoke;
76° F; 30.01

SOURCE: Westberg et al. (1979)

Figure 41. Ozone concentrations (ppb) at 1500 ft msl from approximately 1825 to 2040 CST, 1 October 1978.

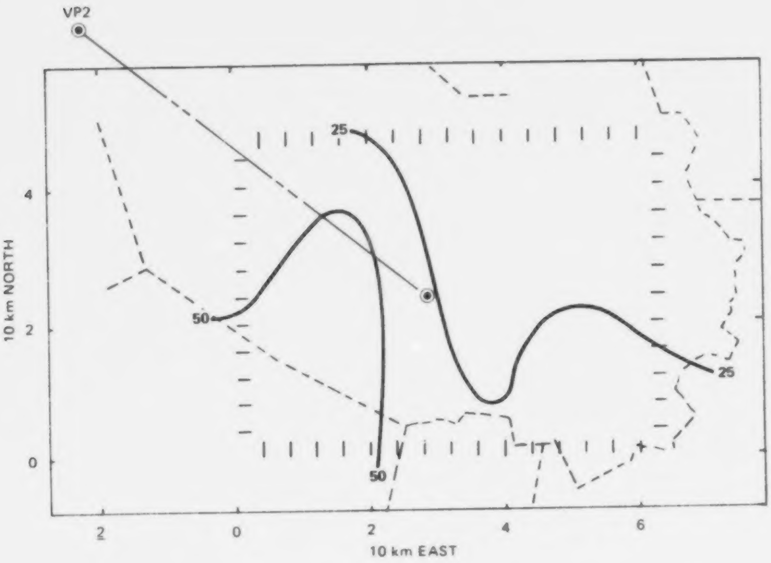

Figure 42. Ozone concentrations (ppb) at ground level, 1900 CST, 1 October 1978.

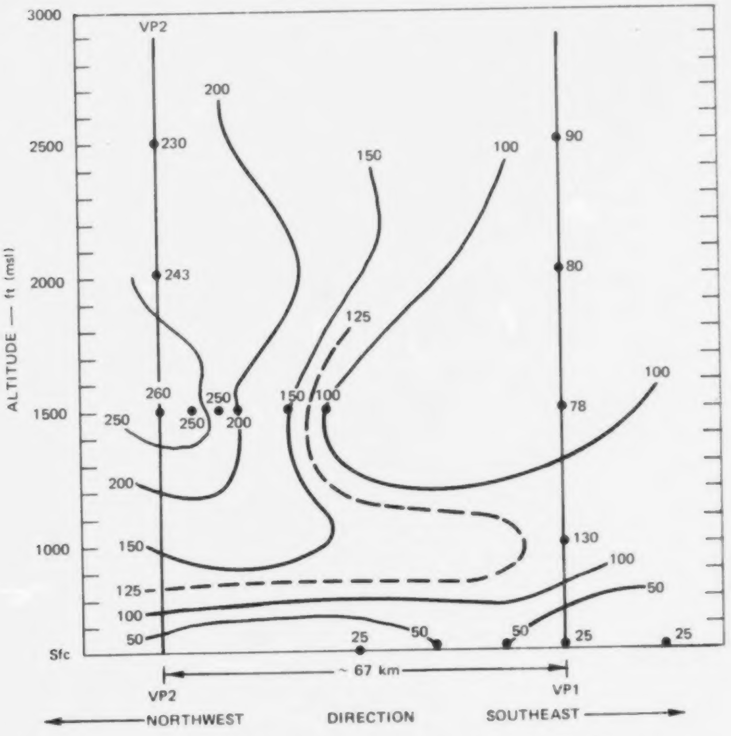

Figure 43. Vertical cross section of ozone concentrations (ppb) in the Houston area at approximately 1900 CST, 1 October 1978.

line shown in Figure 42. It shows why the surface and upper-level distributions are so different. There were very strong vertical gradients of ozone concentration in the lowest several hundred feet, indicating destruction of ozone at the surface, while ozone aloft was separated from these destructive processes by a stable layer that formed during the evening. Figure 43 shows what appears to be a cloud of ozone at about 1500 feet and about 60 to 70 kilometers downwind of the center of Houston.

Figure 44 shows the weather maps for the following day, 2 October 1978. The morning pressure gradients were light, but were stronger than during the preceding day because of the approaching front to the northwest. Air flow in the area had shifted more toward the south-southeast than on the preceding day. Aircraft data are available from the morning and the afternoon. Figure 45 shows the distribution of ozone aloft. Although it appears that there is a maximum to the southwest of the center of the city, it is not fully supported by observations. Furthermore, the lack of observations north of the city is a serious shortcoming because it leaves the downwind direction unmonitored.

Figure 46 shows that the ozone concentrations at the surface had a pattern similar to that seen in Figure 45, which gives us somewhat more confidence that the higher ozone concentrations are to the southwest of the city. Figure 46 shows a definite minimum of concentrations in the central part of the modeled region. Figure 47 shows the vertical profiles over the center city area (Spiral 4), and the reason for the minimum ozone concentrations is fairly clear. The higher NO_x concentrations near the surface are responsible for the sharply lower ozone concentrations, which is as expected.

Figure 48 shows that the mid-afternoon surface ozone pattern was very regular, concentrations increasing in the downwind direction from around 75 to 100 ppb in the ship channel area to more than 175 ppb at the northwest corner of the modeling area. Surprisingly, Figure 49 shows that the same pattern is not evident at 1500 feet. The temperature profiles provided by Westberg et al. (1979) are not sufficiently detailed to determine the depth of the mixing layer, but it appears that most of the higher ozone concentrations were confined below about 1500 ft.

Figure 50 is a vertical cross section along the lines shown in Figure 48. Figure 50 provides the basis for the statement made in the preceding paragraph with regard to ozone concentration. Although it appears that most of the ozone was confined to a layer below about 1500 feet, there are not enough aircraft data to confirm this completely.

Concluding Remarks

The preceding analyses clearly indicate that the processes involved in the formation and transport of ozone are very three-dimensional, and that every effort must be made to provide the models with well-resolved initial conditions in three dimensions. The performance of the models must be verified with observations made throughout the complete volume of air over the Houston region.

Reproduced from
best available copy.

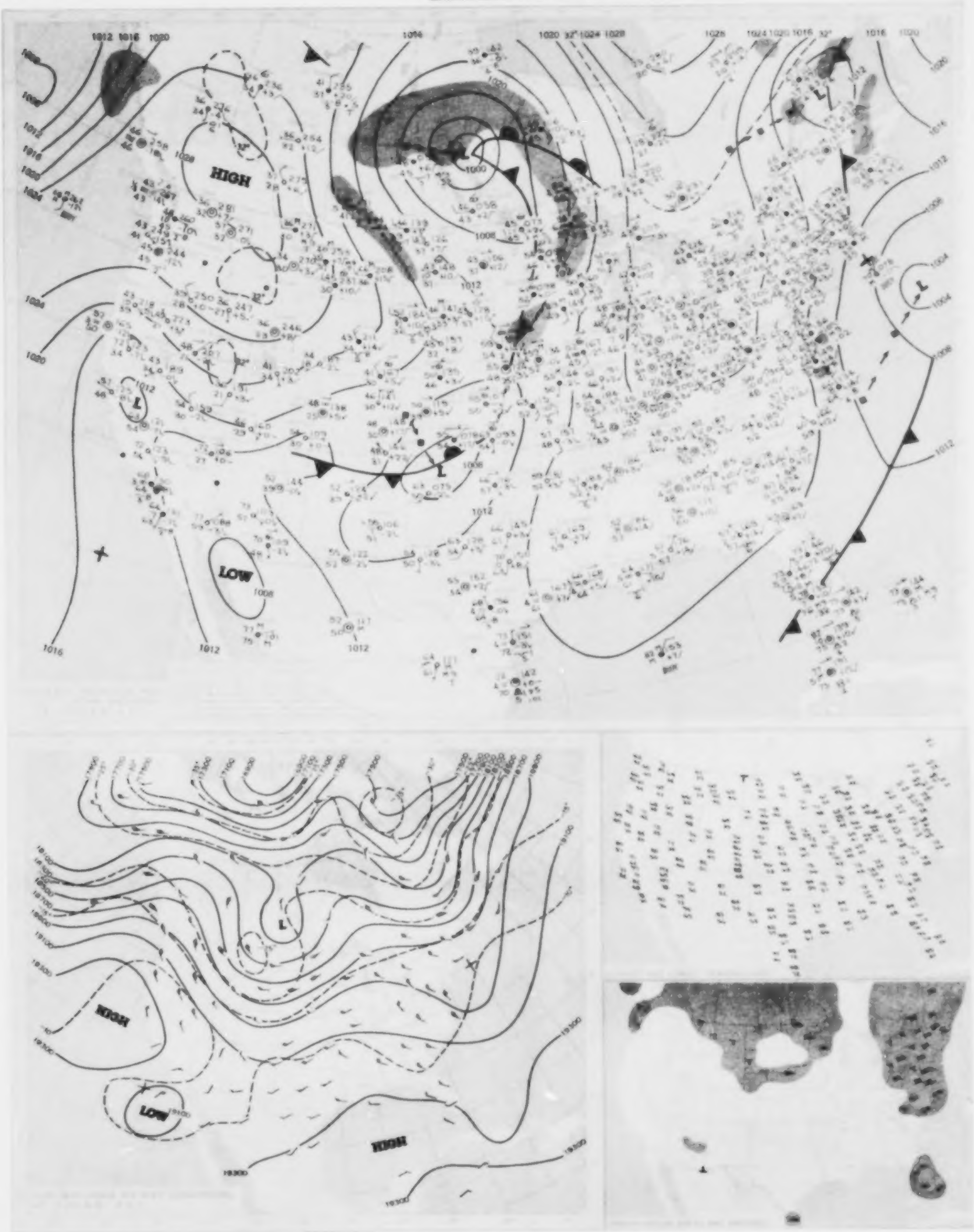

Figure 44. Weather maps for 0600 CST, 2 October 1978.

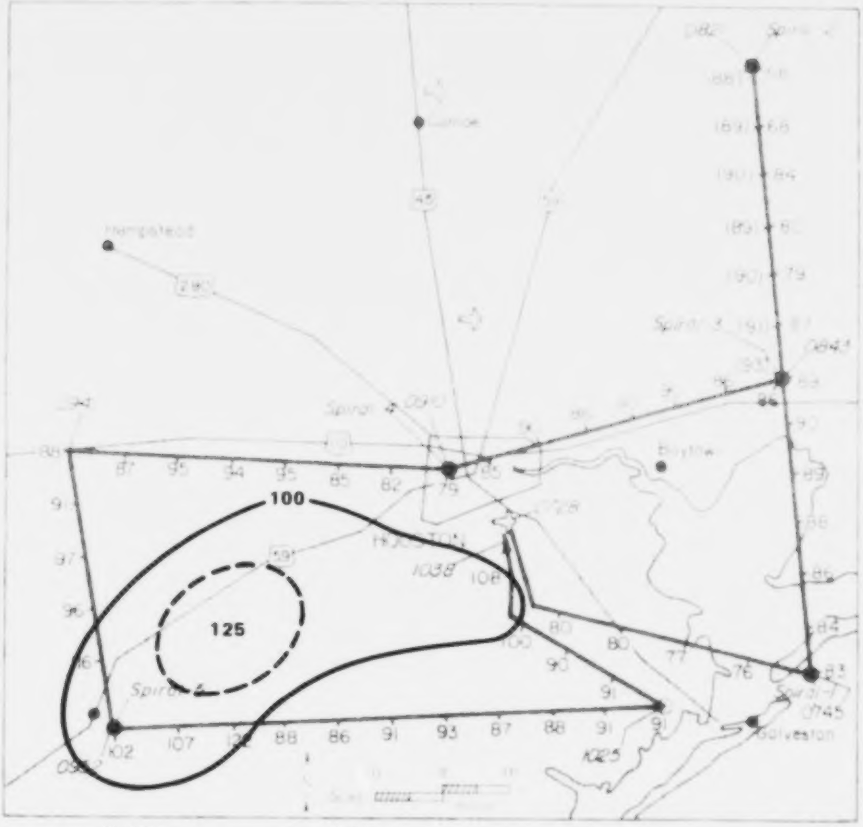

WIND: Calm

FLIGHT ALTITUDE: 1500 ft with spirals to 6000 ft; leg with O_3 concentrations in parentheses was at 6000 ft

WEATHER: Clear; 3 miles fog/haze/smoke; 68° F; 30.03

SOURCE: Westberg et al. (1979)

Figure 45. Ozone concentrations (ppb) at 1500 ft msl from approximately 0730–1040 CST, 2 October 1978.

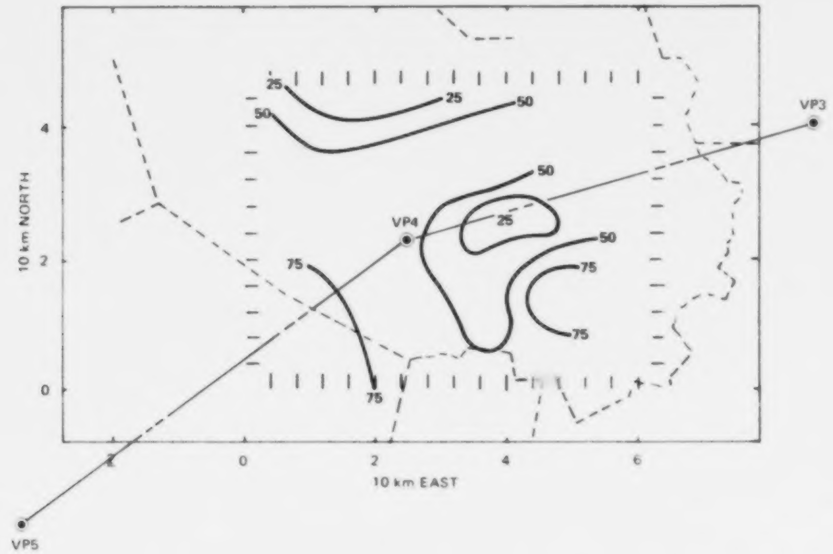

Figure 46. Ozone concentrations (ppb) at ground level, 0900 CST, 2 October 1978.

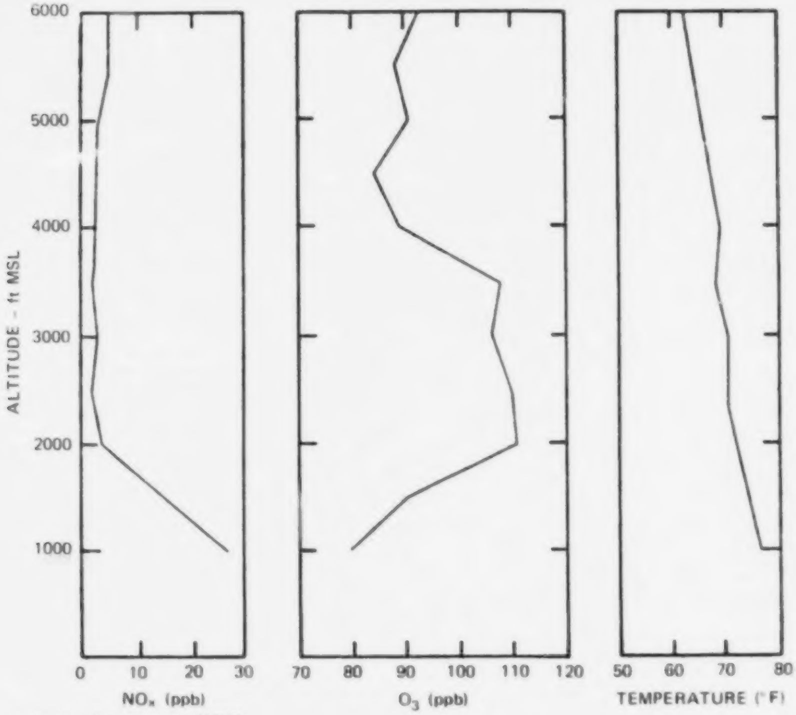

SOURCE: Westberg et al. (1979)

Figure 47. Vertical NO$_x$, O$_3$, and temperature profiles recorded over central Houston during the morning flight of 2 October 1978.

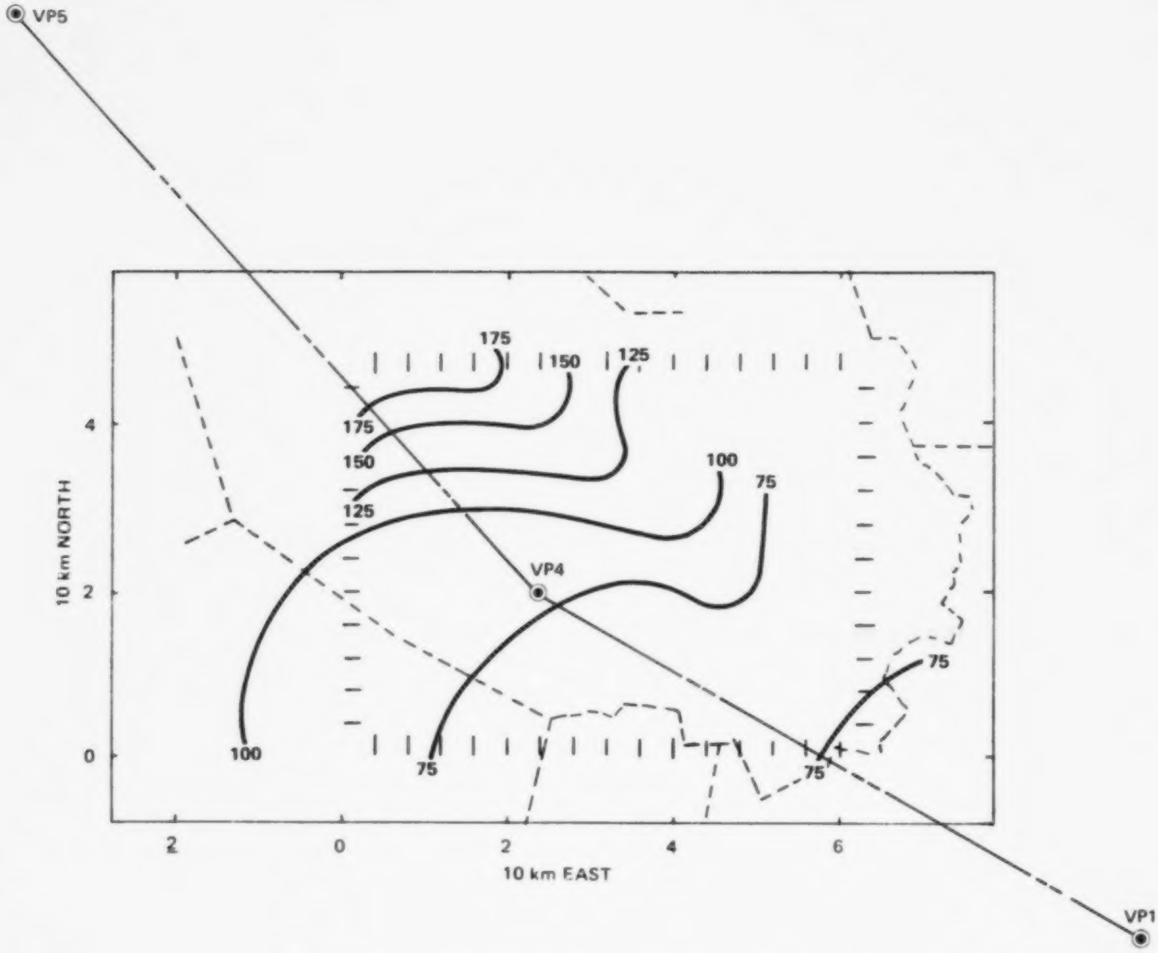

Figure 48. Ozone concentrations (ppb) at ground level, 1500 CST, 2 October 1978.

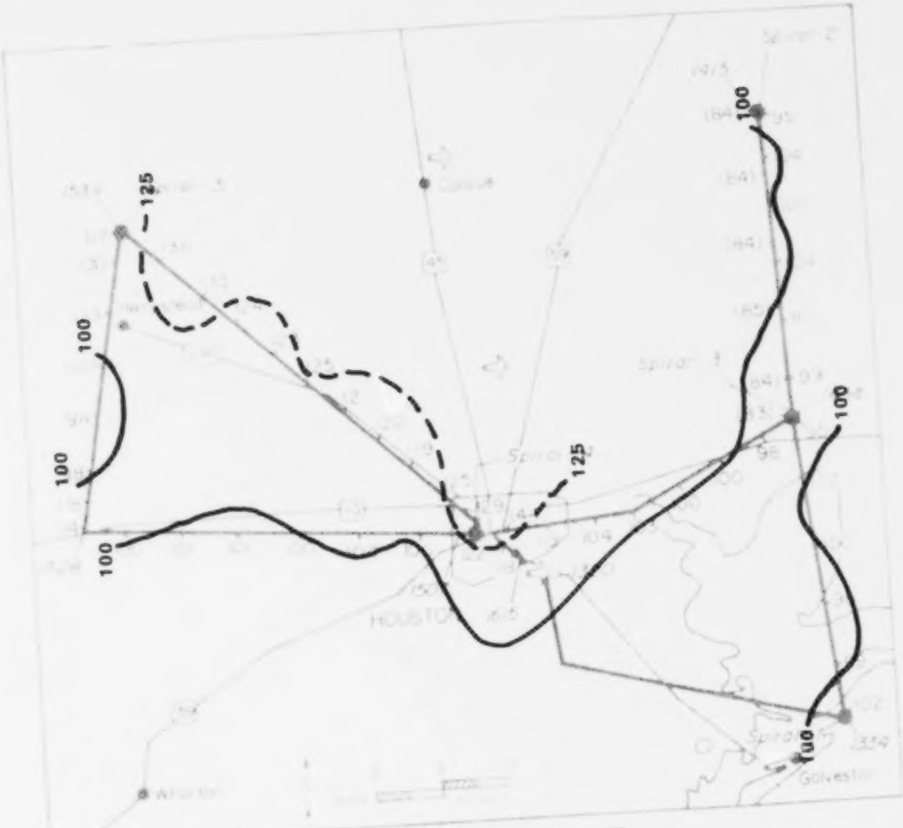

WIND:	HUB 120/8 (take-off) HUB 130 variable to 180/10 gusts to 15 (landing)
FLIGHT ALTITUDE:	1500 ft with spirals to 7000 ft; leg with O_3 concentrations in parentheses was at 7000 ft
WEATHER:	3500 broken; 6 miles haze/smoke; 85° F; 29.97

SOURCE: Westberg et al. (1979)

Figure 49. Ozone concentrations (ppb) at 1500 ft msl from 1320 to 1615 CST, 2 October 1978.

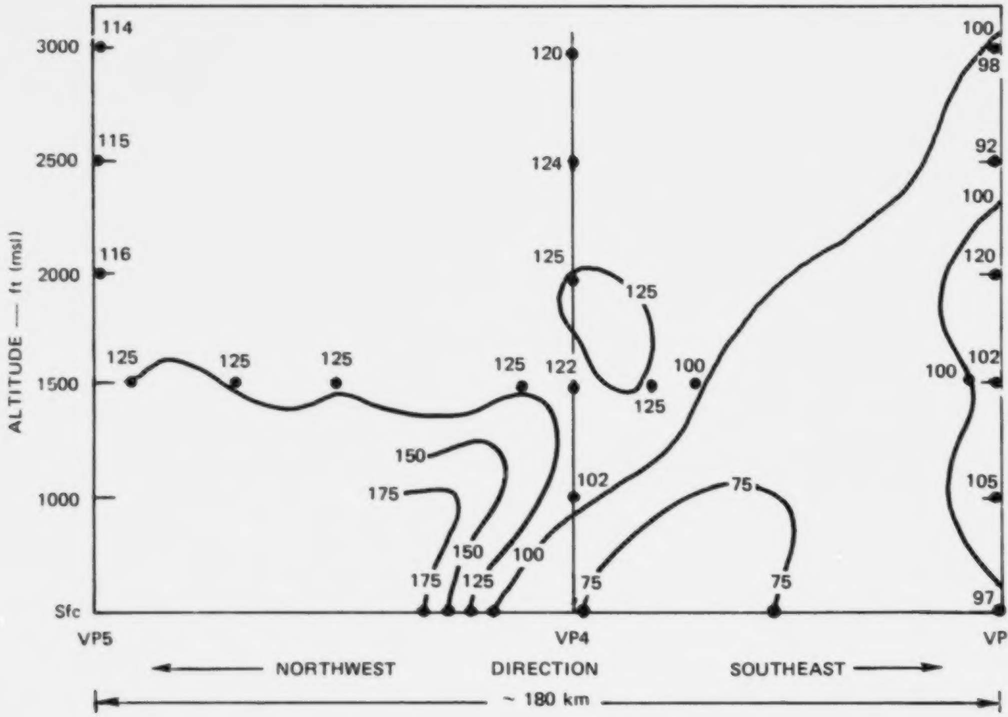

Figure 50. Vertical cross section of ozone downwind of Houston at approximately 1500 CST, 2 October 1978.

SECTION 5

SUMMARY AND CONCLUSIONS

GENERAL

The principal objectives of the HOMS were to obtain a comprehensive data base suitable for use with photochemical air-quality simulation models, and to provide aerometric data that can be used to study and characterize Houston's air quality. In general, our analysis shows that these goals were achieved. In what follows, we summarize the findings of the study and provide recommendations to improve future programs of a similar nature.

EVALUATION OF HOMS DATA BASE

The HOMS monitoring program produced data that describe in detail the spatial and temporal variations of ozone, because the ozone monitoring network was relatively dense. Consequently, there is a rich ozone data base that can be used for testing the ability of photochemical models to predict ozone.

Photochemical models require specification of the initial and boundary concentrations of hydrocarbons and NO_x. In this respect, the HOMS coverage was not as complete as for ozone. The disposition of the monitoring stations left gaps in the southwestern half of the modeling region for both hydrocarbons and NO_x. This can create problems in specifying initial conditions since our analysis, which used empirical orthogonal functions, showed that there are small-scale variations in the spatial patterns of hydrocarbons and NO_x. Since the small-scale changes are not well defined in large areas of the modeling region, the use of interpolation to estimate initial conditions can yield poor approximations of actual concentrations.

Because three-dimensional effects are so important in the formation and transport of ozone, we focused our attention on the 19 days when aircraft data were available. About half were judged to have reasonably good data for defining initial conditions. Data were deemed suitable for specifying boundary conditions at the upwind edge of the region on 13 of these days. Regarding boundary conditions, we recommend that future programs include aircraft flights that circumnavigate the modeling region, since this would enhance the models's ability to specify accurate boundary conditions. Several of the HOMS flight paths ranged far from the modeling region, and consequently the data obtained are not very useful for purposes of modeling conditions in the urban area itself.

Aldehydes are an important input in modern photochemical models but they are seldom measured. Total aldehydes and formaldehyde were monitored during the HOMS on a limited basis. Although the data obtained are useful, the amount is insufficient to permit a detailed characterization of temporal and spatial fluctuations. Future monitoring programs should include more extensive efforts to measure aldehydes. Specifically, it would be preferable to measure aldehydes for an extended period at a few well-chosen locations than to monitor for short periods at several sites, as was done in the HOMS.

The 0600-0900 (CDT) NMHC/NO_x ratio is an important descriptor of ozone-precursor conditions. Both NMHC and NO_x were measured concurrently at only six of the monitoring sites and the data capture rate at four of the sites was rather low, so the ratio could be estimated for only 30 of the maximum possible 108 site-days at those four sites. The two remaining sites had a combined data capture rate of 45 of a possible 54 site-days. Thus, the analysis of patterns of NMHC/NO_x ratios in the HOMS is limited by the relatively small amount of data. Incidentally, the HAOS data are similarly afflicted, having captured about 26 percent of the possible NMHC/NO_x ratios at five sites.

The number of monitoring sites where meteorological parameters were measured varied between one and five during the 19 days of aircraft operations. Such coverage is very sparse, and may be inadequate for modeling applications. To compensate for the sparseness of the meteorological data, mass-conserving interpolation methods should be used to generate the wind field that is an input of photochemical air-quality models (e.g., Ludwig and Byrd, 1980). The need for a good wind-field generator for modeling studies is also suggested by the case studies of particular days. These show that wind-shear effects can be important determinants of ozone levels. Although current models treat such effects, they can do so only if the proper wind inputs are provided.

The HOMS coincided with a period when the Houston area recorded some of its highest ozone levels ever. This is fortunate in the sense that the air quality data can be used to model worst-case or near-worst-case conditions, which of course are of interest for regulatory reasons.

Despite the high ozone levels, both PAN and NO_2 concentrations were relatively low, a result that confirms the findings previously reported for the HAOS (Ludwig and Martinez, 1979). The HOMS analysis showed that the highest NO_2 levels occurred in downtown Houston and in locations west and northwest of downtown. PAN was measured at one rural location (Sheldon, Site 18) and one suburban site (Jackrabbit, Site 20). Mean PAN values do not differ very much at these two sites, but the maximum PAN at Jackrabbit is more than twice that at Sheldon.

Detailed hydrocarbon analyses were conducted at ten sites located in industrial, urban, suburban, and rural areas. The analysis of 11 selected compounds for the period 0800-0900 showed that ethane and propane are relatively uniformly distributed. Acetylene and propylene concentrations have similar, nonuniform spatial distributions. Isopentane and isobutane exhibit considerable spatial fluctuations, as do toluene and the xylenes. Benzene shows a dichotomous spatial pattern: industrial, urban, and suburban sites have similar mean concentrations that are significantly higher than for sites on the fringes of the urban envelope. N-butane follows a comparable pattern, except that the industrial site clusters with the outlying locations.

Mobile sources were found to be responsible for acetylene and propylene at several locations, including downtown Houston, which was expected. However, evidence of stationary sources contributed by propylene was also found at a number of sites. Benzene was found to follow the same pattern as propylene. At all the sites examined, toluene and the xylenes appeared to receive substantial contributions from stationary sources. The same is true for isopentane and the two butanes.

The HOMS and HAOS hydrocarbon data were compared and found to be generally consistent in the pattern of concentrations and hydrocarbon/acetylene ratios. However, the benzene/toluene ratio in the HOMS data was different from that in the HAOS measurements. The indications are that the benzene/toluene ratio in the HAOS may not be correct.

The 0600-0900 detailed hydrocarbon data for the HOMS were compared with similar data from Denver and southern California. Denver's hydrocarbon mixture was found to be similar to that in suburban Houston. The mixtures in downtown Houston and Los Angeles were also found to be similar except for toluene and the xylenes, for which levels in Los Angeles were considerably higher than in Houston. In general, the southern California data differ most markedly from Houston's in the higher content of aromatics, which appear to be mainly due to stationary sources.

The 0600-0900 n-butane/propylene ratio is used as an indicator of the reactivity of the hydrocarbon mixture in some air-quality models. For this reason, we compared these ratios in Houston, Denver, and southern California. The mean and median ratios at four of five sites in southern California were somewhat lower than in Houston or Denver, which suggests that the mixture may be slightly more reactive. In particular, the ratio in downtown Houston is higher than in downtown Los Angeles, but is similar to the ratio at Long Beach.

The analysis of the aldehyde data showed that formaldehyde ranged from 1 to 28 ppb, and total aldehydes from 4 to 40 ppb. The highest aldehyde levels were associated with elevated ozone concentrations. However, although formaldehyde exceeded 20 ppb only when maximum daily ozone was at least 100 ppb, the converse is not generally true.

Examination of 0600-0900 (CDT) NMHC/NO_x ratios showed that they ranged from 1 to 210, with six ratios having values exceeding 100. Ninety-two percent of the ratios did not exceed 85. The median ratio for the area was 14, which is similar to the median ratio of 12 found in the HAOS. The distributions of the HOMS and HAOS ratios were compared and found to diverge substantially at the high end. The divergence is caused by the presence of several very high values in the HOMS data, ratios that are high because the NO_x was very low, not because NMHC was high.

The spatial patterns of NMHC, NO_x, and ozone were analyzed using empirical orthogonal functions. The analysis showed that the spatial distribution of ozone has a high degree of uniformity, and is characterized by large-scale features. By contrast, the spatial distibutions of NMHC and NO_x are less uniform and show evidence of small-scale influences. These results imply that the ozone-monitoring network need not be as dense as it was, but that the number of stations monitoring NMHC and NO_x probably should be more numerous, to capture the small-scale features. For NMHC and NO_x, these results imply that it may be inaccurate to estimate initial conditions for a grid-type model by interpolation or extrapolation based on the monitoring network.

Several days were identified that may be of interest for modeling applications. An ozone episode occurring from 1 through 5 October 1978 seemed particularly interesting. Case studies of potential modeling days were performed for 20 and 29 September and 1 and 2 October. The case studies showed the influence of conditions aloft on ground-level concentrations. It is clear from these and other studies that the processes affecting the formation and transport of ozone are very three-dimensional. Thus, if modeling efforts are to succeed, it is important that the models be provided with accurate, well-resolved initial and boundary conditions. Moreover, the performance of the models should be evaluated at both the ground-level stations and at points aloft for which measurements exist.

REFERENCES

Decker, C.E., L.A. Ripperton, J.J.B. Worth, F.M. Vukovich, W.D. Bach, J.B. Tommerdahl, F. Smith, and D.E. Wagner (1976): "Formation and Transport of Oxidants Along Gulf Coast and in Northern U.S.," EPA-450/3-76-033 (August).

Ferman, M.A., R.S. Eisinger, and P.R. Monson (1977): "Characterization of Denver Air Quality," in P.A. Russell, ed., *Denver Air Pollution Study--1973: Proceedings of a Symposium*, EPA-600/9-77-001 (February).

Graedel, T.E. (1978): *Chemical Compounds in the Atmosphere*, Academic Press, New York.

Hendry, D.G., A.C. Baldwin, J.R. Barker, and D.M. Golden (1978): "Computer Modeling of Simulated Photochemical Smog," EPA 600/3-78-059 (June).

Joshi, S.B. (1979): "Houston Field Study (1978) Formaldehyde and Total Aldehydes Monitoring Program," Northrop Services, Inc., Report ESC-TR-79-22, (February).

Lonneman, W.A. and J.J. Bufalini (1973): "Hydrocarbon Analysis of Houston Atmosphere," U.S. Environmental Protection Agency Memorandum (September).

Lonneman, W.A., S.L. Kopcznynski, P.E. Daily, and F.D. Satterfield (1974): "Hyrocarbon Composition of Urban Air Pollution," *Environ. Sci. Technol.*, 8, pp. 229-236.

Lorenz, E.N. (1956): "Empirical Orthogonal Functions and Statistical Weather Prediction," Scientific Report No. 1, Statistical Forecasting Project, Massachusetts Institute of Technology, Cambridge, Massachusetts, Defense Document Center No. 110268, 49 pp.

Ludwig, F.L. (1979): "Assessment of Vertical Distributions of Photochemical Pollutants in the Vicinity of Urban Areas," Final Report, EPA Contract 68-02-2662, SRI International Project 6809, EPA Report No. 450/4-79-017, 167 pp.

Ludwig, F.L. and J.R. Martinez (1979): "Aerometric Data Analysis for the Houston Area Oxidant Study--Volume 2," Final Report, SRI International, Project 7106 (July).

Ludwig, F.L., J.R. Martinez, and K.C. Nitz (1979): "Data Summaries for the Houston Area Oxidant Study," Final Report, SRI International, Project 7106 (July).

Ludwig, F.L. and G. Byrd (1980): "An Efficient Method for Deriving Mass-Consistent Flow Fields from Wind Observations in Rough Terrain," Atmos. Environ., 14, pp. 585-587.

Martinez, J.R. and F.L. Ludwig (1979): "First Analyses and Interpretations of the 1978 Houston Air Quality Data," Proc. of the Specialty Conference on Ozone/Oxidants, Air Pollution Control Assoc., Houston, Texas (October).

Mayrsohn, H. and J.H. Crabtree (1976): "Source Reconciliation of Atmospheric Hydrocarbons," Atmos. Environ., 10, pp. 137-143.

Mayrsohn, H., M. Kuramoto, J.H. Crabtree, R.D. Sothern, and S.H. Mano (1975): "Atmospheric Hydrocarbon Concentrations, June-September 1974," California Air Resources Board, Atmospheric Studies Section (April).

Scheffe, H. (1959): The Analysis of Variance, John Wiley and Sons, Inc., New York.

Shauck, M.E. and W.M. Alexander (1978): "Houston Area Oxidant Study: Airborne Ozone Study, Volume II: Data," Baylor University, Waco, Texas.

Siddiqi, A.A. and F.L. Worley (1977): "Urban and Industrial Air Pollution in Houston, Texas: Vol. I, Hydrocarbons," Atmos. Environ., 11, pp. 131-143.

U.S. Environmental Protection Agency (1977): "Uses, Limitations, and Technical Basis of Procedures for Quantifying Relationships Between Photochemical Oxidants and Precursors," EPA 450/2-77-021a.

U.S. Environmental Protection Agency (1978): "Procedures for Quantifying Relationships Between Photochemical Oxidants and Precursors: Supporting Documentation," EPA 450/2-77-021b.

Westberg, H., K. Allwine, and E. Robinson (1978): "Measurement of Light Hydrocarbons and Oxidant Transport--Houston Study, 1976", EPA-600/3-78-062 (July).

Westberg, H., K. Sexton, and M. Holdren (1979): "Measurement of Ambient Hydrocarbons and Oxidant Transport--Volume I: Houston Study, 1978," Washington State University, College of Engineering (September).

Whitten, G.Z. and H. Hogo (1978): "Users Manual for Kinetics Model and Ozone Isopleth Plotting Package," EPA 600/8-78-014a (July).

APPENDIX A

SUMMARY OF HOMS DATA AVAILABILITY FOR DAYS WITH AIRCRAFT DATA

ITEM	FLIGHT 1	FLIGHT 2
AIRCRAFT COVERAGE		
START TIME	0925	
END TIME	1135	
FLIGHT LEVEL (ft)	1500 (6000)	
APPROXIMATE MIXING DEPTH (ft)	1500	
NUMBER OF VERTICAL PROFILES	4	
OTHER UPPER-LEVEL DATA		
TETHERSONDE		
TIMES		
LOCATION		
PILOT BALLOON (T DENOTES TEMPERATURESONDE)		
TIMES	8T,9,10,13T	
LOCATION	25 and 17	
SURFACE DATA — NUMBER OF SITES AVAILABLE:		
O_3	10	
NO_x	2	
NMHC	6	
PAN	0	
METEOROLOGICAL	3	
CONDITIONS		
DAILY O_3 PEAK CONCENTRATION (ppb)	60	
HOUR (CST)	1200	
SITE	Aldine	
GENERAL WINDS (DIRECTION/SPEED)		
850 mb	150°/5 kts	
SURFACE	210°/7 kts	
AIRCRAFT DATA USEFULNESS FOR		
ESTIMATION OF INITIAL CONDITIONS	Good	
ESTIMATION OF BOUNDARY CONDITIONS	Good	
MODEL VERIFICATION	Reasonably good	
ESTIMATION OF MIXING	Good	
DETERMINATION OF RESOLUTION REQUIREMENTS		
VERTICAL	Good	
HORIZONTAL	Good	

Maximum height of vertical profiles shown in parentheses. Location of vertical profiles is denoted by symbol ◉. Arrows denote surface and 850-mb wind direction. Dots denote location of ground monitoring sites.

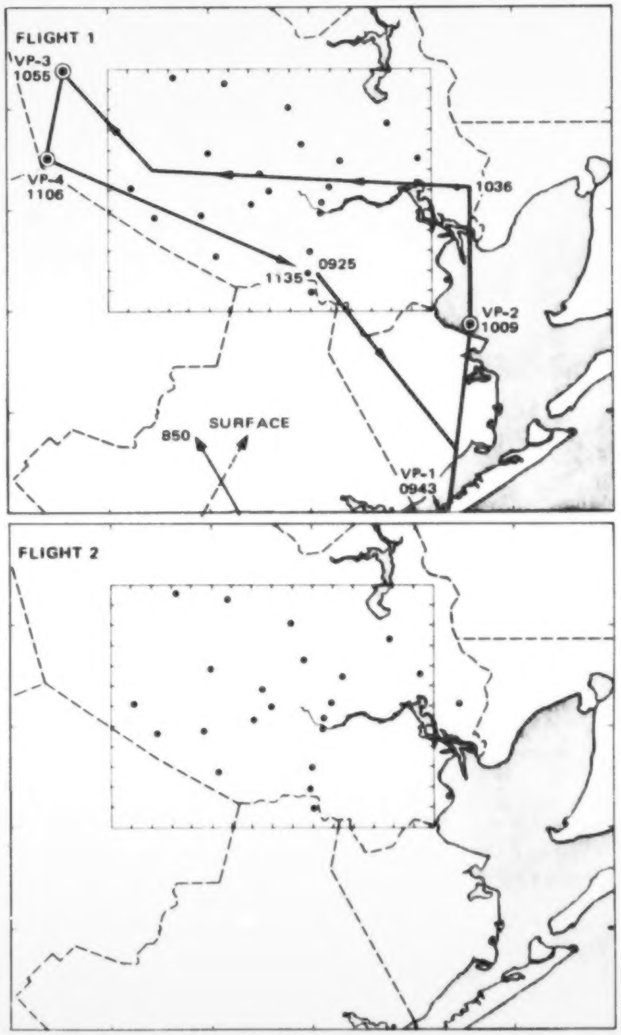

Figure A-1. Summary of data availability and usefulness for 15 September 1978.

ITEM	FLIGHT 1	FLIGHT 2
AIRCRAFT COVERAGE		
START TIME	1005	1510
END TIME	1225	1732
FLIGHT LEVEL (ft)	1500 (6000)	1500 (10000)
APPROXIMATE MIXING DEPTH (ft)	6000	5000
NUMBER OF VERTICAL PROFILES	5	2
OTHER UPPER-LEVEL DATA		
TETHERSONDE		
TIMES		
LOCATION		
PILOT BALLOON (T DENOTES TEMPERATURESONDE)		
TIMES	8T,9,10,11,13T	14,15,16,17
LOCATION	25 and 17	25 and 17
SURFACE DATA — NUMBER OF SITES AVAILABLE:		
O_3	8	8
NO_x	3	3
NMHC	7	7
PAN	0	0
METEOROLOGICAL	3	3
CONDITIONS		
DAILY O_3 PEAK CONCENTRATION (ppb)	90	90
HOUR (CST)	1500	1500
SITE	Aldine	Aldine
GENERAL WINDS (DIRECTION/SPEED)		
850 mb	180°/10 kts	180°/10 kts
SURFACE	210°/5 kts	180°/8 kts
AIRCRAFT DATA USEFULNESS FOR		
ESTIMATION OF INITIAL CONDITIONS	Reasonably good	Poor
ESTIMATION OF BOUNDARY CONDITIONS	Reasonably good	Fair
MODEL VERIFICATION	Reasonably good	Fair
ESTIMATION OF MIXING	Good	Good
DETERMINATION OF RESOLUTION REQUIREMENTS		
VERTICAL	Good	Good
HORIZONTAL	Good	Good

Maximum height of vertical profiles shown in parentheses. Location of vertical profiles is denoted by symbol ◉. Arrows denote surface and 850-mb wind direction. Dots denote location of ground monitoring sites.

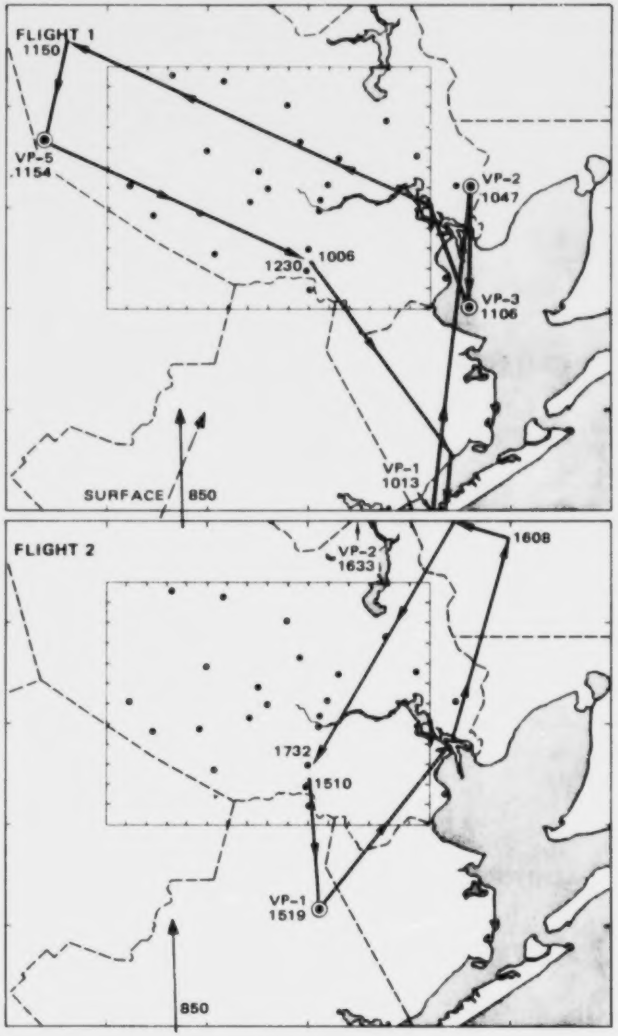

Figure A-2. Summary of data availability and usefulness for 16 September 1978.

ITEM	FLIGHT 1	FLIGHT 2
AIRCRAFT COVERAGE		
START TIME	0925	1950
END TIME	1210	2230
FLIGHT LEVEL (ft)	1500 (9000)	1500 (8000)
APPROXIMATE MIXING DEPTH (ft)	2500 (?)	2000
NUMBER OF VERTICAL PROFILES	1	2
OTHER UPPER-LEVEL DATA		
TETHERSONDE		
TIMES		
LOCATION		
PILOT BALLOON (T DENOTES TEMPERATURESONDE)		
TIMES (LOCATION)	8T,9,11,13T (25 and 17)	17 (25 and 17)
	10 (17)	
SURFACE DATA — NUMBER OF SITES AVAILABLE		
O_3	10	10
NO_x	3	3
NMHC	6	6
PAN	0	0
METEOROLOGICAL	4	4
CONDITIONS		
DAILY O_3 PEAK CONCENTRATION (ppb)	70	70
HOUR (CST)	1300	1300
SITE	Aldine	Aldine
GENERAL WINDS (DIRECTION/SPEED)		
850 mb	180°/15 kts	160°/15 kts
SURFACE	160°/8 kts	150°/7 kts
AIRCRAFT DATA USEFULNESS FOR		
ESTIMATION OF INITIAL CONDITIONS	Fair	Poor
ESTIMATION OF BOUNDARY CONDITIONS	Good	Good
MODEL VERIFICATION	Good	Good
ESTIMATION OF MIXING	Reasonably good	Reasonably good
DETERMINATION OF RESOLUTION REQUIREMENTS		
VERTICAL	Poor	Reasonably good
HORIZONTAL	Good	Good

Maximum height of vertical profiles shown in parentheses. Location of vertical profiles is denoted by symbol ⊙. Arrows denote surface and 850-mb wind direction. Dots denote location of ground monitoring sites.

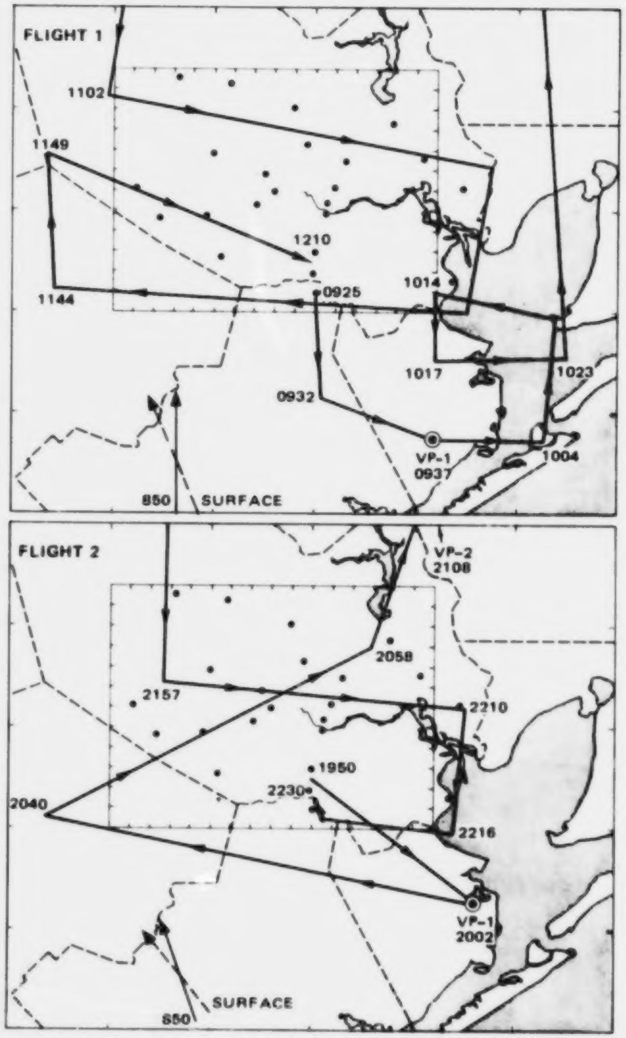

Figure A-3. Summary of data availability and usefulness for 17 September 1978.

ITEM	FLIGHT 1	FLIGHT 2
AIRCRAFT COVERAGE		
START TIME	0930	
END TIME	1220	
FLIGHT LEVEL (ft)	1500 (10000)	
APPROXIMATE MIXING DEPTH (ft)	> 6000 ft	
NUMBER OF VERTICAL PROFILES	1	
OTHER UPPER-LEVEL DATA		
TETHERSONDE		
TIMES		
LOCATION		
PILOT BALLOON (T DENOTES TEMPERATURESONDE)		
TIMES	8T,9,10,11,13T	
LOCATION	25 and 17	
SURFACE DATA — NUMBER OF SITES AVAILABLE		
O_3	12	
NO_x	3	
NMHC	7	
PAN	1	
METEOROLOGICAL	3	
CONDITIONS		
DAILY O_3 PEAK CONCENTRATION (ppb)	80	
HOUR (CST)	1500	
SITE	Aldine	
GENERAL WINDS (DIRECTION/SPEED)		
850 mb	160°/25 kts	
SURFACE	140°/12 kts	
AIRCRAFT DATA USEFULNESS FOR		
ESTIMATION OF INITIAL CONDITIONS	Poor	
ESTIMATION OF BOUNDARY CONDITIONS	Poor	
MODEL VERIFICATION	Poor	
ESTIMATION OF MIXING	Poor	
DETERMINATION OF RESOLUTION REQUIREMENTS		
VERTICAL	Poor	
HORIZONTAL	Fair	

Maximum height of vertical profiles shown in parentheses. Location of vertical profiles is denoted by symbol ⊙. Arrows denote surface and 850-mb wind direction. Dots denote location of ground monitoring sites.

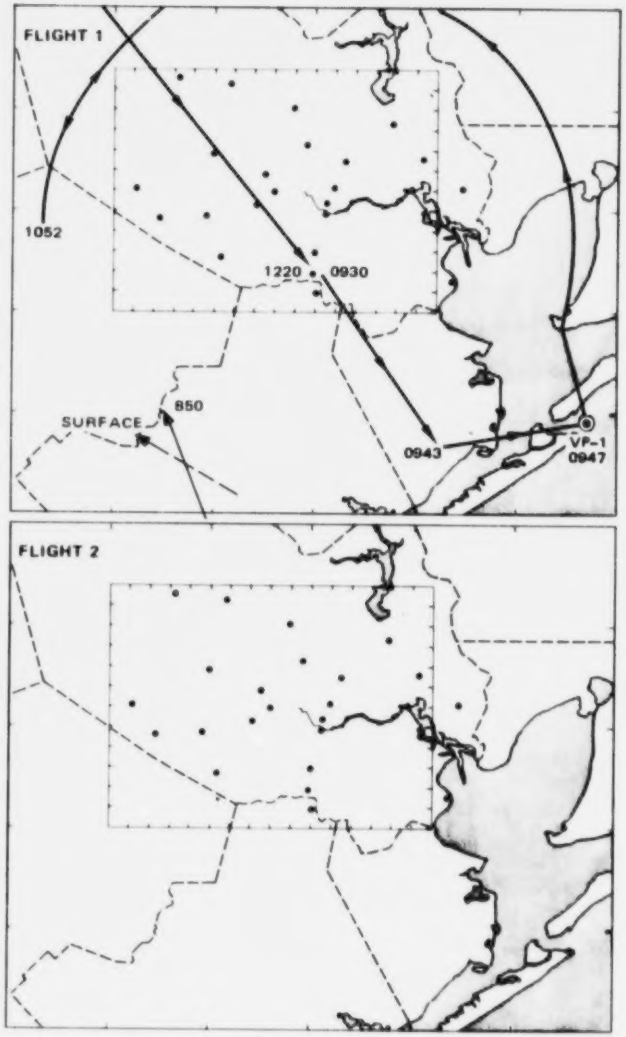

Figure A-4. Summary of data availability and usefulness for 18 September 1978.

ITEM	FLIGHT 1	FLIGHT 2
AIRCRAFT COVERAGE		
START TIME	0742	1424
END TIME	1055	1707
FLIGHT LEVEL (ft)	1500 (7000)	1500 (8000)
APPROXIMATE MIXING DEPTH (ft)	3000	5000
NUMBER OF VERTICAL PROFILES	5	2
OTHER UPPER-LEVEL DATA		
TETHERSONDE		
TIMES	0925,1000	
LOCATION	12	
PILOT BALLOON (T DENOTES TEMPERATURESONDE)		
TIMES	8T,9,10,11	13T,14,15,16,17
LOCATION	25 and 17	25 and 17
SURFACE DATA — NUMBER OF SITES AVAILABLE:		
O_3	12	12
NO_x	2	2
NMHC	7	7
PAN	1	1
METEOROLOGICAL	3	3
CONDITIONS		
DAILY O_3 PEAK CONCENTRATION (ppb)	110	110
HOUR (CST)	1600	1600
SITE	Aldine	Aldine
GENERAL WINDS (DIRECTION/SPEED)		
850 mb	170°/25 kts	120°/10 kts
SURFACE	120°/5 kts	120°/13 kts
AIRCRAFT DATA USEFULNESS FOR		
ESTIMATION OF INITIAL CONDITIONS	Good	Poor
ESTIMATION OF BOUNDARY CONDITIONS	Good	Good
MODEL VERIFICATION	Good	Good
ESTIMATION OF MIXING	Good	
DETERMINATION OF RESOLUTION REQUIREMENTS		
VERTICAL	Good	Reasonably good
HORIZONTAL	Good	Good

Maximum height of vertical profiles shown in parentheses. Location of vertical profiles is denoted by symbol ◉. Arrows denote surface and 850-mb wind direction. Dots denote location of ground monitoring sites.

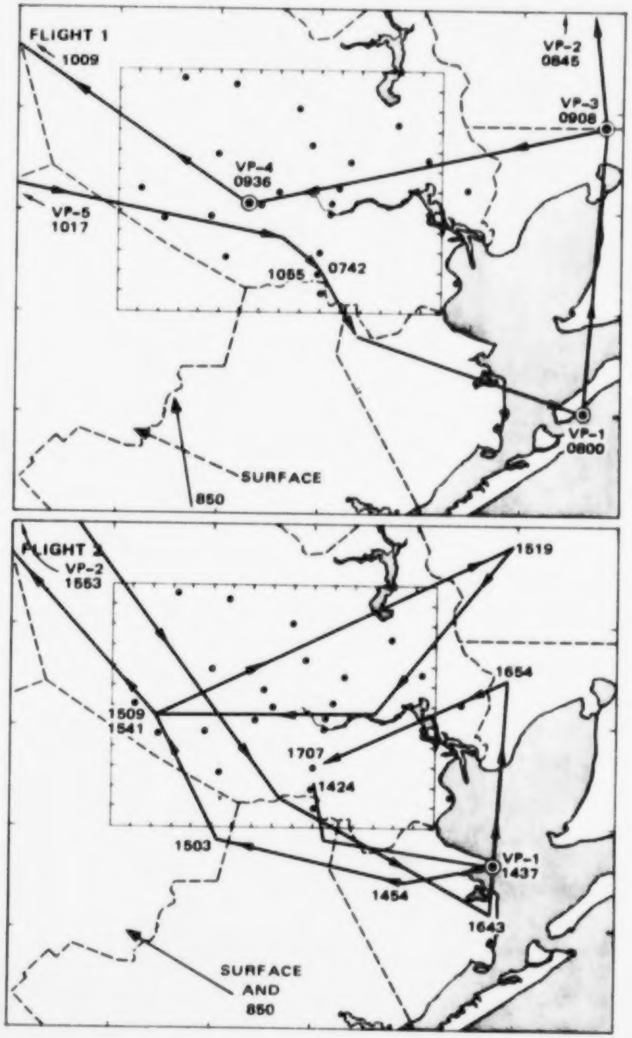

Figure A-5. Summary of data availability and usefulness for 19 September 1978.

ITEM	FLIGHT 1	FLIGHT 2
AIRCRAFT COVERAGE		
START TIME	0551	1055
END TIME	0748	1400
FLIGHT LEVEL (ft)	1500 (6000)	1500 (10000)
APPROXIMATE MIXING DEPTH (ft)	1000	3000
NUMBER OF VERTICAL PROFILES	4	2
OTHER UPPER-LEVEL DATA		
TETHERSONDE		
TIMES (SITE 12)	0800	1020,1110,1195 1230
PILOT BALLOON (T DENOTES TEMPERATURESONDE)		
TIMES	7,8T	13T,14 (25)
LOCATION	(25 and 17)	11 (25 and 17)
SURFACE DATA — NUMBER OF SITES AVAILABLE		
O_3	11	11
NO_x	2	2
NMHC	7	7
PAN	1	1
METEOROLOGICAL	3	3
CONDITIONS		
DAILY O_3 PEAK CONCENTRATION (ppb)	120	120
HOUR (CST)	1300	1300
SITE	Aldine	Aldine
GENERAL WINDS (DIRECTION/SPEED)		
850 mb	150°/12 kts	100°/5 kts
SURFACE	020°/6 kts	010°/5 kts
AIRCRAFT DATA USEFULNESS FOR		
ESTIMATION OF INITIAL CONDITIONS	Fair	Fair
ESTIMATION OF BOUNDARY CONDITIONS	Fair	Good
MODEL VERIFICATION	Poor	Good
ESTIMATION OF MIXING	Good	Fair
DETERMINATION OF RESOLUTION REQUIREMENTS		
VERTICAL	Good	Good*
HORIZONTAL	Fair	Good

Maximum height of vertical profiles shown in parentheses. Location of vertical profiles is denoted by symbol ◉. Arrows denote surface and 850-mb wind direction. Dots denote location of ground monitoring sites.

*Multiple flight levels on downwind edge of town

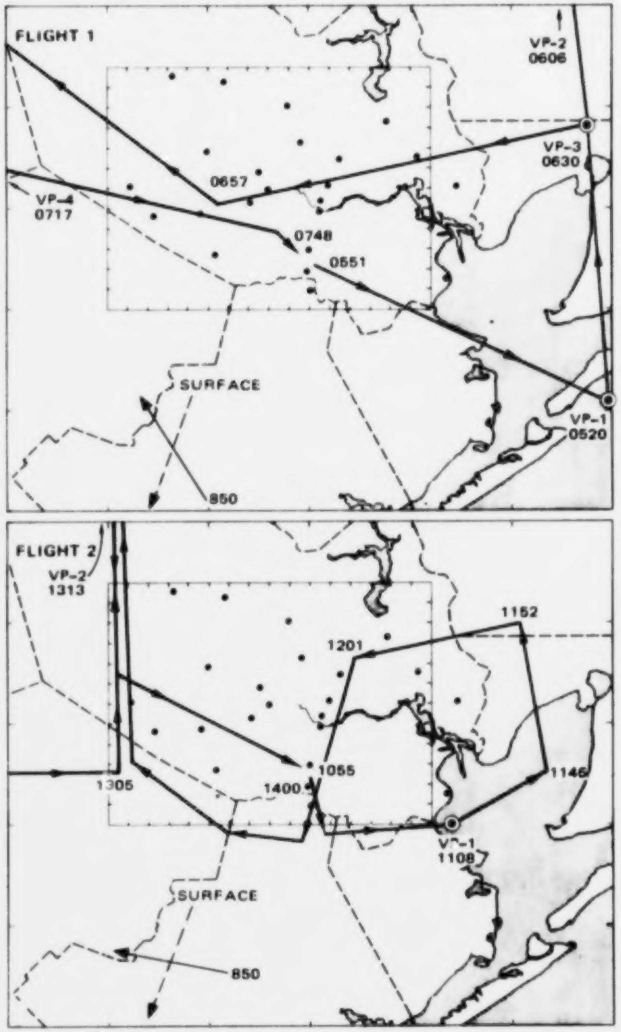

Figure A-6. Summary of data availability and usefulness for 20 September 1978.

ITEM	FLIGHT 1	FLIGHT 2
AIRCRAFT COVERAGE		
START TIME	0545	
END TIME	0842	
FLIGHT LEVEL (ft)	1500 (6000)	
APPROXIMATE MIXING DEPTH (ft)	4000	
NUMBER OF VERTICAL PROFILES	5	
OTHER UPPER-LEVEL DATA		
TETHERSONDE		
TIMES	0810,1015	
LOCATION	12	
PILOT BALLOON (T DENOTES TEMPERATURESONDE)		
TIMES	7,8T,9	
LOCATION	25 and 17	
SURFACE DATA — NUMBER OF SITES AVAILABLE:		
O_3	12	
NO_x	4	
NMHC	5	
PAN	1	
METEOROLOGICAL	5	
CONDITIONS		
DAILY O_3 PEAK CONCENTRATION (ppb)	135	
HOUR (CST)	1600	
SITE	Beasley	
GENERAL WINDS (DIRECTION/SPEED)		
850 mb	100°/10 kts	
SURFACE	040°/10 kts	
AIRCRAFT DATA USEFULNESS FOR		
ESTIMATION OF INITIAL CONDITIONS	Good	
ESTIMATION OF BOUNDARY CONDITIONS	Fair	
MODEL VERIFICATION	Poor	
ESTIMATION OF MIXING	Good	
DETERMINATION OF RESOLUTION REQUIREMENTS		
VERTICAL	Good	
HORIZONTAL	Good	

Maximum height of vertical profiles shown in parentheses. Location of vertical profiles is denoted by symbol ◉. Arrows denote surface and 850-mb wind direction. Dots denote location of ground monitoring sites.

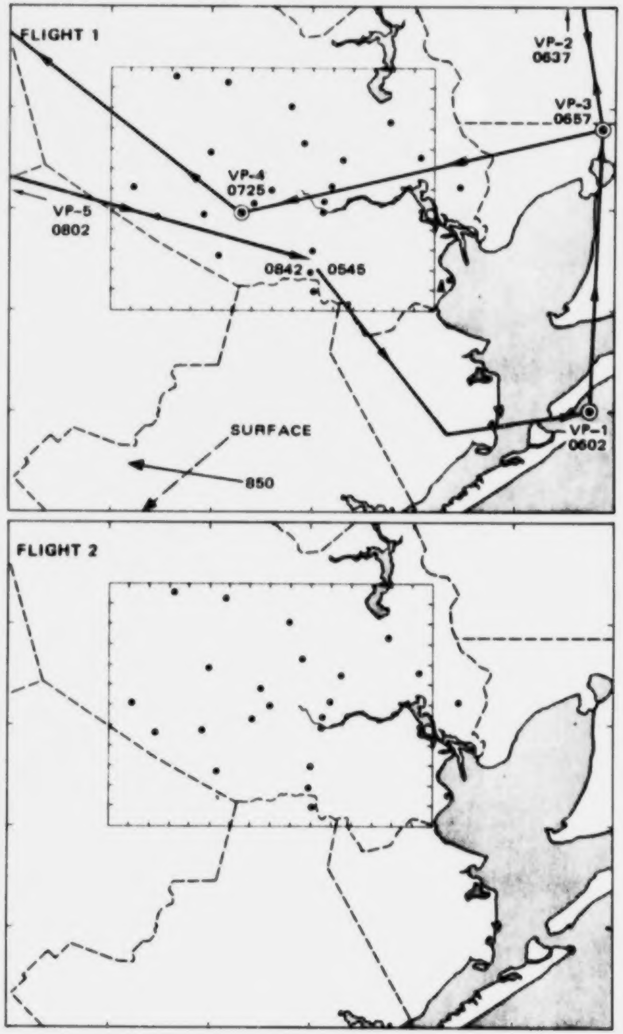

Figure A-7. Summary of data availability and usefulness for 23 September 1978.

ITEM	FLIGHT 1	FLIGHT 2
AIRCRAFT COVERAGE		
START TIME	0625	1135
END TIME	0937	1520
FLIGHT LEVEL (ft)	1500 (10000)	1500 (12000)
APPROXIMATE MIXING DEPTH (ft)	2000	2500
NUMBER OF VERTICAL PROFILES	5	2
OTHER UPPER-LEVEL DATA		
TETHERSONDE		
TIMES		
LOCATION		
PILOT BALLOON		
TIMES		
LOCATION		
SURFACE DATA — NUMBER OF SITES AVAILABLE:		
O_3	11	11
NO_x	3	3
NMHC	4	4
PAN	1	1
METEOROLOGICAL	3	3
CONDITIONS		
DAILY O_3 PEAK CONCENTRATION (ppb)	123	123
HOUR (CST)	1400	1400
SITE	Pearland	Pearland
GENERAL WINDS (DIRECTION/SPEED)		
850 mb	070°/5 kts	060°/15 kts
SURFACE	060°/8 kts	040°/12 kts
AIRCRAFT DATA USEFULNESS FOR		
ESTIMATION OF INITIAL CONDITIONS	Fair	Poor
ESTIMATION OF BOUNDARY CONDITIONS	Fair	Fair
MODEL VERIFICATION	Fair	Good
ESTIMATION OF MIXING	Good	Good
DETERMINATION OF RESOLUTION REQUIREMENTS		
VERTICAL	Good	Fair
HORIZONTAL	Fair	Good

Maximum height of vertical profiles shown in parentheses. Location of vertical profiles is denoted by symbol ◉. Arrows denote surface and 850-mb wind direction. Dots denote location of ground monitoring sites.

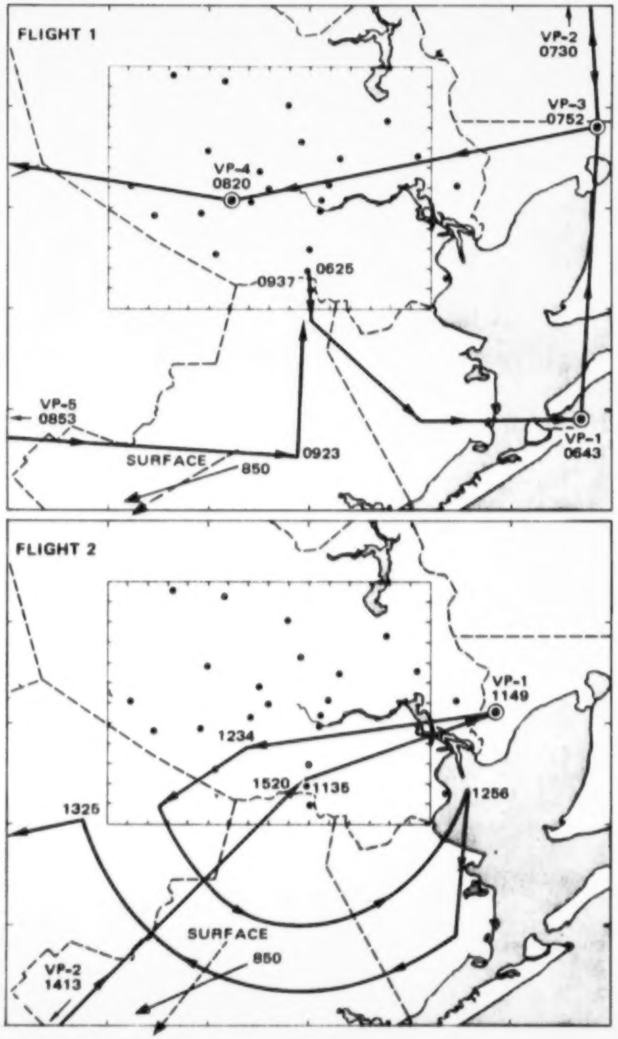

Figure A-8. Summary of data availability and usefulness for 24 September 1978.

ITEM	FLIGHT 1	FLIGHT 2
AIRCRAFT COVERAGE		
START TIME	0500	1200
END TIME	0900	1500
FLIGHT LEVEL (ft)	1500 (8000)	1500 (8000)
APPROXIMATE MIXING DEPTH (ft)	Surface and 2500	3000
NUMBER OF VERTICAL PROFILES	5	1
OTHER UPPER-LEVEL DATA		
TETHERSONDE		
TIMES (SITE 12)	0800,0833,0905	1200,1225,1300, 1400,1435
PILOT BALLOON (T DENOTES TEMPERATURESONDE)		
TIMES	7,8T,9	13T,14,15
LOCATION	25 and 17	25 and 17
SURFACE DATA — NUMBER OF SITES AVAILABLE:		
O_3	12	12
NO_x	6	6
NMHC	5	5
PAN	1	1
METEOROLOGICAL	5	5
CONDITIONS		
DAILY O_3 PEAK CONCENTRATION (ppb)	164	164
HOUR (CST)	1400	1400
SITE	Pearland	Pearland
GENERAL WINDS (DIRECTION/SPEED)		
850 mb	030°/5 kts	030°/7 kts
SURFACE	050°/10 kts	020°/8 kts
AIRCRAFT DATA USEFULNESS FOR		
ESTIMATION OF INITIAL CONDITIONS	Reasonably good	Fair
ESTIMATION OF BOUNDARY CONDITIONS	Reasonably good	Fair
MODEL VERIFICATION	Reasonably good	Good
ESTIMATION OF MIXING	Reasonably good	Fair
DETERMINATION OF RESOLUTION REQUIREMENTS		
VERTICAL	Good	Fair
HORIZONTAL	Good	Good

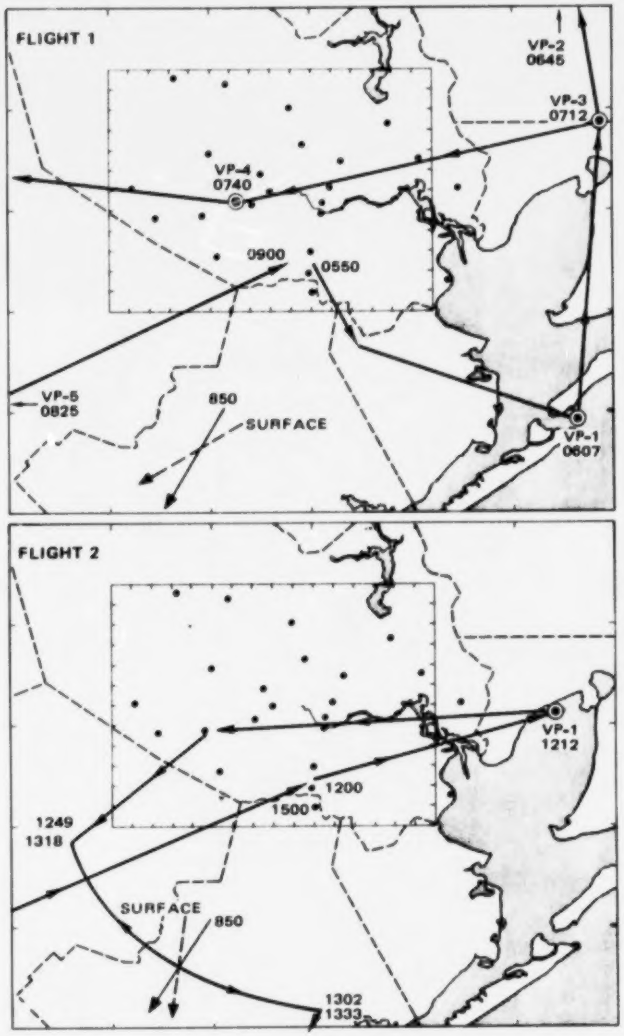

Maximum height of vertical profiles shown in parentheses. Location of vertical profiles is denoted by symbol ⊙. Arrows denote surface and 850-mb wind direction. Dots denote location of ground monitoring sites.

Figure A-9. Summary of data availability and usefulness for 25 September 1978.

ITEM	FLIGHT 1	FLIGHT 2
AIRCRAFT COVERAGE		
START TIME	0610	1030
END TIME	0905	1325
FLIGHT LEVEL (ft)	1500 (6000)	1500 (8000)
APPROXIMATE MIXING DEPTH (ft)	1000	4500
NUMBER OF VERTICAL PROFILES	5	2
OTHER UPPER-LEVEL DATA		
TETHERSONDE		
TIMES (SITE 12)	0945	1100,1130,1200, 1225,1300
PILOT BALLOON (T DENOTES TEMPERATURESONDE)		
TIMES	7,8T,9	10,11,13T,14
LOCATION	25 and 17	25 and 17
SURFACE DATA — NUMBER OF SITES AVAILABLE		
O_3	11	11
NO_x	7	7
NMHC	6	6
PAN	1	1
METEOROLOGICAL	5	5
CONDITIONS		
DAILY O_3 PEAK CONCENTRATION (ppb)	182	182
HOUR (CST)	1200	1200
SITE	Pearland	Pearland
GENERAL WINDS (DIRECTION/SPEED)		
850 mb	120°/5 kts	080°/5 kts
SURFACE	085°/10 kts	070°/8 kts
AIRCRAFT DATA USEFULNESS FOR		
ESTIMATION OF INITIAL CONDITIONS	Good	Poor
ESTIMATION OF BOUNDARY CONDITIONS	Good	Poor
MODEL VERIFICATION	Fair	Fair
ESTIMATION OF MIXING	Good	Good
DETERMINATION OF RESOLUTION REQUIREMENTS		
VERTICAL	Good	Fair
HORIZONTAL	Good	—

Maximum height of vertical profiles shown in parentheses. Location of vertical profiles is denoted by symbol ⊙. Arrows denote surface and 850-mb wind direction. Dots denote location of ground monitoring sites.

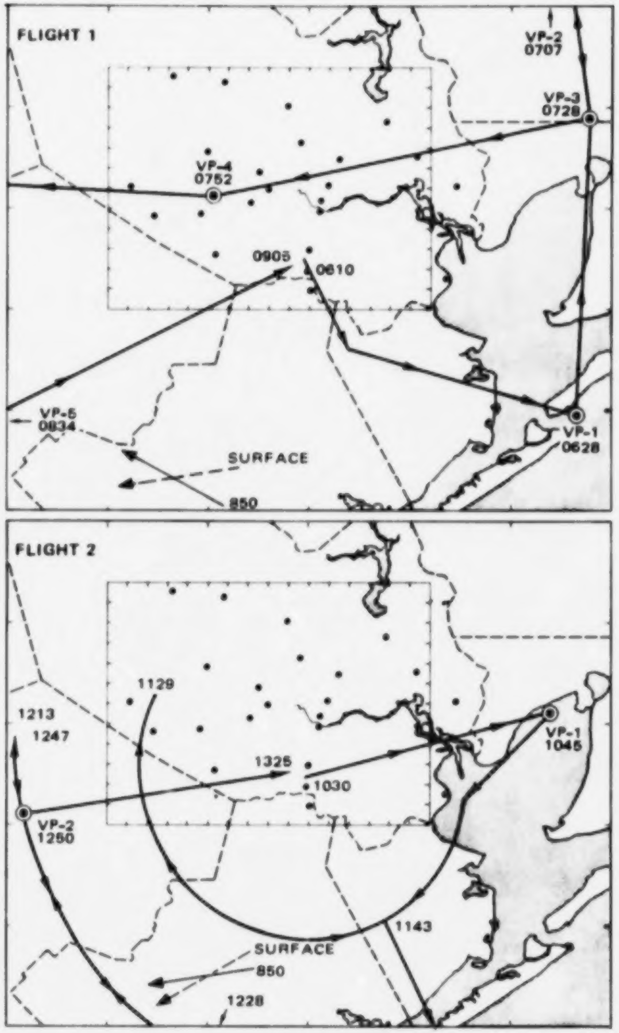

Figure A-10. Summary of data availability and usefulness for 26 September 1978.

ITEM	FLIGHT 1	FLIGHT 2
AIRCRAFT COVERAGE		
START TIME	0745	
END TIME	0935	
FLIGHT LEVEL (ft)	1500 (20000)	
APPROXIMATE MIXING DEPTH (ft)	200	
NUMBER OF VERTICAL PROFILES	1	
OTHER UPPER-LEVEL DATA		
TETHERSONDE		
TIMES (SITE 12)	0800,0825,0900, 0925	
PILOT BALLOON (T DENOTES TEMPERATURESONDE)		
TIMES	7,8T,9,10	
LOCATION	25 and 17	
SURFACE DATA — NUMBER OF SITES AVAILABLE:		
O_3	12	
NO_x	7	
NMHC	6	
PAN	1	
METEOROLOGICAL	5	
CONDITIONS		
DAILY O_3 PEAK CONCENTRATION (ppb)	106	
HOUR (CST)	1400	
SITE	Pearland	
GENERAL WINDS (DIRECTION/SPEED)		
850 mb	040°/2 kts	
SURFACE	030°/10 kts	
AIRCRAFT DATA USEFULNESS FOR		
ESTIMATION OF INITIAL CONDITIONS	Poor	
ESTIMATION OF BOUNDARY CONDITIONS	Poor	
MODEL VERIFICATION	Poor	
ESTIMATION OF MIXING	Poor	
DETERMINATION OF RESOLUTION REQUIREMENTS		
VERTICAL	Fair	
HORIZONTAL	Poor	

Maximum height of vertical profiles shown in parentheses. Location of vertical profiles is denoted by symbol ◉. Arrows denote surface and 850-mb wind direction. Dots denote location of ground monitoring sites.

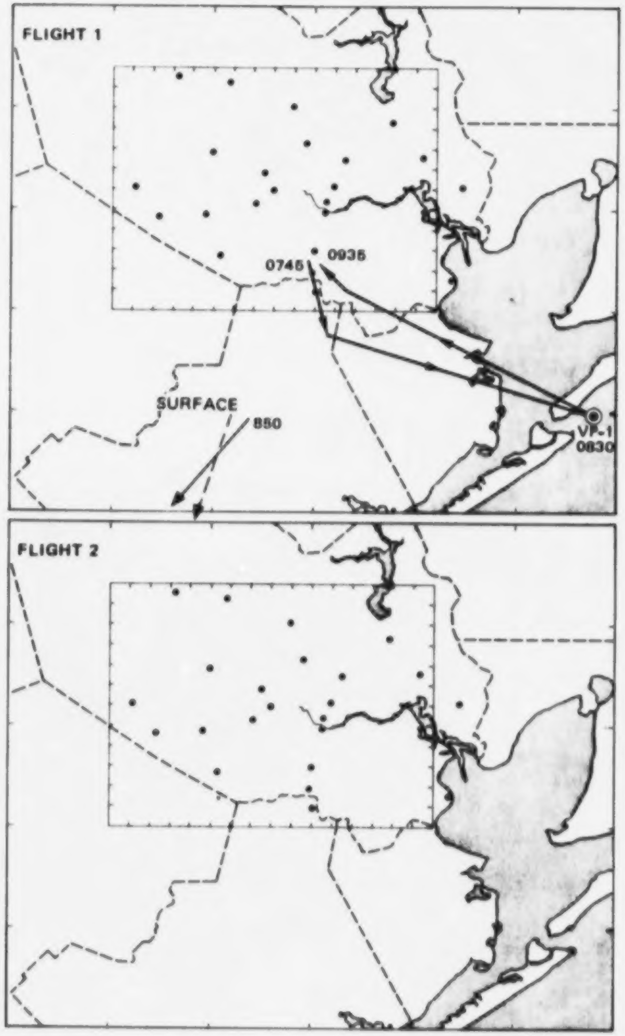

Figure A-11. Summary of data availability and usefulness for 27 September 1978.

ITEM	FLIGHT 1	FLIGHT 2
AIRCRAFT COVERAGE		
START TIME	1010	
END TIME	1025	
FLIGHT LEVEL (ft)	1500	
APPROXIMATE MIXING DEPTH (ft)	—	
NUMBER OF VERTICAL PROFILES	0	
OTHER UPPER-LEVEL DATA		
TETHERSONDE		
TIMES		
LOCATION		
PILOT BALLOON		
TIMES	10,11	
LOCATION	25 and 17	
SURFACE DATA — NUMBER OF SITES AVAILABLE:		
O_3	13	
NO_x	8	
NMHC	6	
PAN	1	
METEOROLOGICAL	5	
CONDITIONS		
DAILY O_3 PEAK CONCENTRATION (ppb)	88	
HOUR (CST)	1600	
SITE	Beasley	
GENERAL WINDS (DIRECTION/SPEED)		
850 mb	050°/8 kts	
SURFACE	360°/12 kts	
AIRCRAFT DATA USEFULNESS FOR		
ESTIMATION OF INITIAL CONDITIONS	Poor	
ESTIMATION OF BOUNDARY CONDITIONS	Poor	
MODEL VERIFICATION	Poor	
ESTIMATION OF MIXING	Poor	
DETERMINATION OF RESOLUTION REQUIREMENTS		
VERTICAL	Poor	
HORIZONTAL	Poor	

Maximum height of vertical profiles shown in parentheses. Location of vertical profiles is denoted by symbol ◉. Arrows denote surface and 850-mb wind direction. Dots denote location of ground monitoring sites.

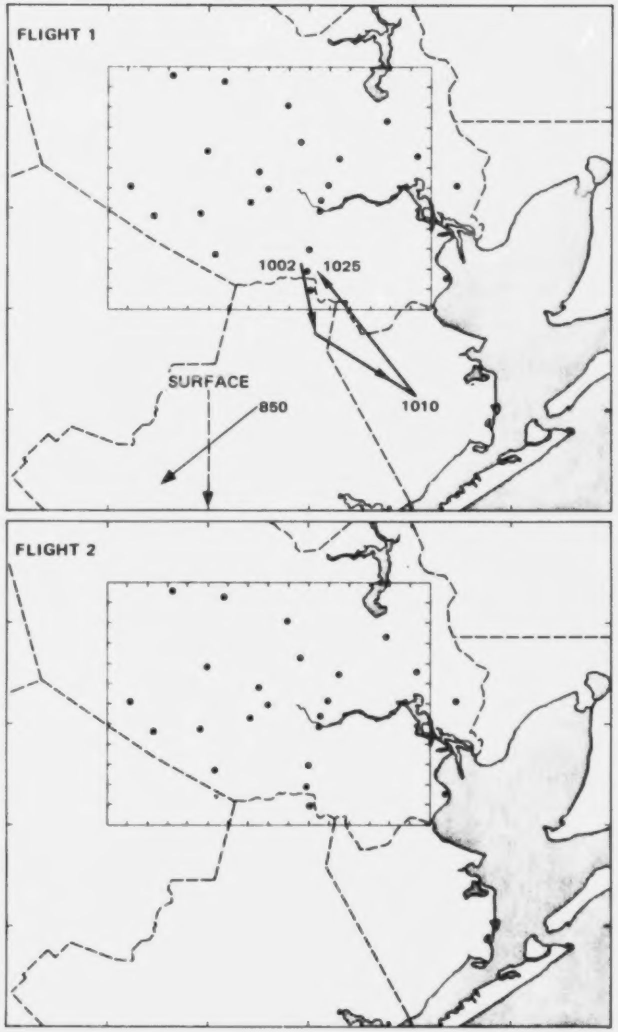

Figure A-12. Summary of data availability and usefulness for 28 September 1978.

ITEM	FLIGHT 1	FLIGHT 2
AIRCRAFT COVERAGE		
START TIME	0820	1310
END TIME	1112	1458
FLIGHT LEVEL (ft)	1500 (6000)	1500 (7500)
APPROXIMATE MIXING DEPTH (ft)	1500	3000
NUMBER OF VERTICAL PROFILES	5	2
OTHER UPPER-LEVEL DATA		
TETHERSONDE		
TIMES (SITE 12)	0820,1015,1045, 1100,1115	1330,1400,1415, 1430,1445,1500
PILOT BALLOON (T DENOTES TEMPERATURESONDE)		
TIMES	8T,9,10,11	13T,14,15
LOCATION	25 and 17	25 and 17
SURFACE DATA — NUMBER OF SITES AVAILABLE:		
O_3	13	13
NO_x	8	8
NMHC	6	6
PAN	1	1
METEOROLOGICAL	5	5
CONDITIONS		
DAILY O_3 PEAK CONCENTRATION (ppb)	141	141
HOUR (CST)	1600	1600
SITE	Pearland	Pearland
GENERAL WINDS (DIRECTION/SPEED)		
850 mb	020°/7 kts	010°/10 kts
SURFACE	090°/8 kts	050°/8 kts
AIRCRAFT DATA USEFULNESS FOR		
ESTIMATION OF INITIAL CONDITIONS	Reasonably good	Fair
ESTIMATION OF BOUNDARY CONDITIONS	Reasonably good	Fair
MODEL VERIFICATION	Fair	Good
ESTIMATION OF MIXING	Good	Good
DETERMINATION OF RESOLUTION REQUIREMENTS		
VERTICAL	Good	Reasonably good
HORIZONTAL	Reasonably good	Reasonably good

Maximum height of vertical profiles shown in parentheses. Location of vertical profiles is denoted by symbol ⊙. Arrows denote surface and 850-mb wind direction. Dots denote location of ground monitoring sites.

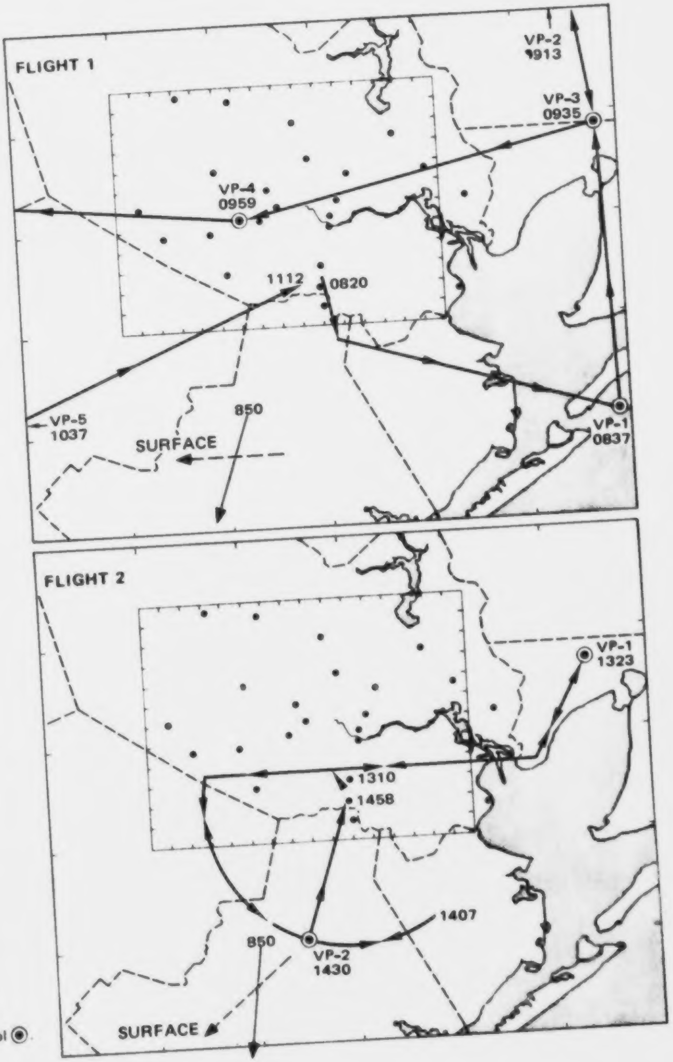

Figure A-13. Summary of data availability and usefulness for 29 September 1978.

ITEM	FLIGHT 1	FLIGHT 2
AIRCRAFT COVERAGE		
START TIME	0715	1200
END TIME	1018	1525
FLIGHT LEVEL (ft)	1500 (7500)	1500 (7000)
APPROXIMATE MIXING DEPTH (ft)	1500	5000
NUMBER OF VERTICAL PROFILES	5	4
OTHER UPPER-LEVEL DATA		
TETHERSONDE		
TIMES (SITE 12)	0800,0825,0845, 0910,0930,1000	1220,1230,1300, 1330,1400,1425, 1505,1535
PILOT BALLOON (T DENOTES TEMPERATURESONDE)		
TIMES	7T,8,9,10,11	13T,14,15,16
LOCATION	25 and 17	25 and 17
SURFACE DATA — NUMBER OF SITES AVAILABLE:		
O_3	13	13
NO_x	8	8
NMHC	3	3
PAN	1	1
METEOROLOGICAL	5	5
CONDITIONS		
DAILY O_3 PEAK CONCENTRATION (ppb)	105	105
HOUR (CST)	1500	1500
SITE	Darlinghurst	Darlinghurst
GENERAL WINDS (DIRECTION/SPEED)		
850 mb	020°/5 kts	050°/10 kts
SURFACE	050°/5 kts	360°/5 kts
AIRCRAFT DATA USEFULNESS FOR		
ESTIMATION OF INITIAL CONDITIONS	Fair	Fair
ESTIMATION OF BOUNDARY CONDITIONS	Fair	Fair
MODEL VERIFICATION	Fair	Good
ESTIMATION OF MIXING	Reasonably good	Good
DETERMINATION OF RESOLUTION REQUIREMENTS		
VERTICAL	Good	Good
HORIZONTAL	Good	Good

Maximum height of vertical profiles shown in parentheses. Location of vertical profiles is denoted by symbol ◉. Arrows denote surface and 850-mb wind direction. Dots denote location of ground monitoring sites.

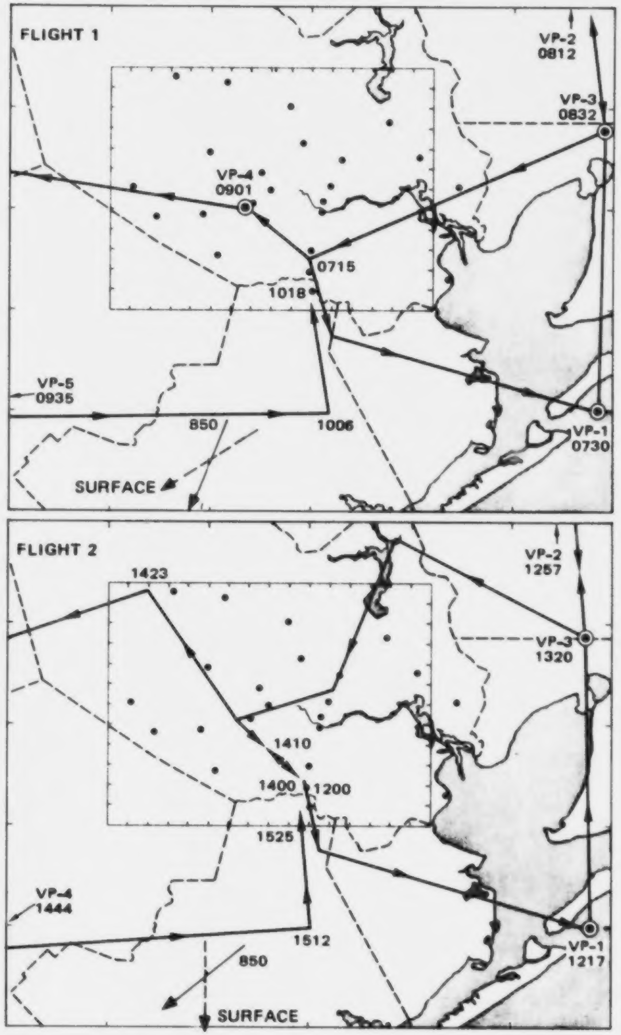

Figure A-14. Summary of data availability and usefulness for 30 September 1978.

ITEM	FLIGHT 1	FLIGHT 2
AIRCRAFT COVERAGE		
START TIME	1152	1825
END TIME	1500	2040
FLIGHT LEVEL (ft)	1500 (6000)	1500 (6000)
APPROXIMATE MIXING DEPTH (ft)	4000	5000
NUMBER OF VERTICAL PROFILES	5	3
OTHER UPPER-LEVEL DATA		
TETHERSONDE		
TIMES		
LOCATION		
PILOT BALLOON (T DENOTES TEMPERATURESONDE)		
TIMES	11,13T,14,15	17T
LOCATION	25 and 17	25 and 17
SURFACE DATA — NUMBER OF SITES AVAILABLE:		
O_3	11	11
NO_x	8	8
NMHC	6	6
PAN	1	1
METEOROLOGICAL	5	5
CONDITIONS		
DAILY O_3 PEAK CONCENTRATION (ppb)	310	310
HOUR (CST)	1400	1400
SITE	Hornwood	Hornwood
GENERAL WINDS (DIRECTION/SPEED)		
850 mb	100°/5 kts	100°/5 kts
SURFACE	015°/6 kts	150°/7 kts
AIRCRAFT DATA USEFULNESS FOR		
ESTIMATION OF INITIAL CONDITIONS	Reasonably good	Poor
ESTIMATION OF BOUNDARY CONDITIONS	Reasonably good	Poor
MODEL VERIFICATION	Reasonably good	Reasonably good
ESTIMATION OF MIXING	Good	Reasonably good
DETERMINATION OF RESOLUTION REQUIREMENTS		
VERTICAL	Good	Reasonably good
HORIZONTAL	Good	Reasonably good

Maximum height of vertical profiles shown in parentheses. Location of vertical profiles is denoted by symbol ◉. Arrows denote surface and 850-mb wind direction. Dots denote location of ground monitoring sites.

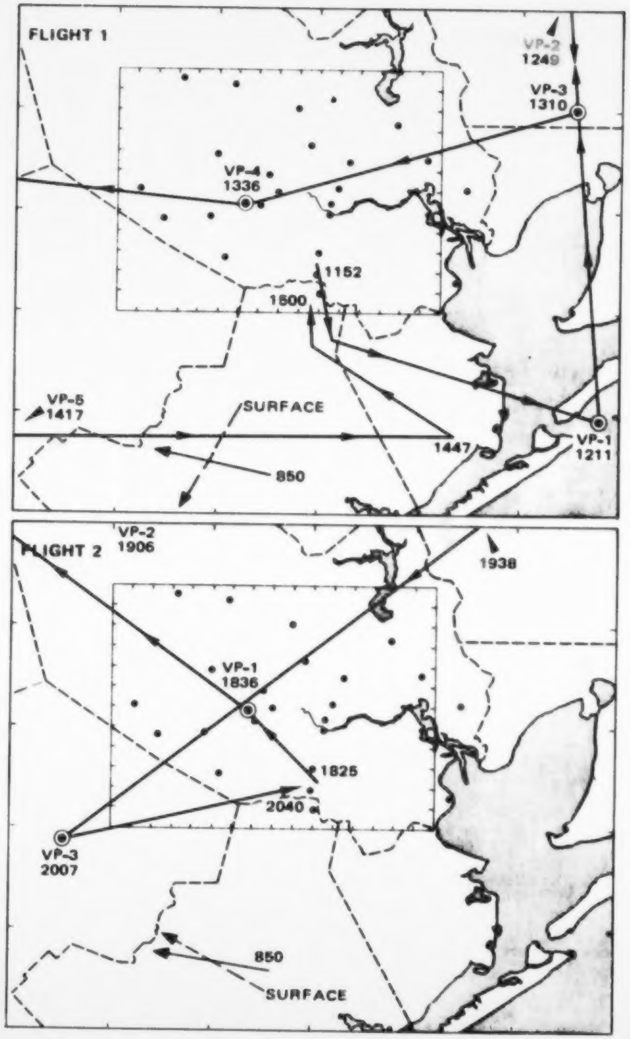

Figure A-15. Summary of data availability and usefulness for 1 October 1978.

ITEM	FLIGHT 1	FLIGHT 2
AIRCRAFT COVERAGE		
START TIME	0728	1320
END TIME	1038	1615
FLIGHT LEVEL (ft)	1500 (6000)	1500 (7000)
APPROXIMATE MIXING DEPTH (ft)	1500	3500
NUMBER OF VERTICAL PROFILES	5	5
OTHER UPPER-LEVEL DATA		
TETHERSONDE		
TIMES (SITE 12)	0900,0925,1000, 1025	1340,1430,1500, 1525,1550,1615
PILOT BALLOON (T DENOTES TEMPERATURESONDE)		
TIMES	7T,8,9,10,11	13T,14,15,16,17
LOCATION	25 and 17	25 and 17
SURFACE DATA — NUMBER OF SITES AVAILABLE:		
O_3	11	11
NO_x	8	8
NMHC	6	6
PAN	1	1
METEOROLOGICAL	5	5
CONDITIONS		
DAILY O_3 PEAK CONCENTRATION (ppb)	210	210
HOUR (CST)	1200/1300	1200/1300
SITE	Aldine	Aldine
GENERAL WINDS (DIRECTION/SPEED)		
850 mb	120°/10 kts	200°/7 kts
SURFACE	Calm	150°/10 kts
AIRCRAFT DATA USEFULNESS FOR		
ESTIMATION OF INITIAL CONDITIONS	Reasonably good	Poor
ESTIMATION OF BOUNDARY CONDITIONS	Reasonably good	Reasonably good
MODEL VERIFICATION	Reasonably good	Good
ESTIMATION OF MIXING	Reasonably good	Good
DETERMINATION OF RESOLUTION REQUIREMENTS		
VERTICAL	Good	Good
HORIZONTAL	Reasonably good	Good

Maximum height of vertical profiles shown in parentheses. Location of vertical profiles is denoted by symbol ⊙. Arrows denote surface and 850-mb wind direction. Dots denote location of ground monitoring sites.

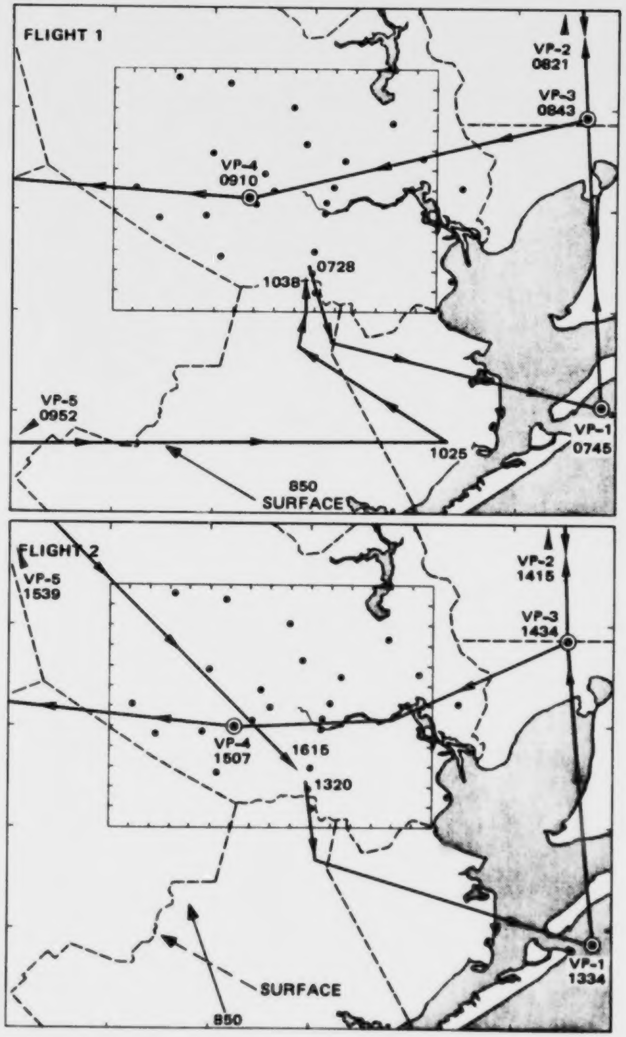

Figure A-16. Summary of data availability and usefulness for 2 October 1978.

ITEM	FLIGHT 1	FLIGHT 2
AIRCRAFT COVERAGE		
START TIME	0800	1655
END TIME	0915	2008
FLIGHT LEVEL (ft)	1500 (6000)	1500 (6000)
APPROXIMATE MIXING DEPTH (ft)	1200	2500
NUMBER OF VERTICAL PROFILES	1	2
OTHER UPPER-LEVEL DATA		
TETHERSONDE		
TIMES	0745,0930	1645
LOCATION	12	12
PILOT BALLOON (T DENOTES TEMPERATURESONDE)		
TIMES	7T,8,9,10	16,17
LOCATION	25 and 17	25 and 17
SURFACE DATA — NUMBER OF SITES AVAILABLE:		
O_3	12	12
NO_x	9	9
NMHC	5	5
PAN	1	1
METEOROLOGICAL	5	5
CONDITIONS		
DAILY O_3 PEAK CONCENTRATION (ppb)	150	150
HOUR (CST)	1200/1400	1200/1400
SITE	Hornwood/Aldine	Hornwood/Aldine
GENERAL WINDS (DIRECTION/SPEED)		
850 mb	080°/5 kts	180°/5 kts
SURFACE	040°/5 kts	130°/8 kts
AIRCRAFT DATA USEFULNESS FOR		
ESTIMATION OF INITIAL CONDITIONS	Poor	Poor
ESTIMATION OF BOUNDARY CONDITIONS	Fair	Good
MODEL VERIFICATION	Poor	Good
ESTIMATION OF MIXING	Poor	Reasonably good
DETERMINATION OF RESOLUTION REQUIREMENTS		
VERTICAL	Fair	Fair
HORIZONTAL	Poor	Good

Maximum height of vertical profiles shown in parentheses. Location of vertical profiles is denoted by symbol ⦿. Arrows denote surface and 850-mb wind direction. Dots denote location of ground monitoring sites.

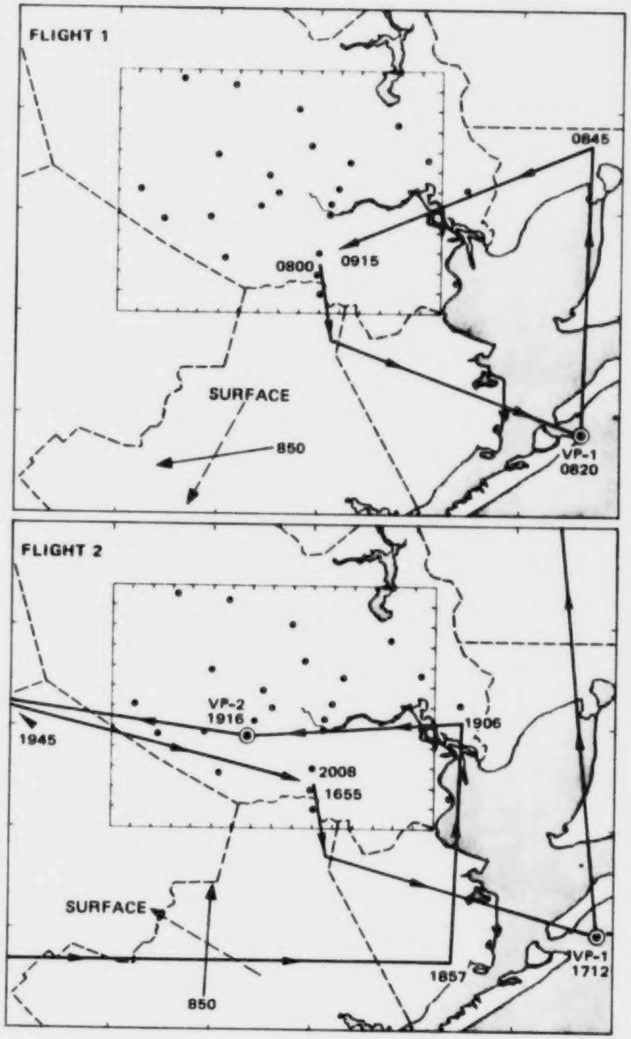

Figure A-17. Summary of data availability and usefulness for 4 October 1978.

ITEM	FLIGHT 1	FLIGHT 2
AIRCRAFT COVERAGE		
START TIME	0950	
END TIME	1302	
FLIGHT LEVEL (ft)	1500 (6000)	
APPROXIMATE MIXING DEPTH (ft)	3000	
NUMBER OF VERTICAL PROFILES	5	
OTHER UPPER-LEVEL DATA		
TETHERSONDE		
TIMES (SITE 12)	1000,1100,1125, 1145,1205	
PILOT BALLOON (T DENOTES TEMPERATURESONDE)		
TIMES	8,9,10,11,13T	
LOCATION	25 and 17 (8T — Site 25)	
SURFACE DATA — NUMBER OF SITES AVAILABLE:		
O_3	12	
NO_x	8	
NMHC	5	
PAN	1	
METEOROLOGICAL	5	
CONDITIONS		
DAILY O_3 PEAK CONCENTRATION (ppb)	190	
HOUR (CST)	1300	
SITE	Crawford	
GENERAL WINDS (DIRECTION/SPEED)		
850 mb	040°/5 kts	
SURFACE	070°/5 kts	
AIRCRAFT DATA USEFULNESS FOR		
ESTIMATION OF INITIAL CONDITIONS	Fair	
ESTIMATION OF BOUNDARY CONDITIONS	Good	
MODEL VERIFICATION	Reasonably good	
ESTIMATION OF MIXING	Good	
DETERMINATION OF RESOLUTION REQUIREMENTS		
VERTICAL	Good	
HORIZONTAL	Good	

Maximum height of vertical profiles shown in parentheses. Location of vertical profiles is denoted by symbol ◉. Arrows denote surface and 850-mb wind direction. Dots denote location of ground monitoring sites.

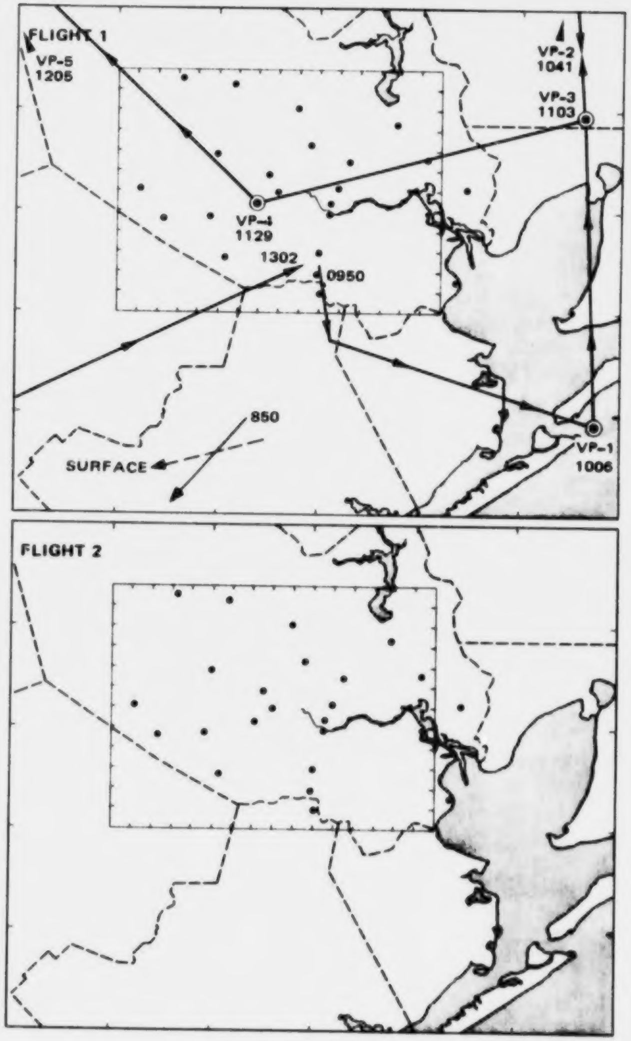

Figure A-18. Summary of data availability and usefulness for 5 October 1978.

ITEM	FLIGHT 1	FLIGHT 2
AIRCRAFT COVERAGE		
START TIME	0617	
END TIME	0940	
FLIGHT LEVEL (ft)	1500 (6000)	
APPROXIMATE MIXING DEPTH (ft)	1500	
NUMBER OF VERTICAL PROFILES	5	
OTHER UPPER-LEVEL DATA		
TETHERSONDE		
TIMES	0750,0915,0935	
LOCATION	12	
PILOT BALLOON (T DENOTES TEMPERATURESONDE)		
TIMES (LOCATION)	7T,8,9,10 (25)	
	7,8T,9,10 (17)	
SURFACE DATA — NUMBER OF SITES AVAILABLE:		
O_3	13	
NO_x	8	
NMHC	6	
PAN	1	
METEOROLOGICAL	5	
CONDITIONS		
DAILY O_3 PEAK CONCENTRATION (ppb)	163	
HOUR (CST)	1600	
SITE	Darlinghurst	
GENERAL WINDS (DIRECTION/SPEED)		
850 mb	360°/10 kts	
SURFACE	060°/7 kts	
AIRCRAFT DATA USEFULNESS FOR		
ESTIMATION OF INITIAL CONDITIONS	Reasonably good	
ESTIMATION OF BOUNDARY CONDITIONS	Reasonably good	
MODEL VERIFICATION	Reasonably good	
ESTIMATION OF MIXING	Reasonably good	
DETERMINATION OF RESOLUTION REQUIREMENTS		
VERTICAL	Good	
HORIZONTAL	Good	

Maximum height of vertical profiles shown in parentheses. Location of vertical profiles is denoted by symbol ◉. Arrows denote surface and 850-mb wind direction. Dots denote location of ground monitoring sites.

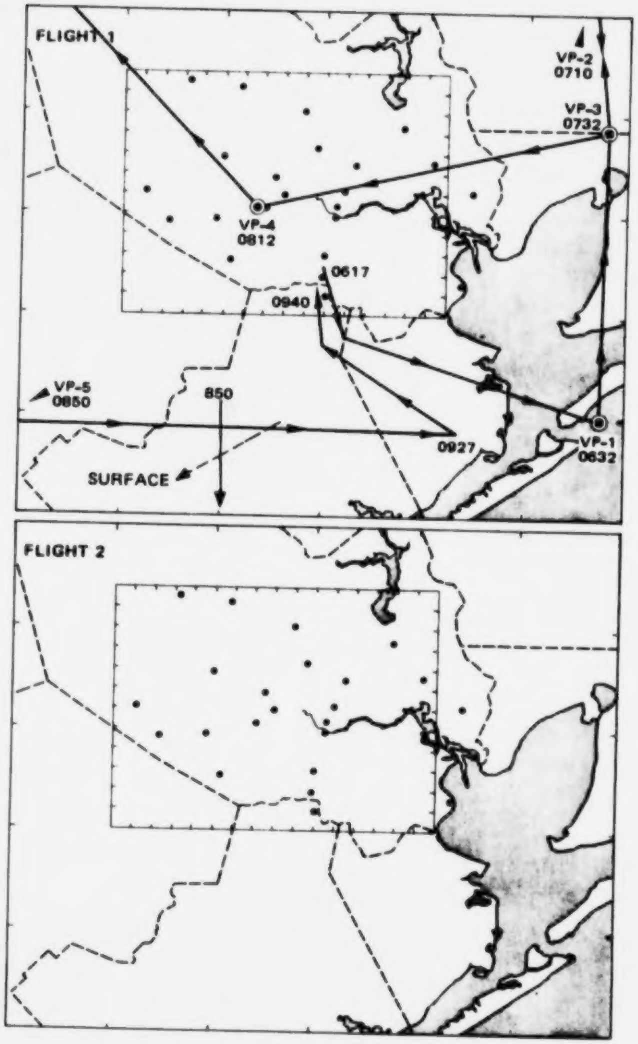

Figure A-19. Summary of data availability and usefulness for 7 October 1978.

APPENDIX B

MATHEMATICAL DEFINITIONS FOR EMPIRICAL ORTHOGONAL FUNCTIONS

Lorenz adapted factor-analysis methods to the treatment of meteorological parameters. The methods he developed are quite useful as analytical tools because they provide descriptions of the most important patterns of fluctuation in a field of data, e.g. pollutant concentrations. We have used Lorenz's concepts and methods to examine the HOMS NMHC, NO_x, and ozone data. The following description of the approach is derived from the work of Lorenz (1956).

Consider the set of M observations $\overset{*}{p}_1(t)\ldots\overset{*}{p}_m(t)$, each observed at the N times $t_1\ldots t_n$, where p_i is the deviation of the observation at point i from the mean value for that point. Let V be the total variance of the observations that make up the data set

$$V = \sum_{m=1}^{N} \overline{\overset{*}{p}_m^{2}} \quad , \tag{1}$$

where the bar denotes an average. Let $q_1(t)\ldots q_k(t)$ be any K quantities where $K < M$, and let

$$\overset{*}{p}_m(t) = \sum_{k=1}^{K} y_{km} q_k(t_i) + r_m(t_i) \quad , \tag{2}$$

where the coefficients y_{km} are selected to minimize the value of r_m^2 for each of the cases, and where r is the remainder or difference between observed and estimated $p_m(t)$. This will also minimize the quantity

$$R = \sum_{m=1}^{M} r_m^2 \quad , \tag{3}$$

which represents the total variance in the observation data set that is not explained by the relationship given in Eq. (2).

Values of y_{km} are chosen to minimize R, but R also depends on the choice of the quantities q_k. Lorenz's method chooses the quantities q_k to minimize the minimum value of R. The quantity $(V - R)/V$ represents the fraction of the total variance in the observed data set that can be represented by K quantities.

Let us consider the expression

$$\overset{*}{p}_m(t) = \sum_{k=1}^{M} Y_{km}Q_k(t) \quad , \tag{4}$$

where y_m and $Q_k(t)$ satisfy the following relations

$$\sum_{m=1}^{M} Y_{km}Y_{jm} = \delta_{kj} \equiv \begin{cases} 1 \text{ when } k=j \\ 0 \text{ when } k\neq j \end{cases} \tag{5}$$

and

$$N\overset{*}{Q}_k\overset{*}{Q}_j = a_k\delta_{kj} \quad . \tag{6}$$

From the above, it follows that the quantities $\overset{*}{Q}_1 \ldots \overset{*}{Q}_k$ (if they exist) satisfy the requirements for the desired functions $q_1 \ldots q_k$. Moreover,

$$V = \frac{1}{N}\sum_{k=1}^{M} a_k \tag{7}$$

and

$$V - R = \frac{1}{N}\sum_{k=1}^{K} a_k \quad . \tag{8}$$

Lorenz has provided a proof of these results.

Equation (4) above is the equivalent of the column vector equation

$$\begin{bmatrix} \overset{*}{p}_1 \\ \overset{*}{p}_2 \\ \cdot \\ \cdot \\ \cdot \\ \overset{*}{p}_M \end{bmatrix} = q_1(t) \begin{bmatrix} y_{11} \\ y_{21} \\ \cdot \\ \cdot \\ \cdot \\ y_{M1} \end{bmatrix} + q_2(t) \begin{bmatrix} y_{12} \\ y_{22} \\ \cdot \\ \cdot \\ \cdot \\ y_{M2} \end{bmatrix} + \ . \ . \ . + \begin{bmatrix} y_{1M} \\ y_{2M} \\ \cdot \\ \cdot \\ \cdot \\ y_{MM} \end{bmatrix} \quad , \tag{9}$$

where the elements of the column vector ($\overset{*}{p}_1$, $\overset{*}{p}_2$, etc.) on the left side of the equation, in this application, represent the deviation of the observed values for a given time t from their means. Lorenz shows that the column vectors on the right side of the equation are the eigenvectors of a covariance matrix derived from the data set if the relations presented in Eqs. (5) through (8) are satisfied. The coefficients, q_k, are unique for the observations at a given time. They are given by the inner products of the observation column vector [the left side of Eq. (9)] and the corresponding eigenvectors. The eigenvectors, or empirical orthogonal functions in Lorenz' terminology, can be arranged according to the amount of variance explained by each. If this is done so that the first empirical orthogonal function explains the most variance and the second explains the second most variance and so on, then the right-hand side of the vector equation above can be truncated after a few terms and will remain approximately correct for most cases. By so doing, we have transformed the variables that describe the pollutant field, thus reducing the number required to describe the field while still maintaining most of the information within the original data set.

Lorenz points out that each of the points in the original data set is likely to contain some noise--where noise is used in the broad sense and includes errors both in observations and in observed values that are little related to other values in the data set--either elsewhere at the same time or at different times at the same place. When the variables are transformed, most of this noise tends to be associated with those q_k's with small variances, i.e., those associated with the least important empirical orthogonal functions. Those q_k's with large variances may also contain considerable noise, but that noise will be less relative to the total variance. The patterns with which the most important empirical orthogonal functions are associated are likely to represent the more important physical features in the set of observations.